Universidade de Lisboa

Faculdade de Farmácia

RESTORING CHOLESTEROL HOMEOSTASIS IN NEURONS BY CYP46A1 DOES NOT STALL THE PROGRESSION OF NIEMANN-PICK TYPE C DISEASE

Joana Pinheiro Leite da Anunciação Reis

Dissertation supervised by Dr. Maria João de Jesus Nunes and co-supervised by Professor Elsa Margarida Teixeira Rodrigues

Confidential

Master in Biopharmaceutical Sciences

2022

Universidade de Lisboa

Faculdade de Farmácia

RESTORING CHOLESTEROL HOMEOSTASIS IN NEURONS BY CYP46A1 DOES NOT STALL THE PROGRESSION OF NIEMANN-PICK TYPE C DISEASE

Joana Pinheiro Leite da Anunciação Reis

Dissertation supervised by Dr. Maria João de Jesus Nunes and co-supervised by Professor Elsa Margarida Teixeira Rodrigues

Confidential

Master in Biopharmaceutical Sciences

2022

This work was supported by FEDER and national funds from Fundação para a Ciência e Tecnologia (FCT) (PTDC/MED-NEU/29455/2017), Bolsa de Investigação da Sociedade Portuguesa de Doenças Metabólicas (SPDM), and BrainVectis Technologies.

Acknowledgments

Em primeiro lugar, gostaria de agradecer à Professora Doutora Cecília Rodrigues, pela oportunidade de desenvolver a minha tese de mestrado no Cell Function and Therapeutic Targeting Lab e pela preocupação e disponibilidade para resolver qualquer questão.

À minha orientadora, Doutora Maria João Nunes, agradeço por me ter guiado e ensinado tanto ao longo deste ano, partilhando comigo o seu saber e toda a sua experiência de vida de laboratório. Agradeço toda a disponibilidade para seguir sempre de perto o meu trabalho, bem como a preocupação em me ensinar e motivar, desenvolvendo as minhas capacidades laboratoriais.

À Professora Doutora Elsa Rodrigues, que me acolheu e orientou desde os projetos do primeiro ano de mestrado, obrigada pela oportunidade de trabalhar e aprender com este grupo fantástico. Obrigada pela presença constante – a qualquer hora – e por me ensinar, não só o entusiasmo da vida de investigação, mas também a encarar os desafios de forma concisa – "Keep It Short and Simple".

Agradeço também o apoio prestado pela Professora Doutora Maria João Gama. À Professora Doutora Margarida Castro-Caldas, agradeço por me ter ensinado os segredos da imunohistoquímica e do microscópio. À Doutora Andreia Carvalho, obrigada por estar sempre pronta para esclarecer os nossos impasses, para encontrar protocolos e, sempre que necessário, vir connosco descobrir os reagentes aos armários mistério no piso de cima. Agradeço também ao restante grupo do CellFun, pela disponibilidade e interajuda no laboratório, bem como pela oportunidade de aprender sobre diversos projetos e temáticas nos Lab Meetings.

À Inês, obrigada por seres um apoio constante, por estares sempre pronta a desvendar os nossos problemas, com a preocupação de quem, acima de tudo, quer o bem para o seu grupo. Às minhas companheiras, Daria e Margarida, obrigada por tornarem especial esta aventura, em que os desafios de cada uma passavam a ser das três. Vou ter saudades do nosso dia-a-dia, dos almoços, das viagens à máquina do andar de cima, dos lanches que tornavam os dias mais fáceis, dos donuts em feriados de trabalho e do jantar na nossa sala em dia de Western. Conseguimos, amigas!

Por fim, obrigada aos meus pais, avós e tio pelo apoio, sempre de perto. E ao Diogo, pela paciência e motivação.

Abstract

Cholesterol 24-hydroxylase (CYP46A1) is a neuronal-specific cytochrome P450, which catalyzes the major elimination pathway of brain cholesterol, through its conversion into 24S-hydroxycholesterol. Our previous studies in different models of Niemann-Pick type C disease (NPC) suggested CYP46A1 to be a potential therapeutic target, since the ectopic expression of this protein could correct the unesterified cholesterol accumulation in late endosome/lysosomes (LE/L) characteristic of this disease. The deregulation of cholesterol homeostasis is the main hallmark of this fatal neurodegenerative and lysosomal storage disorder, leading to autophagic flux impairment and neuroinflammation. The goal of the present work was to evaluate how CYP46A1 ectopic expression in the $Npc1^{tm(I1061T)}$ animal model is improving the disease phenotype, by focusing on the main pathologic hallmarks, cholesterol homeostasis dysregulation, neuroinflammation, and autophagy impairment.

Increased expression of CYP46A1 by adeno-associated virus-mediated gene therapy in NPC mice partially prevented weight loss and hepatomegaly. Additionally, CYP46A1 corrected the transcript levels of genes involved in cholesterol synthesis, uptake, efflux, and esterification, also promoting a redistribution of the cholesterol accumulated in the LE/L. In NPC, neuroinflammation is first evidenced by microglia activation that begins a neurodegenerative cascade, leading to astrocytosis. CYP46A1 expression partially corrected the increased levels of pro-inflammatory markers along with a decrease of Anti-ionized calcium-Binding Adapter Molecule 1 (Iba-1) immunostaining in NPC mice cerebellum, suggesting CYP46A1 is decreasing microgliosis. However, no CYP46A1-dependent effect was observed in astrogliosis. Moreover, expression of this cholesterol hydroxylase was able to partially rescue lysosomal deregulation, by restoring Cathepsin D mRNA levels in NPC animals. *In vitro* studies in HeLa NPC-KO cells confirmed previous results obtained in the NPC animal model, showing that CYP46A1 restores the autophagy flux, as observed by a reduction in the accumulation of lipidated microtubule-associated protein 1 light chain 3 (LC3-II), as well as by autophagy-related transcriptome analysis. Although several pathological features were improved in response to CYP46A1 expression, Purkinje cell degeneration was not reversed in the cerebellum of NPC mice. Overall, this work further characterizes the effect of CYP46A1 in ameliorating important

pathological features of NPC and highlights that correction of cholesterol accumulation is not sufficient to halt neurodegeneration in NPC.

Keywords: Niemann-Pick Type C disease (NPC); Cholesterol 24-hydroxylase (CYP46A1); brain cholesterol metabolism; neuroinflammation; autophagy

Resumo

A enzima colesterol 24-hidroxilase (CYP46A1) consiste num citocromo P450 neuro-específico, que catalisa a conversão do colesterol em 24S-hydroxycholesterol, constituindo a principal via de eliminação do colesterol no encéfalo. Tem assim um papel crucial na manutenção do normal metabolismo do colesterol, tendo em conta que o encéfalo é o órgão do corpo humano com maior teor de colesterol. Em estudos prévios do nosso grupo, em que foram utilizados diferentes modelos celulares da doença de Niemann-Pick type C (NPC), o CYP46A1 foi sugerido como um potencial alvo terapêutico nesta patologia. Isto deve-se à capacidade do CYP46A1 em corrigir a acumulação de colesterol não-esterificado nos endossomas tardios /lisossomas (LE/L), que constitui a principal característica da doença de NPC. Este fenótipo é originado por mutação na proteína NPC1, localizada na membrana dos LE/L, e responsável pelo efluxo e reciclagem do colesterol internalizado sob a forma de lipoproteínas. A doença de NPC é uma doença rara, com alternativas terapêuticas muito limitadas. A sintomatologia que a caracteriza é diversa e afeta o encéfalo, fígado e o baço. Na maioria dos casos, a doença manifesta-se durante a infância ou início da adolescência, sendo que os pacientes apresentam um comprometimento progressivo da função motora e intelectual, que geralmente levam à morte nas duas primeiras décadas de vida. Entre as alterações patológicas neuro-viscerais, um sintoma principal da doença de NPC é a ataxia cerebelar, que é resultante da perda progressiva de células de Purkinje. O mecanismo responsável pela perda neuronal acentuada não se encontra ainda definido, porém, o desequilíbrio induzido pela acumulação de colesterol é frequentemente tido em conta como agravante, senão mesmo a causa da doença. De facto, a desregulação da homeostase do colesterol está subjacente ao processo neurodegenerativo, induzindo um bloqueio do fluxo autofágico e um aumento da neuro-inflamação. Desta forma, o objetivo deste trabalho foi avaliar se a expressão do CYP46A1 promove a melhoria do fenótipo da doença, com foco nas principais características patológicas, incluindo a desregulação da homeostase do colesterol, neuro-inflamação e bloqueio da autofagia. Para isso, aumentámos os níveis de CYP46A1 utilizando vírus adeno-associados, num modelo murganho da doença de NPC. Estes animais, Npc1$^{tm(I1061T)}$, possuem o *knock-in* da mutação I1061T no gene que codifica para a proteína NPC1, que é a mais frequente encontrada nos humanos.

Os nossos resultados mostraram que a expressão ectópica de CYP46A1 impediu parcialmente a perda de peso e a hepatomegalia observada os murganhos NPC. Além

disso, o CYP46A1 promoveu uma correção significativa dos níveis de mRNA de genes envolvidos na síntese, captação, efluxo e esterificação do colesterol. A este efeito, foi também associada uma promoção da redistribuição do colesterol não esterificado acumulado nos LE/L, que foi sugerida através da análise por marcação de cortes parasagitais do córtex dos animais com filipina III. A partir destes resultados, foi possível concluir que as células do cerebelo e córtex dos animais NPC estão de facto a responder à normalização da homeostase do colesterol promovida pela expressão do CYP46A1.

Outra característica impactante da doença de NPC é a neuro-inflamação, que é evidenciada pela ativação de microglia, que inicia uma cascata neurodegenerativa e leva à ativação de astrócitos. A expressão de CYP46A1 corrigiu parcialmente os níveis de mRNA aumentados de alguns marcadores de microglia característicos de um fenótipo mais pró-inflamatório no cerebelo dos murganhos NPC, e em simultâneo induziu um aumento dos níveis de expressão de Arginase 1 e do Fator de Transformação do crescimento β1. Esta alteração do perfil inflamatório da microglia foi corroborada por ensaios de imunohistoquímica, em que foram analisados os níveis da molécula adaptadora de ligação ao cálcio 1 (Iba-1), em várias regiões do cerebelo dos murganhos, nomeadamente o núcleo cerebelar profundo e as camadas molecular e granular dos lóbulos do cerebelo, e que sugerem uma diminuição da ativação da microglia por parte do CYP46A1. No entanto, não foi observada nenhuma melhoria relativamente ao perfil de ativação de astrócitos.

Concomitante com a correção da homeostasia do colesterol, foi também registado um restabelecimento dos níveis de mRNA da enzima lisosomal Catepsina D o que sugere uma melhoria parcial da desregulação lisossomal caraterística da doença de NPC. Visto que a disfunção lisossomal está associada aos defeitos na autofagia verificados nesta doença, foram efetuados estudos *in vitro* recorrendo a células HeLa em que foi efetuado o *knock-down* da proteína NPC (NPC-KO). O aumento da expressão do CYP46A1 com recurso a transdução com vectores de adenovírus, confirmaram os resultados previamente obtidos pelo nosso grupo no modelo animal NPC, ao indicar que a expressão de CYP46A1 promove a restauração do fluxo autofágico. Este efeito foi observado através de uma redução na acumulação da forma lipidada da proteína 1 de cadeia leve 3 associada a microtúbulos (LC3-II), bem como através da análise dos níveis de mRNA de genes envolvidos na regulação da autofagia.

Embora uma melhoria das várias características patológicas principais da doença de NPC tenha sido registada em resposta à expressão de CYP46A1, a degeneração das células de

Purkinje não foi revertida no cerebelo dos murganhos NPC. Esta análise decorreu do cálculo da densidade de células de Purkinje após marcação dos tecidos com Violeta de Cresil e posterior confirmação através de marcação com um anticorpo anti-Calbindina através de imunofluorescência.

Os resultados apresentados neste estudo demonstram que a correção da homeostase do colesterol mediada por CYP46A1 em murganhos NPC não é suficiente para prevenir a morte de células neuronais, realçando o papel de outros lípidos neurotóxicos na etiologia desta doença. No entanto, a expressão de CYP46A1 promoveu a reversão de importantes aspetos patológicos da doença, nomeadamente a normalização do metabolismo do colesterol, regularização do fluxo autofágico e diminuição da neuro-inflamação. Sendo estes aspetos característicos também de variadas outras doenças neurodegenerativas, o CYP46A1 poderá então representar uma abordagem terapêutica válida em diferentes contextos.

Palavras-chave: Doença de Niemann-Pick Tipo C (NPC); Colesterol 24-hidroxilase (CYP46A1); metabolismo do colesterol no encéfalo; neuro-inflamação; autofagia

Table of contents

List of figures

List of tables

Abbreviations

24S-OH - 24S-hydroxycholesterol

ABCA1 - Adenosine Triphosphate-Binding Cassette Subfamily A Member 1

ACAT1 - Cholesterol Acyltransferase 1

adCYP - Adenovirus encoding cholesterol 24-hydroxylase

adGFP - Adenovirus encoding green fluorescent protein

ALT - Alanine Aminotransferase

ApoE - Apolipoprotein E

Arg1 - Arginase 1

ATG - Autophagy-related gene

BBB - Blood-brain barrier

Becn1 - Beclin 1

CD68 - Cluster of Differentiation 68

CSF - Cerebrospinal fluid

CX_3CR1 - C-X_3-C motif Chemokine Receptor 1

CYP46A1 - Cholesterol 24-hydroxylase

DAM - Disease-Associated Microglia

ER - Endoplasmic reticulum

GFAP - Glial Fibrillary Acidic Protein

HDAC - Histone Deacetylase

HDL - High-density lipoprotein

HMGCR - Hydroxy β-methylglutaryl-Coenzyme A (HMG-CoA) reductase

HMGCS - HMG-CoA synthase

Iba-1 - Anti-ionized Calcium-Binding Adapter Molecule 1

IGF1 - Insulin Growth Factor-1

Il-1α - Interleukin-1α

IL-1β - Interleukin-1β

LC3 - Microtubule-Associated Protein 1 Light Chain 3

LDLR - Low-Density Lipoprotein Receptor

LE/L - late endosome/lysosome

LXR - Liver X Receptor

mTOR - Mammalian Target of Rapamycin

mTORC1 - mTOR complex 1

NPC - Niemann-Pick, type C

p62 – Sequestosome 1

Pik3c3 - Phosphatidylinositol 3-Kinase Catalytic Subunit Type 3

Prkaa1 - Protein Kinase AMP-Activated Catalytic Subunit Alpha 1

RT-qPCR - Real-Time Quantitative Polymerase Chain Reaction

SNARE - Soluble N-ethylmaleimide-sensitive factor Attachment protein Receptor

SREBP2 - Sterol Regulatory Element-Binding Protein 2

TGFβ - Transforming Growth Factor β

TNFα - Tumor Necrosis Factor α

TREM2 - Triggering Receptor Expressed on Myeloid cells 2

ULK1 - Unc-51 Like Autophagy Activating Kinase 1

WIPI2 - WD Repeat Domain Phosphoinositide Interacting 2

Part I – General Introduction and Background

1. Brain cholesterol

The brain is the most cholesterol-rich organ in the body[1]. As a constituent of myelin and cell membranes, cholesterol is required for proper brain function in aspects including the formation of axons and dendrites during development, neuronal repair and remodeling, formation of new synapses, as well as learning and memory[2–5]. Therefore, being essential for neuronal physiology during development and in the adult stage, depletion of cholesterol in neurons leads to impairment of synaptic vesicle exocytosis, neuronal activity, and neurotransmission, with consequent degeneration of the dendritic spine and synapse[6–8]. Cholesterol's presence in the brain is divided into two pools, a larger and more concentrated one, accounting for 70% of total cholesterol, which is metabolically stable and found in the myelin membranes of white matter, and a smaller second pool, of a lower concentration, containing 30% of total cholesterol, which is found in the plasma and subcellular membranes of neurons and glial cells of gray matter and is metabolically active[9,10].

Regarding the source of brain cholesterol, as the efficiency of the blood-brain barrier (BBB) does not allow the uptake of lipoproteins from the circulation, and therefore separates cholesterol's metabolism in the brain from that in the rest of the body, the brain has to rely its substantial cholesterol needs on *de novo* synthesis[11] (Figure 1). This process begins with the β-Hydroxy β-methylglutaryl-Coenzime A synthase (HMGCS)-mediated conversion of acetyl-CoA to HMG-CoA, which is then converted into mevalonate by HMG-CoA reductase (HMGCR), which is the rate-limiting and irreversible step of the pathway[8]. Cholesterol is then the final product of a series of enzymatic reactions that include the conversion of mevalonate into 3-isopenenyl pyrophosphate, farnesyl pyrophosphate, squalene, lanosterol, and 19 other steps. Surplus cholesterol is then stored intracellularly in an esterified form in lipid droplets. Cholesterol is esterified by the cholesterol acyltransferase 1 (ACAT1) enzyme, in a process that primarily occurs in the endoplasmic reticulum. This storage process is enhanced in cells with excess unesterified cholesterol, due to increased cholesterol transport from the plasma membrane to the endoplasmic reticulum[8,12].

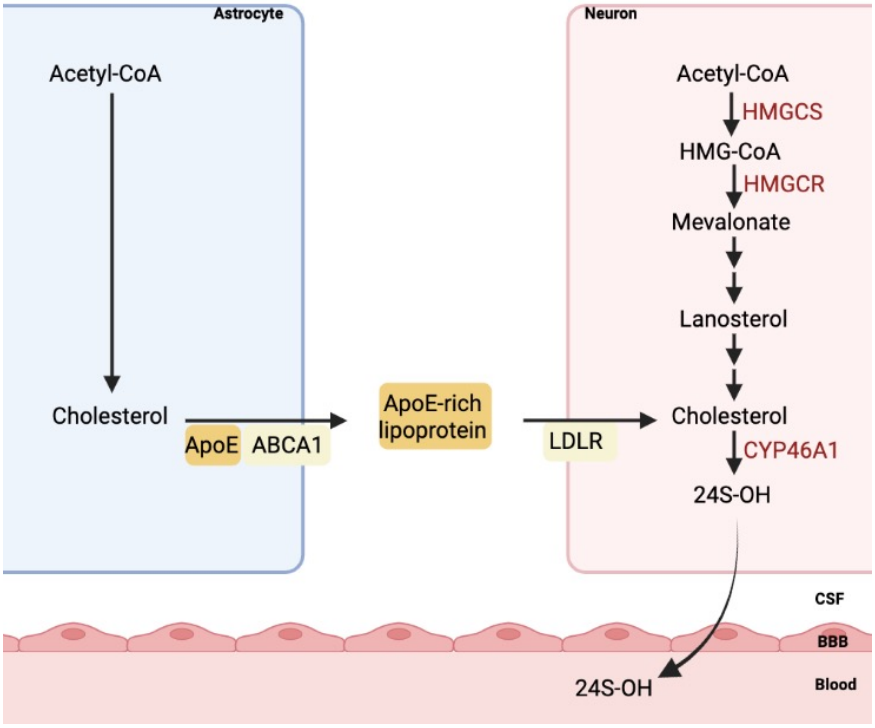

Figure 1 - Brain cholesterol *de novo* synthesis and metabolism. The brain relies its substantial cholesterol needs on *de novo* synthesis. The process begins with the β-Hydroxy β-methylglutaryl-Coenzyme A synthase (HMGCS)-mediated conversion of acetyl-CoA to HMG-CoA, which is then converted into mevalonate by HMG-CoA reductase (HMGCR), consisting of the rate-limiting and irreversible step of the pathway. Cholesterol is the final product of a series of enzymatic reactions. The lipid is also imported from astrocytes, after the secretion of Apolipoprotein E (ApoE)-rich lipoprotein, being its uptake ensured by low-density lipoprotein receptor (LDLR). Neurons handle excess cholesterol and intracellular storage by direct excretion via adenosine triphosphate-binding cassette (ABC) transporters, namely ABC Subfamily A Member 1 (ABCA1), also expressed in astrocytes, through which ApoE-rich lipoprotein is secreted. Two-thirds of the brain-synthetized cholesterol is eliminated through its conversion into 24S-hydroxycholesterol (24S-OH), catalyzed by the neuron-specific cytochrome P450 cholesterol 24-hydroxylase (CYP46A1) protein. 24S-OH is eliminated from the neuronal cells by active transport through ABCA1. 24S-OH can then cross the blood-brain barrier (BBB) by spontaneous diffusion and gain access to the circulation. In plasma, 24S-OH associates with lipoprotein particles to travel to the liver, to be converted into bile acids or excreted into the bile. CSF – cerebrospinal fluid. Adapted from Vance et al., 2012. Figure created in BioRender.com.

Due to the bulk of brain cholesterol having a long half-life, combined with the protection offered by the BBB from the exchange with circulating lipoprotein, specific mechanisms for the removal of excess brain cholesterol are necessary to maintain cholesterol homeostasis[13]. In contrary to every other tissue or organ, knowledge regarding the mechanisms that maintain cholesterol steady-state levels in the brain is still being developed[14]. According to the current knowledge, the synthesis and elimination of cholesterol in the adult brain are compartmentalized, being the astroglial cells responsible for the majority of synthesis, while not relevantly contributing to elimination. The mechanism responsible for the elimination of

two-thirds of the brain-synthetized cholesterol consists of the conversion into 24S-hydroxycholesterol (24S-OH), catalyzed by the neuronal-specific cytochrome P450 cholesterol 24-hydroxylase (CYP46A1)[15–17]. 24S-OH is eliminated from the neuronal cells by active transport through ABC Subfamily A Member 1 (ABCA1), when in the presence of high-density lipoprotein (HDL) as a lipid acceptor, gaining access to the circulation. Although being a more polar sterol, 24S-OH can cross the BBB by spontaneous diffusion[18]. In plasma, 24S-OH associates with lipoprotein particles to travel to the liver, the major site for the turnover of cholesterol, where it is 7α-hydroxylated and can then be converted into bile acids or excreted into the bile as a sulfated and/or glucuronidated metabolite[13,19,20].

Although the mechanism catalyzed by CYP46A1 is the major cholesterol removal pathway, other mechanisms are also recognized, such as a flux of cholesterol in apolipoprotein E (apoE)-containing lipoproteins through cerebrospinal fluid (CSF) into the circulation, a mechanism analogous to reverse cholesterol transport[21]. A CYP46A1-independent pathway for neurons to handle excess cholesterol and intracellular storage is, as previously mentioned, by direct excretion via ABC transporters, namely ABCA1, which, in rodents, has been registered to be expressed in both embryonic and adults' neurons[8,22–24]. Cholesterol is released onto APOA1-containing lipoproteins present in CSF, that can then be removed from the brain through receptors in brain capillary endothelial cells[8,25]. Decreased ABCA1 in neuronal cultures has been shown to reduce the efflux of cholesterol onto apoE whereas increased levels enhanced the release[26]. ApoE is the major transporter of extracellular cholesterol and other lipids and lipidated apoE represents the most frequent form that cholesterol is found in, due to being water insoluble and therefore not frequently detected in an unbound form. ApoE participates in cholesterol homeostasis, mediating a dynamic cholesterol exchange between neuronal and non-neuronal cells in CNS. For that, cholesterol-loaded apoE particles secreted by glial cells bind to lipoprotein receptors in neurons, being taken up by these cells[8,27]. Cholesterol homeostasis in the brain is of crucial importance for normal neuronal function and morphology[28]. As either lack or surplus of cholesterol lead to neuronal impairment, defects in brain cholesterol homeostasis are frequently a pathological feature of neurodegenerative disorders. Neuronal cells regulate their cholesterol content by a number of feedback mechanisms based on sensing their cholesterol levels. One major mechanism involved in the control of cholesterol homeostasis consists in membrane-bound transcription factors, the sterol regulatory element-binding proteins (SREBPs), that regulate the expression of enzymes involved in cholesterol biosynthesis, transport, and metabolism[29]. In case high levels of cholesterol are reached,

CYP46A1 plays a crucial role in re-establishing homeostasis, catalyzing the previously described conversion of cholesterol into 24S-OH.

2. Cholesterol 24-hydroxylase (CYP46A1)

2.1. Characterization of CYP46A1

CYP46A1, as previously mentioned, has a critical role in maintaining brain cholesterol homeostasis, by catalyzing the major cholesterol elimination pathway, its conversion into 24S-OH[15–17].

Regarding the characterization of CYP46A1, from the alignment of the cDNA-deduced sequences of CYP46A1 human and mouse enzymes, it was observed that the proteins contain 500 amino acids and share a degree of sequence identity of 95%, which is considered high when compared to the average 77% identity usually observed in human and mouse P450 orthologs and underlies the potential physiological importance of the enzyme and of cholesterol turnover in the brain[1,30].

The 24-hydroxylases are microsomal members of the cytochrome P450 superfamily, some of the conserved features shared with other microsomal members being a generalized hydrophobicity (with an amino acid content of 46%), a conserved cysteine ligand that binds the heme cofactor and also the ability to hydroxylate a hydrophobic substrate. However, the enzymes are distinguished from other P450s, sharing less than 35% identity, and therefore constitute a subfamily, designated as CYP46. Besides the high sequence identity, 24-hydroxylase genes also differ from other P450s in terms of having a larger number of exons. The isolation of this gene from genomic DNA libraries by hybridization screening and posterior DNA sequencing revealed that the human CYP46A1 encoding gene (*CYP46A1*) contains 15 exons and 14 introns. Regarding its localization, fluorescent *in situ* hybridization and radiation hybrid panel mapping indicated it to be on chromosome 14q32.1.

The 24-hydroxylase genes are selectively expressed in the brain, as previously observed by RNA blotting, *in situ* mRNA hybridization and immunohistochemistry, immunoblotting, and enzyme activity. This is unlike most P450s, as they are usually expressed in tissues active in xenobiotic and endobiotic metabolisms, such as the liver, kidney, and lung. CYP46A1 is expressed in neurons, including pyramidal cells of the cortex and hippocampus, granule cells

of the dentate gyrus and Purkinje cells of the cerebellum. There is not yet any evidence of expression in the peripheral nervous system[30]. The enzyme is expressed since birth, and there is a significant increase in its expression in the brain shortly after birth and, according to ontogeny studies, there is a gradual accumulation in the brain as a function of age. Accordingly, the levels of 24S-OH in circulation increase during the first months of human life[31]. At the age of 1 year, a steady state level of the enzyme is reached, which is maintained during adulthood, as well as 24S-OH levels.

2.2.Roles of CYP46A1 in the Central Nervous System

As previously mentioned, CYP46A1 is the enzyme responsible for initiating the major pathway of cholesterol elimination from the brain into circulation, by catalyzing cholesterol 24S-hydroxylation, and therefore is tremendously important in controlling that organ's cholesterol turnover[30]. Indeed, *Cyp46a1* knock-out mice present a critical reduction of *de novo* cholesterol synthesis, as, in subregions of the brain that express high levels of the enzyme, such as the cortex and hippocampus, rates are decreased by as much as 60%[1].

In addition to catalyzing the conversion of cholesterol into 24S-OH, *in vitro* biochemical studies regarding the enzyme's catalytic activities revealed that CYP46A1 has a broad substrate specificity, as a consequence of a large substrate-binding pocket, and is able to metabolize a number of endogenous and exogenous compounds other than cholesterol, suggesting a role in other metabolic pathways, namely of steroid hormones and drugs[32,33]. Such a diverse role for the enzyme was also suggested by its expression in neurons, rather than the cholesterol-laden support cells or their lipid-rich myelin sheaths[34]. A major finding of those studies was that CYP46A1 is able to catalyze both the formation and further metabolism of the biologically active oxysterol 24S-OH, by sequentially hydroxylating cholesterol. This means that at least part of the 24S-OH originated is released from the active site during catalysis and then, demonstrating that it is even a better substrate than cholesterol, reenters the substrate binding pocket for further processes of hydroxylation, originating 24,25- and 24,27-dihydroxycholesterols. Among the diverse endogenous steroids found to also be hydroxylated by CYP46A1, there is 4β-hydroxycholesterol, 7R-hydroxycholesterol, cholestanol, cortisol, testosterone, and progesterone. Since the brain is a steroidogenic organ, where progesterone

and testosterone are synthesized *de novo* from cholesterol or from blood-born steroidal precursors, the latter two mentioned catalytic activities may be of physiological importance[35].

There is also evidence regarding a biological function for 24S-OH as a ligand for the liver X receptor (LXR), a nuclear hormone receptor that activates the expression of genes involved in lipid metabolism, including several transporters (ABCA1, ABCA2, ABCG1, ABCG4, and ABCG5) and apoE expressing genes, involved in cholesterol transport and homeostasis in the brain[36,37]. The absence of LXR-mediated activity of these genes can lead to a variety of CNS defects upon aging including lipid accumulation, astrocyte proliferation and disorganization of myelin sheaths[38–43]. Recent studies have, however, shown that despite 24S-OH being a highly effective agonist of LXRs *in vitro*, it is not a critical activator of its target genes *in vivo*, either in the brain or in the liver[44,47].

2.3.Correlation of CYP46A1 with cognition

Several aspects of brain function depend on cholesterol turnover, such as axons and dendrites formation during development, neuronal repair and remodeling, new synapses formation, and learning and memory[2,4]. Therefore, recent studies have focused on understanding how CYP46A1 is important for memory and learning. In order to further determine the role of CYP46A1 in brain development, Lund et al. performed studies in mice lacking the *Cyp46a1* gene (*Cyp46a1*$^{-/-}$ mice)[38]. The loss of CYP46A1 led to a slower cholesterol excretion from the brain, accounting for a reduction of 50% and a compensatory similar decrease in cerebral cholesterol *de novo* synthesis, maintaining the steady-state cholesterol levels in the brain of knockout mice, yet with a reduction of cerebral cholesterol turnover and possibly of the production of the biosynthetic intermediate geranylgeraniol, necessary for normal learning and hippocampal plasticity[34]. Geranylgeraniol is synthesized from mevalonate, alongside with cholesterol and other nonsterol isoprenoids through the mevalonate pathway[45]. This suppression of the mevalonate pathway, shown in a study published by Kotti et al., underlies learning and memory defects presented in this mice[45]. As a result, *Cyp46a1*$^{-/-}$ mice show severe deficiencies in spatial, associative, and motor learning as well as in hippocampal long-term potentiation (LTP), having a significantly impaired cognitive performance. That study has shown that cholesterol turnover in the brain via CYP46A1 ensures the activation of the mevalonate pathway and suggests that a constant production of geranylgeraniol in neurons is

essential for LTP and learning. In a posterior study, Kotti et al. further explored the dependence of LTP on geranylgeraniol, showing that this polyisoprenol acts rapidly (within 5 minutes) and is required for both the induction and maintenance of hippocampal LTP[46]. The requirement for geranylgeraniol was observed to be both chemically selective, as related compound farnesol cannot substitute it, and genetically selective for CYP46A deficiency, as hippocampal slices from mice lacking apoE (another animal model of LTP impairment) do not respond to geranylgeraniol. This compound was concluded to act specifically and locally to modulate LTP, as localized delivery of geranylgeraniol to the dendritic trees from hippocampal neurons restored LTP in CYP46A1 knockout slices. Our group also contributed to elucidating the molecular mechanisms activated by CYP46A1 and the increase in geranylgeraniol supply and showed that increased expression of CYP46A1 enhanced prenylation and activation of small GTPases (sGTPases) of the Rho and Rab (Ras-genes from rat brain) family, and that this effect was dependent on the activation of the mevalonate pathway[47]. Moreover, we showed that CYP46A1 triggers an increase in neuronal dendritic outgrowth and dendritic protrusion density and elicits *in vitro* and *in vivo* increase of synaptic proteins in crude synaptosomal fractions. Strikingly, in neurons, these effects were abolished by pharmacological inhibition of geranylgeranyl transferase I (GGTase-I) activity. Furthermore, CYP46A1 expression increased tropomyosin-related kinase (Trk) receptors phosphorylation, its interaction with GGTase-I, and the activity of GGTase-I. This interaction Trk-GGTase-I was shown to be crucial for the enhanced dendritic outgrowth mediated by CYP46A1[48]. Following the related severe deficiencies in *Cyp46a1*$^{-/-}$ mice that indicated CYP46A1 to be important for normal memory formation, along with results of studies that indicated the involvement of CYP46A1 gene polymorphisms in the rate of cognitive deterioration, a study by Maioli et al. tested the hypothesis that increased activity of CYP46A1 improves memory function in old mice[49,50]. The mice model used was homozygotes generated from mice previously described by the group as having a stable CYP46A1 overexpression, which was obtained by using a ubiquitous expression vector[44]. Female homozygous CYP46A1 transgenic mice of an advanced age of 15 months showed an improvement in spatial memory retention in the Morris water maze test, compared to the wild-type controls. Biochemical modifications consistent with this observed improvement were analyzed in hippocampal lysate by western blotting. The results showed an increase in hippocampal levels of N-methyl-D-aspartate (NMDA) receptor subunits NMDAR1 and p-NMDAR2, the hippocampus' primary mediators of excitatory synaptic transmission. CYP46A1 transgenic mice also showed significantly higher levels of Postsynaptic density protein 95 (PSD95), involved in the assembly and function of the postsynaptic density complex.

Presynaptic proteins synaptophysin, a marker for intact synapses, and synapsin-1, which regulates neurotransmitter release, were also increased in the transgenic mice[49]. The enhancement of spatial memory processes may be linked with these increased levels, which suggested a protective effect of CYP46A1 on cognition and synaptic plasticity in normal aging processes.

2.4.Modulation of CYP46A1 in the brain

Evidence that deregulation of cholesterol balance is related to the onset of neurodegenerative disorders has shown a need to further develop the knowledge on the molecular mechanisms that underlie the expression of *CYP46A1*, namely of its transcriptional and allosteric modulation, in order to find possible therapeutics for treatment or prevention of associated disorders[42].

2.4.1. Transcriptional regulation of CYP46A1

Our group has performed an extensive analysis of the human *CYP46A1* promoter, that revealed a GC-rich region that comprises Sp transcription factors binding elements that are indispensable for basal expression of this TATA and CAAT-less promoter[42]. Finding that the CYP46A1 promoter is extremely GC-rich led to another study that suggested that *CYP46A1* might be regulated by epigenetic modifications, such as DNA methylation and histone modifications[51]. The fact that the *CYP46A1* proximal promoter is completely demethylated in tissues where CYP46A1 mRNA cannot be detected, led us to focus on the role of histone modifications. Increased histone acetylation, achieved by histone acetyltransferases (HAT) can cause remodeling of chromatin to a more loosely packed configuration, leading to transcriptional activation, while a decrease in histone acetylation leads to transcriptional silencing. Therefore, our group investigated the effect of histone deacetylase (HDAC) inhibitors on *CYP46A1* expression. The study demonstrated a potent induction of human *CYP46A1* expression by inhibition of HDAC activities with trichostatin A (TSA), anti-epileptic drug valproic acid (VA) and sodium butyrate (NaB). Another study, published by Shafaati et al. revealed that in agreement with the previously mentioned findings, acute TSA treatment was shown to significantly increase mRNA levels of CYP46A1 in the brain and liver of mice, while a chronic treatment did not show effects on these levels in the brain, only a similar increase in the liver.

Treatment with VA also resulted in a modest induction of the mRNA levels of *Cyp46a1* in the liver and in the brain.

Inhibitors of HDACs have been approved for cancer treatment, having an apoptotic effect on proliferative cells. These compounds have also been shown to have a protective role in post-mitotic neurons, emerging as a therapeutic option for the treatment of neurodegenerative disorders, such as AD where it provides protection against Amyloid β-induced neuronal damage[52]. CYP46A1 was shown by Ohyama et al. to be resistant towards a broad spectrum of factors expected to regulate it at the transcriptional level, such as statins, cholesterol, or oxysterols[11]. Also, steroid hormones, insulin, growth hormone, thyroid hormone, cAMP, or bile acids failed to show transcriptional regulation of CYP46A1. This observed low need for transcriptional control of the major brain cholesterol elimination pathway was understood to be consequent to the effectiveness of the BBB in blocking the entrance of extracerebral cholesterol. However, oxidative stress was discovered to be an influencing factor, as the promoter was found to be rich in putative binding sites for oxidative stress-inducible transcription factor Sp1[53]. Sp1, suggested as responsible for the enzyme's basal expression, as a positive as well as negative regulator of transcription rate, functions to promote neuronal survival, being involved in the expression of a large number of genes, including housekeeping genes[54].

2.4.2. Modulation of CYP46A1 activity

The substrate-bound and ligand-free crystal structures of human CYP46A1, published by Mast et al., revealed specific interactions with the high-affinity substrate cholesterol sulfate (CH-3S). The conformational flexibility of CYP46A1 demonstrated in these structural studies suggested that, besides the mentioned cholesterol, it is able to bind compounds other than sterols, including possible stimulators and inhibitors, indicating that the enzyme's activity is possible to modulate by therapeutic agents. This finding led to a search for inhibitory properties of marketed drugs and non-pharmaceuticals. The CNS active imidazole-containing drugs clobenpropit (H3-receptor antagonist), tranylcypromine, and thioperamide (H3/H4 receptor antagonist) showed a significant inhibitory effect on CYP46A1. The known P450 activators quinine, quinidine, lansoprazole, and dapsone were shown to (modestly) inhibit CYP46A1 activity. A drug that was proven, in other studies, to be an efficient inhibitor of brain CYP46A1

was the antifungal drug voriconazole, which binds with high affinity to CYP46A1. The activity inhibition was demonstrated *in vitro* and also *in vivo* through intraperitoneal injections of the drug in mice, given that voriconazole was found to be able to cross the BBB and therefore very high levels of the drug were measured in the brain[56]. Mast et al. also contributed to the search for CYP46A1 inhibitors among therapeutic agents, identifying the antidepressant fluvoxamine as a strong one[57].

The initially conformational study by Mast et al. also demonstrated the CYP46A1-activating action (although in a modest way) of phenacetin and acetaminophen, which induced an activity increase of >30%, as well as of the phenacetin analog 4'-(2-hydroxyethoxy)-acetanilide, which caused an increase by 45%[55]. Although the observed activation was probably not enough to significantly affect cholesterol turnover *in vivo*, it still had relevance due to proving that, in theory, CYP46A1 stimulation is possible. In a posterior study, Mast et al. confirmed that, as the pharmaceuticals efavirenz (EFV), acetaminophen, mirtazapine, and galantine increased the enzyme's activity *in vitro*. Also, the anti-human immunodeficiency virus drug depending on the concentration range, could stimulate cerebral cholesterol turnover, confirming an *in vivo* CYP46A1 stimulation, and also had the ability to inhibit CYP46A1 activity when more concentrated[58].

3. Niemann-Pick type C disease

Niemann-Pick Disease, type C (NPC) is a rare neurodegenerative disorder that affects the viscera and CNS[59] caused by reduced function of NPC1 protein[60], being inherited in an autosomal recessive manner. To date, there are no Food and Drug Administration-approved therapies, however, miglustat (Zavesca®), an imino sugar that blocks glycosphingolipid synthesis and slows the neurological progression in both NPC animal models and human patients, has been approved by the European Medicines Agency[61,62]. Also, some drug trials have recently been implemented, in which 2-hydroxypropyl-β-cyclodextrin (VTS-270) has shown to be promising as a potential therapy to decrease neurological progression[63]**.** Regardless, therapeutic approaches are still limited, reinforcing a critical need for the development of knowledge regarding this pathology.

Mutations of the NPC1-encoding gene (*NPC1*) account for approximately 95% of the NPC cases, only 5% being due to pathogenic variants or defects in *NPC2*[64]. *NPC1* encodes for a polytopic, highly glycosylated transmembrane protein that localizes to the limiting membrane of the late endosome/lysosome (LE/L)[59,65], and *NPC2* for a soluble lysosomal protein. These proteins are jointly responsible for the egress and recycling of lipoprotein-derived cholesterol from LE/L towards other cell compartments, such as the endoplasmic reticulum (ER) or plasma membrane[66]. Therefore, decreased function of these proteins leads to endolysosomal dysfunction due to the accumulation of unesterified cholesterol and other lipids, such as glycosphingolipids, sphingomyelin, and sphingosine, leading to the impairment of mobilization and re-esterification of LDL cholesterol[67] (Figure 2).

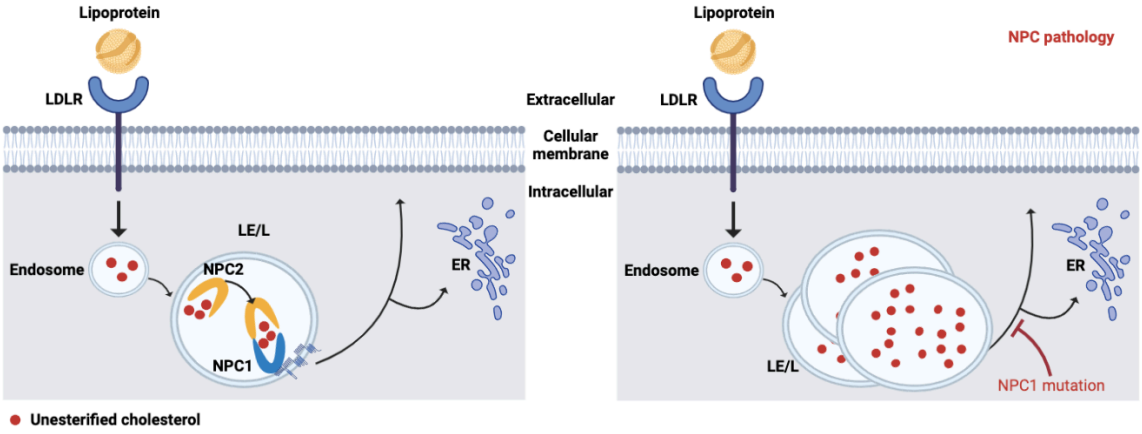

Figure 2 - Late endosome/lysosome (LE/L) unesterified cholesterol export impairment in NPC. NPC1, a transmembrane protein that localizes to the limiting membrane of the LE/L, and NPC2, a soluble lysosomal protein, are jointly responsible for the egress and recycling of lipoprotein-derived cholesterol from the late endosome/lysosome (LE/L) towards other cell compartments, such as the endoplasmic reticulum (ER) or plasma membrane. The NPC disease is characterized by decreased function of these proteins, leading to endolysosomal dysfunction due to the accumulation of unesterified cholesterol and other lipids, such as glycosphingolipids, sphingomyelin, and sphingosine, there being impairment of mobilization and re-esterification of LDL cholesterol. LDLR - Low-Density Lipoprotein Receptor. Adapted from Pacheco et al. and Vance et al., 2012. Figure created in BioRender.com.

Clinically, NPC is characterized by diverse symptoms affecting the brain, liver, spleen, and motor control. Early-onset NPC manifests a variety of symptoms that precede neurological involvement, including infantile jaundice, hepatosplenomegaly, or isolated splenomegaly. In most cases, NPC manifests during childhood or early adolescence[68], and patients present a progressive impairment of motor and intellectual function and usually die within the first two decades of life[64], although the phenotypic spectrum also includes a more indolent adult-onset

disorder. Despite this wide range of age of onset and variability of symptoms among patients, NPC is typically characterized by progressive supranuclear saccade and gaze palsy, gelastic cataplexy, epileptic seizures, cerebellar ataxia, and cognitive impairment[69], due to progressive neurodegeneration, leading to premature death[66]. Furthermore, psychiatric symptoms comprise bipolar disorder, schizophrenia-like psychosis, or major depression.

Among the mentioned broad array of neurovisceral pathological changes, cerebellar ataxia is a cardinal symptom of NPC, resulting from the progressive loss of cerebellar Purkinje neurons. These are large inhibitory GABAergic neurons that function to integrate cerebellar neuronal input and provide an output of the cerebellum via axons that project to the deep cerebellar nuclei. The cerebellum accounts for more than half of the total neurons in the CNS, coordinating motor control and coordination, and has also been suggested to play a role in cognition[60]. The molecular mechanism responsible for neuronal death in NPC is still not fully understood, although it has been proposed before to be induced by phagocytosis during neuroinflammation and it is also possible that Purkinje cell death by necroptosis promotes and amplifies neuroinflammation[70]. It has been proposed that the accumulation of lipids, particularly sphingosine, can induce an imbalance in calcium homeostasis and affect lysosomal trafficking, subsequently leading to autophagy defects, another feature of NPC disorder[66,71]. Additionally, lipid accumulation within lysosomes and mitochondrial membranes may induce oxidative stress, another potentially pathological mechanism in NPC[72].

Restoring NPC1 function in the cerebellum has been shown to prevent neurodegeneration and premature lethality in a mouse model of the disease[73] but it does not fully rescue the phenotype and still results in lethality, suggesting that the NPC1 protein is functionally important in other brain cells as well[66]. Besides neurons, supporting glial cells are also present in the cerebellum, including astrocytes, ependymal cells, and oligodendrocytes, as well as vascular-associated cells, and myeloid, comprising microglia and monocytes/macrophages. Being ubiquitously expressed throughout the brain[74], *NPC1* has a particularly high expression in oligodendrocytes and microglia. Accordingly, it was shown that NPC1 function is crucial for the correct maturation of oligodendrocyte progenitor cells and maintenance of the existing myelin. Therefore, although Purkinje neuron loss has been reported to be cell autonomous, histopathological changes are observed in astrocytes and oligodendrocytes, along with microglial activation, which is a predominant aspect and likely contributor to NPC neuropathology[60,75].

3.1.Neuroinflammation in NPC

Neuroinflammation is a common feature in NPC, being found in most CNS-affecting disorders. The progressive CNS degeneration that takes place in NPC is one of the most relevant clinical problems, as it contributes to the onset of disease hallmarks such as seizures, progressive dementia, and an apathetic state, leading to death[76]**.** The first line of defense of the CNS consists of the innate immune system of microglia, astrocytes, and perivascular macrophages[77,78]. During the inflammatory process, microglia and astrocytes switch to an activated state, resulting in morphological changes characterized by specific identifiable inflammation markers.

Microglia activation (microgliosis) is the first evidence of neuroinflammation in $Npc1^{-/-}$ mouse models, occurring at an approximate age of 2 weeks, and begins the neurodegenerative cascade, with subsequent marked activation of astrocytes at around 4 weeks post birth, beneath the Purkinje neuron layer corresponding to the sites of early apoptosis in NPC disease[79,80]. Microgliosis is an immunological hallmark of several neurodegenerative diseases such as amyotrophic lateral sclerosis (ALS), Alzheimer's disease (AD), and Parkinson's disease (PD)[68]. This way, despite being the primary innate immune cells of the CNS and regulating brain homeostasis by controlling myelination and synaptogenesis[81], microglia also actively contribute to the pathophysiology of neurodegenerative disorders[66].

Brain microglia are typically in an immunosurveillance state but become activated in the context of injury or disease[82]. The activated state allows aiding in clearing cellular debris or innate immunity functions and is dependent on the local microenvironment, which differs between different pathologies[83]. Therefore, the microglial phenotype is disease-dependent and is mostly regulated by pathogens, hormones, neurotransmitters, and other molecules released by surrounding cells, including neurons, microglial cells, and astrocytes. In the past, microglial phenotypes were characterized according to the presence of particular cell surface molecules and expression of specific sets of cytokines, being strictly classified as either M1-like, exhibiting pro-inflammatory signaling and neurotoxicity, or M2-like, being more directed to the resolution of inflammation[84]. However, more recently, it has become clear that this simplistic view of microglial phenotypes does not respond to the phenotype variety found in the brain[83] and has therefore been redefined in both mice and humans as newly developed technologies emerged, including RNA-sequencing, quantitative proteomics, and epigenetic studies. This allowed for the identification of a broad array of activation profiles and

phenotypes, especially in relation to neurodegenerative diseases. A unique transcriptional signature has also been described for homeostatic microglia in adult mice, including expression of P2Y purinoceptor 12 (*P2ry12*), transmembrane protein 119 (*Tmem119*), sialic acid binding Ig-like lectin H (*Siglech*), G protein-coupled receptor 34 (*Gpr34*), suppressor of cytokine signaling 3 (*Socs3*), β-hexosaminidase subunit β (*Hexb*), olfactomedin-like protein 3 (*Olfml3*) and Fc receptor-like S, scavenger receptor (*Fcrls*)[82]. This homeostatic molecular signature and functions, such as roles in synaptic plasticity, are lost during the course of disease states, as well as aging, and microglia acquire different phenotypes and activate specific transcriptional programs that result in both protective and disease-associated microglia (DAM). The DAM signature that has been identified for diseases such as ALS, AD and multiple sclerosis includes the upregulation of *Axl*, *ApoE*, *Clec7a*, *Itgax*, *Lgals3* and *Cst7*, first identified in Amyloid β plaque-associated microglia but then observed by several groups to be a common neurodegenerative-associated signature, although being highly dynamic, even during the course of each disease progression[85,86].

As a massive microgliosis has been reported in several studies of NPC, specific inflammatory markers have also been identified in the tissue of *Npc1* mutant mice as well as NPC human tissue[68] (Figure 3). The microglial activation in NPC results in a classic progressive morphological change from a ramified appearance to a rounded amoeboid one and is especially characterized in NPC by positive staining for Cluster of Differentiation 68 (CD68), in both the cerebellum and frontal cortex[79]. Also, a less conventional polarization was demonstrated by Cougnoux et al., with decreased expression of lineage markers CD11b and C-X_3-C motif chemokine receptor 1 (CX_3CR1) and unaffected expression of activation markers: major histocompatibility complex class II (MHCII), F4/80, CD86 [68]. In both NPC patients and Npc1$^{-/-}$ mouse model[87], there is a notable upregulation of several inflammatory markers, but most notably of the complement protein C3 and C-C motif chemokine ligand 3 (CCL3)[68,79]. Other inflammatory markers have also been identified in NPC, including upregulation of interleukin-1β (IL-1β), tumor necrosis factor α (TNFα), and insulin growth factor-1 (IGF1), as well as down-regulation of transforming growth factor β (TGFβ) in NPC mice models' brain tissue[68,79]. However, regarding classical markers of inflammation IL-6, IL-8, and monocyte chemoattractant protein-1 (MCP1/CCL2), Cologna et al. found the levels in cerebrospinal fluid

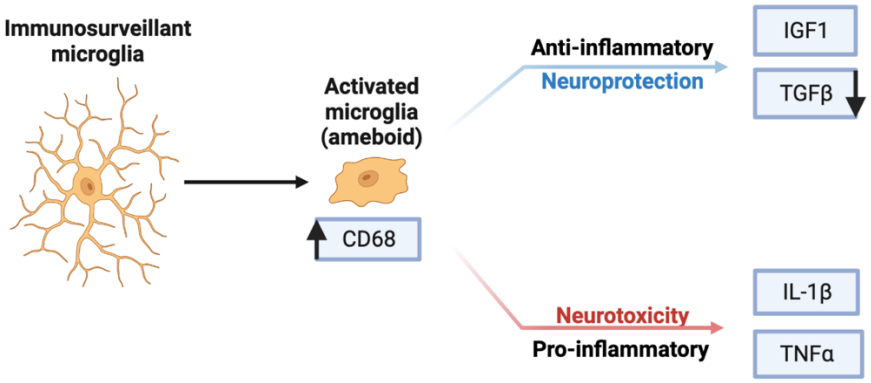

Figure 3 - Microglia activation in NPC. Brain microglia are typically in an immunosurveillance state but become activated in the context of injury or disease, losing the homeostatic molecular signature and functions, and acquiring different phenotypes by activation of specific transcriptional programs that result in both protective and disease-associated microglia (DAM). The activated state is dependent on the local microenvironment, which differs between different pathologies. The microglial activation in Niemann-Pick Type C (NPC) disease results in a classic progressive morphological change from a ramified appearance to a rounded amoeboid one and is especially characterized by positive staining for Cluster of Differentiation 68 (CD68). The role of microglia activation in NPC has yet to be determined, particularly whether it plays a causative role in the pathology, or if it is resultant of the initial trafficking defects. In fact, mixed expression of both neurotoxic (cytokines interleukin-1β (*Il-1β*) and Tumor Necrosis Factor α (*Tnfα*)) as well as neuroprotective genes (Insulin Growth Factor-1 (*Igf1*) and down-regulation of transforming growth factor β (TGFβ)) has been registered, suggesting that the active microglia profile may be both beneficial and detrimental for the pathology progression, although not having yet been extensively described. Figure created in BioRender.com.

of patients and controls to be comparable, suggesting that in NPC the neuroinflammation process might be different from other diseases. Microglial activation has been hypothesized to be trigged by neuroinflammation activating signals, such as neuronal cell death, rather than by the accumulation of unesterified cholesterol. This was based on the morphological changes and altered expression of markers only becoming apparent in the Npc1$^{-/-}$ mice model weeks after significant unesterified cholesterol storage being already present[80].

The role of microglial activation in chronic neurodegeneration can be beneficial, harmful, or non-significant[88] and in the case of disease progression of NPC, the role has yet to be determined, particularly whether it is a primary pathological process and plays a causative role in the pathology, or if it results from the initial trafficking defects. In fact, mixed expression of both neurotoxic as well as neuroprotective genes has been observed, suggesting that the active microglia profile may be both beneficial and detrimental for the pathology progression[68]. However, the potentially damaging cytokines released by microglia suggest it plays a more critical role in NPC[80]. Indeed, genetic inhibition of microglia activation in *Irf8* mutant Npc1$^{-/-}$

mice has led Cougnoux et al. to suggest a direct role of microglia in NPC disease progression (that is amendable to therapeutic intervention), as it resulted in a delay of the Purkinje neurons loss and onset of neurological signs, increasing lifespan[68]. The mechanism through which the activated microglia in NPC could be contributing to the degeneration of Purkinje cells was suggested to be phagocytosis of stressed or damaged cells, based on the increased levels of CSF sCD22, normally expressed by neurons to inhibit microglial proinflammatory cytokine production and, therefore, microglial activation[68,89].

As previously mentioned, microglial activation precedes neuronal degeneration, beginning the neurodegenerative cascade in NPC and leading to the activation of astrocytes, also denominated by astrocytosis. Astrocytes have a crucial role in maintaining CNS homeostasis, by supporting neuronal function. An increased number of reactive astrocytes have been described in commonly used NPC mouse models, especially in the thalamus and cerebellum[90,91]. Once active, a morphological change of astrocytes occurs, as NPC1 astrocytes have been reported to swell in size and display inclusions consisting of myelin figures of concentric membranous lamellae, along with the presence of ubiquitin-positive substances, similar to what happens in neurons and macrophages[76,92].

By mapping the expression of NPC1 in the brain, Patel et al. indicated that the protein is predominantly present in astrocytes, being involved in astrocytic processes associated with synapses[93]. Also, a study by Vance et al. suggested that neuronal processes require cholesterol delivery from endogenous sources such as astrocytes, as axons possess the ability to synthesize phospholipids and sphingomyelin, but not cholesterol, while astrocytes are the major site of cholesterol synthesis in the brain, secreting it through the ABCA1 transporter to make HDL-like particles[94–96]. However, the cholesterol-binding protein apolipoprotein D is markedly reduced in NPC astrocytes[97]. This, taken together with terminal fields of axons and dendrites being the earliest site of degeneration in NPC, even before degeneration of neuronal cell bodies takes place, suggests that a great contributor to the pathologic neuronal degeneration would be the disruption of NPC1-mediated vesicular trafficking in astrocytes. Baudry et al. considered it conceivable that astrocytic impairment, resulting from the loss of NPC1 protein function, leads to the release of toxic cytokines and consequent abnormal phagocytosis, causing terminal and neuronal degeneration[80]. Also, as astrocyte swelling has been found to cause a release of glutamate from the astrocyte[98], which can activate NMDA receptors on neurons, inducing apoptotic cell death, and as neuronal loss in $Npc1^{-/-}$ mice has been concluded in previous studies

to be due to apoptosis[99], this evidence also favors active astrocytes to be able to cause neurodegeneration in NPC[90]. Indeed, more recently, Zhang et al. found that glial fibrillary acidic protein (GFAP, astrocyte marker) promoter-driven replacement of expression of wild-type NPC1 protein in astrocytes of $Npc1^{-/-}$ mice profoundly ameliorates degeneration and lipid accumulation in neurons, confirming an implication of astrocytes in the pathogenesis of the neurodegeneration, even though it appeared to not be sufficient in preventing Purkinje cell loss[96].

Even though neuroinflammation is a common feature of neurodegenerative diseases, the contribution of immune cells to NPC pathogenesis and progression is not yet clear[68]. While the drastic morphological changes observed in neurons and microglia have been taken more into consideration when studying both human and animal models, astrocyte alterations are also determinant for NPC pathologic process, which requires further studies[76]. Overall, understanding the role of neuroinflammation and identifying biomarkers associated with this aspect of NPC pathology is necessary for the development and transition of potential therapies to NPC patients, as results point to anti-inflammatory therapy as a useful delay of pathological manifestations.

3.2.Impaired autophagy in NPC

Autophagy is a process through which portions of cytoplasm are delivered to lysosomes, for degradation and recycling. This allows cells to dispose not only of aberrant protein aggregates but also of other macromolecules (such as glycogens, lipids, and nucleotides), damaged organelles (including mitochondria, peroxisomes, and endoplasmic reticulum), as well as of entire pathogenic invading organisms such as viruses or bacteria[100–102].

Among the three known subtypes of autophagy, macroautophagy, characterized by the delivery of cytosolic contents to the lysosomes by autophagosomes, is the major pathway and will therefore hereafter be referred to as autophagy[103]. The other subtypes are microautophagy and chaperone-mediated autophagy, the first characterized by an inward invagination of the LE/L membrane and the latter by direct translocation across the lysosomal membrane upon binding to the lysosomal-associated membrane protein 2A (LAMP2A)[104,105].

The autophagic process is essential for cellular homeostasis as, along with the ubiquitin-proteasome system, these are the two main systems for the degradation of eukaryotic cells' intracellular components, autophagy being the less selective system. During its course, this process is comprised of the formation of autophagosomes, large double-membrane vesicles that sequester the components targeted for destruction. The autophagosomes then fuse with late endosomes, resulting in amphisomes that, through fusion with lysosomes, membrane-bound organelles, form autophagolysosomes, exposing cargo to the lysosomal degradation machinery[106,107].

The selection of the components in autophagy was initially thought to be a nonselective process, as immature autophagosomes (phagophores) were thought to engulf surrounding cytoplasm and cargo. However, the discovery of several adaptor proteins - including p62 (or sequestosome 1 (SQSTM1)), NBR1, Nix, NDP52 (or calcium binding and coiled-coil domain 2), Alfy/WDFY3 (or autophagy linked FYVE) and optineurin (OPTN) - that target specific cargo for autophagic clearance, suggested that the process can also be selective, depending on the inducing factor being an intracellular component or extracellular stimuli, such as nutrients or cytokines[108–110]. Once the selected autophagic cargo is delivered to the lysosome, it can be degraded and released into the cytoplasm for metabolization or reutilization in synthesizing new macromolecules. However, an alternative mechanism to the conventional autophagy flux has also been proposed, as lysosomal exocytosis can also take place[107]. Following activation of the P2X7 receptor, lysosomes or autolysosomes translocate to the plasma membrane, fusing with the plasma membrane subsequent to triggering of SNARE (soluble N-ethylmaleimide-sensitive factor attachment protein receptor) proteins, and releasing into the extracellular space contents such as intracellular microorganisms or cytosolic proteins, including pro-inflammatory cytokines and amyloidogenic proteins[111]. In fact, although the lysosomes are frequently located in the perinuclear area of the cell soma, these vesicles are in a continuous and dynamic transport process, as the membrane contains diverse machinery, channels, and transporters that allow trafficking and fusion. This includes SNARE proteins and RAB GTPases, as RAB5 and RAB7 are involved in tethering and docking of endolysosomal membranes[107,112,113].

A group of autophagy-related genes (*ATG*) have been identified as necessary for autophagy and related processes, allowing a better understanding of the process. Among the proteins encoded by *ATG*, microtubule-associated protein 1 light chain 3 (LC3), a mammalian orthologue of yeast Atg8, is the only localized to all types of autophagic membranes, including both the immature

and processed autophagosome, as well as the autolysosome[114–116]. After synthesis, the nascent form of LC3 (proLC3), is modified via a ubiquitynation-like system by cysteine proteases of the Atg4-family, through a reaction where the carboxyl terminal region of LC3 is cleaved, generating a cytosolic form, LC3-I, and exposing a carboxyl terminal glycine, essential for further reactions[114,115,117,118]. During the course of autophagy, LC3-I is modified to a membrane-bound form, LC3-II, by conjugation to phosphatidylethanolamine, a process mediated by an activating and a conjugating enzyme, Atg7 and Atg3 respectively, and also facilitated by the Atg12-Atg5 conjugate and Atg16L1[114,119,120]. LC3-II is then engulfed by the autophagosome and, embedded in the autophagosomal membrane, acting as an adaptor protein that binds cargo. LC3-II is then degraded when the fusion of the autophagosome occurs[115,117]. Thus, the conversion of LC3-I to LC3-II and subsequent lysosomal degradation of LC3-II are often used to monitor autophagy progress. Another widely used autophagy marker is protein receptor p62, which binds directly to LC3 and GABARAP family proteins – other Atg8 orthologues that, as well as LC3, are crucial for the growth and closure of the autophagosome. As p62 is degraded by autophagy, the autophagic flux can be assessed by a decrease of its levels when autophagy is induced, while inhibition of the process translates into an accumulation of p62. As p62, many of the previously mentioned adaptors have their avidity of binding to cargo increased due to containing ubiquitin- and LC3-interacting regions, often undergoing oligomerization[107].

Identifying the highly conserved *ATG* genes has provided a better understanding of the diverse autophagy roles. It has revealed the evolutionarily conserved role of autophagy in adaptation to starvation, as the process can be induced by starvation as a mechanism of amino acids (and, overall, energy) production within cells. Indeed, a severe insufficiency of nutrients and energy is present in mice deficient for essential components of autophagosome formation Atg5 and Atg7[121–123]. Starvation-induced autophagy is, for many organisms, the primary process of this pathway, however, it also is of physiological relevance for intracellular clearance even under basal, non-stressful conditions. The physiological roles this process seems to take part in include regulation of mammalian embryonic development, both on oocyte-to-embryo and embryo-to-neonate transitions[104]. Roles are also related to the differentiation and plasticity of cells such as erythrocytes, presumably through mitochondrial clearance, lymphocytes, and adipocytes, as a housekeeping function becomes of great importance in terminally differentiated or senescent cells. Autophagy is suggested to have a critical homeostatic role in post-mitotic differentiated cells, as tissue-specific knock-out of *ATG* genes, and consequent inhibition of autophagy, in the brain or liver of mice leads to degeneration and dysfunction of

the affected organs, even in the absence of a disease-associated mutant protein[124]. Quiescent cells such as neurons, are where this function gains particular importance, as impairment of protein quality-control and normal turnover of cytoplasmic contents has been observed in several neurodegenerative disease models *in vitro* and *in vivo*[125–128] to exacerbate the accumulation of inclusion aggregates that are ubiquitin- and autophagy substrate p62-positive[104,129]. This suggests that a basal autophagy-mediated clearance of diffuse cytosolic proteins is necessary to prevent abnormal protein accumulation and consequent disease-related phenotypes in neurodegenerative diseases[124].

Another function of autophagy is the regulation of lipid metabolism, including cholesterol. This has been identified by Singh et al. in a study that showed that inhibiting autophagy in mice hepatocytes led to an increase in triglyceride storage in lipid droplets *in vivo* and *in vitro*, due to a decrease in triglyceride breakdown[130]. Also, during nutrient deprivation, triglycerides and lipid droplets' structural proteins co-localized with autophagic components and LC3 associated with lipid droplets. This study also showed a reverse interconnection, as autophagy was impaired when an abnormal increase in intracellular lipids took place in hepatocytes. The authors suggest that, combined, this interrelationship can lead hepatocytes into a cycle where a decreased autophagy, due to either aging or disease, promotes lipid accumulation that can then further suppress autophagic function, further increasing lipid retention.

Along with other neurodegenerative disorders, where it contributes to misfolded protein accumulation and cellular toxicity, as well as in certain liver diseases, autophagy dysfunction has also been implicated in NPC disease, characterized by both neurodegeneration and liver dysfunction. Defects of autophagy have been described as involved in NPC pathogenesis since Liao et al. provided the first evidence of cholesterol accumulation leading to alteration of autophagy-lysosome function and promoting neurodegeneration in NPC disease[131]. This conclusion was based on the regions of $Npc1^{-/-}$ postnatal mice brains most affected by early-onset neurodegeneration presenting changes in lysosomal function, indicated by factors such as deregulation of lysosomal cathepsins B and D, responsible for driving proteolytic degradation within the lysosome and critical for maintaining lysosomal-dependent protein homeostasis in the brain[132,133]. Purkinje cell death was also suggested to result from an abnormal autophagy-lysosome system, as these cells showed autophagosome aggregation with cholesterol clusters. Since then, several studies have reported autophagic dysfunction as an error in the maturation of autophagosomes, as they fail to fuse with lysosomes[134,135].

However, how alterations in cholesterol homeostasis in lipid-storage disorders might perturb autophagy has still to be completely understood. Sarkar et al. have suggested that the NPC1 protein functions at a critical junction of autophagy and endocytosis, regulating amphisome formation[136]. The loss of function of this protein in NPC disease impairs autophagy-specific traffic – exhibited by increased LC3-II levels –, by impairing autophagosome maturation, that then fail to fuse with late endosomes, compromising amphisome formation, as shown by a decrease in colocalization of LC3- and Rab7-positive vesicles (Figure 4). This late block in the autophagy pathway is associated with an accumulation of LC3-positive autophagosomes and autophagy substrates including p62 and mitochondria. By showing that LC3-II accumulation is caused by impaired degradation of autophagosomes, this data contradicts previous reports that have attributed the increase in the steady-state number of autophagosomes in NPC models to autophagy being in an activated status, and therefore translating into an increased autophagosome synthesis[135,137,138]. In fact, the impaired fusion originating the autophagic block is due to the very characteristic cholesterol accumulation in the LE/L compartments, which restrains late endosomes from recruiting SNARE machinery components, such as those that regulate the fusion process, VAMP8 and VAMP3[136]. The study has concluded that upregulation of autophagy overcomes the block and restores the clearance of autophagic cargo in NPC1 mutant cells, by facilitating autophagosome maturation in an amphisome formation-independent manner. Also, an increase in the expression of NPC1 protein was able to rescue the autophagy impairment.

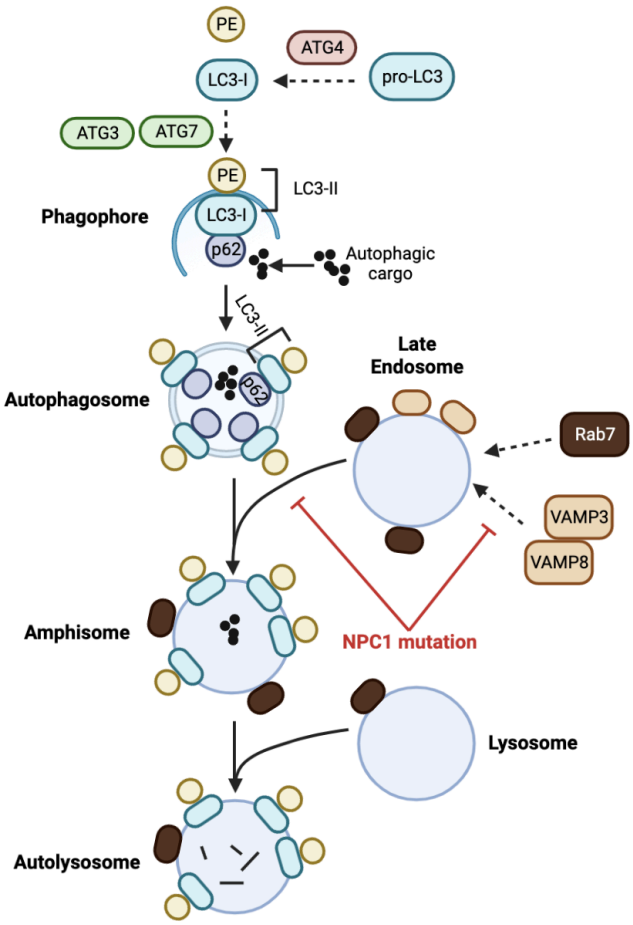

Figure 4 - Autophagy dysfunction in NPC. The NPC1 protein has been suggested to function at a critical junction of autophagy and endocytosis, regulating amphisome formation. The loss of function of this protein in NPC disease impairs autophagy-specific traffic, by impairing autophagosome maturation, which then fail to fuse with late endosomes, compromising amphisome formation – accompanied by a decrease in colocalization of LC3- and Rab7-positive vesicles. The impaired fusion originating the autophagic block is due to the cholesterol accumulation in the late endosome/lysosome compartments, which restrains late endosomes from recruiting SNARE machinery components, such as those that regulate the fusion process, VAMP8 and VAMP3. This block late in the autophagy pathway is associated with the accumulation of the membrane-bound form of microtubule-associated protein 1 light chain 3 (LC3-II). LC3-II originates during the course of autophagy, from the modification of LC3-I (originated from the nascent form of LC3 (pro-LC3) via modification by cysteine proteases of the Atg4 family), by conjugation to phosphatidylethanolamine (PE), mediated by an activating and a conjugating enzyme, Atg7 and Atg3 respectively. Embedded in the autophagosomal membrane, LC3-II acts as an adaptor protein that binds cargo, being then degraded when the fusion of the autophagosome occurs and therefore accumulating subsequent to the autophagy block in NPC. Another widely used autophagy marker is the protein receptor p62, which binds directly to LC3. As p62 is degraded by autophagy, inhibition of the process translates into an accumulation. Adapted from Sarkar et al.. Figure created in BioRender.com.

Autophagosome accumulation in NPC was also described by Roney et al. with a focus on the neuronal axons, where it contributes to axonal dystrophy[139], a pathological feature of early-onset and neurodegeneration promoter, that consists of bulbous swellings containing accumulated organelles[140,141]. Degradation of autophagic cargo is dependent on lysosome

interaction and, therefore, on lysosomal bidirectional movement along microtubules throughout the cytoplasm[142]. Defects in lysosome trafficking, positioning and function are, however, particularly prone to occur in neurons, as they are especially sensitive to cholesterol accumulation in lysosomal membranes, impairing lysosome transport into axons due to disrupting the assembly of the transport complex on NPC lysosomes – a complex formed by the linkage of lysosomes to microtubule-based kinesin-1 motors through its effector SKIP[143]. This leads to impairment of autophagy-lysosomal clearance and resultant autophagosome accumulation in dystrophic axons.

4. Role of CYP46A1 in the pathophysiology of NPC

As previously mentioned, the CYP46A1 protein has been demonstrated to be able to restore cholesterol homeostasis and have a protective effect on cognition and synaptic plasticity in normal aging. Furthermore, increasing evidence suggests that CYP46A1 has a role in the pathogenesis and progression of neurodegenerative disorders and that increasing its levels in the brain is neuroprotective. Indeed, increased expression of CYP46A1 *in vivo* has been shown by Natalie Cartier and colleagues to contribute to the amelioration of the pathologic features in the brain of mice models of amyloidogenesis in AD APP23, APP/PS and 5XFAD, as it was able to decrease Amyloid β peptide production and deposits, as well as diminishing microgliosis and astrogliosis[144,145]. The group also concluded that increasing the levels of CYP46A1 by stereotaxic injection of adeno-associated virus encoding for CYP46A1 prevented neuronal dysfunction and restored cholesterol homeostasis in a Huntington's Disease knock-in mice model[146], even though the mechanisms underlying the neuroprotection offered by CYP46A1 in neurodegenerative disorders remained to be fully understood[147].

The most striking feature of NPC disease is the impairment of cholesterol homeostasis, as the loss of function of the NPC1 protein gives rise to impaired egress of unesterified cholesterol from LE/L, with subsequent accumulation. Another aspect that contributes to the cholesterol homeostasis dysregulation in NPC is a decrease in the expression of CYP46A1, indicated by a decrease in 24S-OH levels in NPC murine and human plasma[148]. Previous studies from our group hypothesized that increasing the expression of CYP46A1 would be beneficial in NPC. Indeed, adenoviral-mediated CYP46A1 expression in fibroblasts of NPC patients carrying the I1061T mutation led to a remarkable amelioration of the pathological phenotype (Moutinho, 2016). This therapeutic effect included a robust decrease in cholesterol accumulation in LE/L,

as well as a partial normalization of the expression levels of genes involved in cholesterol uptake, synthesis and efflux, that had been reported as dysregulated in NPC fibroblasts[149].

Relevant roles for CYP46A1 have also been highlighted by other studies in several NPC mice models, including the NPC1^{nmf164} mice, which, upon activation of CYP46A1 with efavirenz, registered normalization of synaptic transmission, restoration of LTP, improved performance in behavioral tests such as the object placement recognition test, the Y maze test, and fear conditioning tests, as well as of motor abilities in the rotarod test. The lysosomal phenotype in the hippocampus of the mice model was also recovered, as lysosomal cholesterol accumulation was significantly reduced, overall extending the animal lifespan [150,151].

Increased expression of CYP46A1 has been shown in diverse studies to reverse NPC anomalies, however, further observing this action in diverse NPC models and understanding the involved mechanisms is still necessary.

Objectives

The NPC disease is mainly characterized by cholesterol accumulation in the LE/L, leading to autophagy flux impairment and neuroinflammation, which is first evidenced by microglia activation that begins a neurodegenerative cascade, leading to astrocytosis. Being CYP46A1 responsible for the major brain cholesterol elimination pathway, previous *in vitro* studies from our group suggested that ectopic expression of CYP46A1 in NPC cellular models leads to a remarkable amelioration of the pathological phenotype of intracellular cholesterol accumulation (Moutinho et al., unpublished results). This conclusion was widened in further studies, which suggested CYP46A1 *in vivo* delivery improved cholesterol homeostasis and neuroinflammation in the $Npc1^{tm(I1061T)}$ mice model.

Therefore, the goal of the present work was to further evaluate how CYP46A1 ectopic expression in NPC cellular and animal models is improving the disease phenotype, by focusing on the main pathologic hallmarks, cholesterol homeostasis and neuroinflammation. More specifically, the experimental methodology was designed to evaluate the effect of CYP46A1 expression on:

- NPC cholesterol homeostasis dysregulation: NPC mice brain cholesterol levels and transcriptional profile of genes involved in cholesterol synthesis, uptake, transport, and metabolism, as well as the effect of CYP46A1 ectopic expression on promoting unesterified cholesterol egress from LE/L compartments was determined.
- Inflammatory dysregulation of the NPC mice cerebellum tissue: microglia and astrocyte activation was analyzed by determining the transcriptional levels of activation markers, as well as microglia inflammatory phenotype indicators, combined with the evaluation of inflammatory changes by immunohistochemistry of mice brain sections.
- The *in vivo* hallmark of NPC neurodegeneration: the quantification of cerebellar Purkinje cell loss.
- The characteristic impairment of autophagic flux in cellular models of NPC: the autophagy flux status, including LC3II/I and p62 protein levels, as well as the p70S6K phosphorylation ratio, and the transcript levels of genes involved in the Mammalian Target of Rapamycin (mTOR) pathway and autophagy core markers was determined.

Taken together, the molecular and biochemical analysis resultant from this work attempt to further characterize how CYP46A1 promotes the amelioration of important pathological features of NPC disease.

Part II - Materials and methods

Materials

The materials used in this work are listed in the following Tables (Table 1-6).

1.1. Primers

Table 1 - Details of the mouse primers used for Real-Time qPCR.

Gene	Forward Primer	Reverse Primer
Rpl19	5’ GCA TTG GCG ATT TCA TTG GTC 3’	5’ ATG AGT ATG CTC AGG CTA CAG A 3’
Rpl29	5’ AGTCCAAGAACCACACCACA 3’	5’ ATTCGTATCTTTGCGACCGGGG 3’
Hmgcr	5' CCG GCA ACA ACA AGA TCT GTG 3'	5' ATG TAC AGG ATG GCG ATG CA 3'
Hmgs	5’ GTC TCC TTG CTT TGC TCG TTC 3’	5’ GGA CAG AGA ACT GTG GTC TCC 3’
Ldlr	5' GAA CTC AGG GCC TCT GTC TG 3'	5' AGC AGG CTG GAT GTC TCT GT 3'
Abca1	5’ CCC AGA GCA AAA AGC GAC TC 3’	5’ GGTCATCAT CAC TTT GGT CCT TG 3’
Srebp2	5' GCG TTC TGG AGA CCA TGG A 3'	5' ACA AAG TTG CTC TGA AAA CAA ATC A 3'
Acat1	5’ GAA GGC TCA CTC ATT TGT CAGA 3’	5’ GTC TCG GTA AAT AAG TGT AGG CG 3’
Cd68	5' CCT CCA CCC TCG CCT AGT C 3'	5' TTG GGT ATA GGA TTC GGA TTT GA 3'
Itgax	5' GCC ATT GAG GGC ACA GAG A 3'	5’ GAA GCC CTC CTG GGA CAT CT 3'
Crx3cr1	5’ TCG TCT TCA CGT TCG GTC TG 3’	5’ CTC AAG GCC AGG TTC AGG AG 3’
Tnfα	5’ AGG CAC TCC CCC AAA AGA TG 3’	5’ TGA GGG TCT GGG CCA TAG AA 3’
Arg1	5’ CTT GGC TTG CTT CGG AAC TC 3’	5’ GGA GAA GGC GTT TGC TTA GTT C 3’
Igf1	5’ AGACAGGCATTGTGGATGAG 3’	5’ TGAGTCTTGGGCATGTCAGT 3’
Tgf-β	5´ CTG CTG ACC CCC ACT GAT AC 3’	5’ GTG AGC GCT GAA TCG AAA GC 3’
Il-1α	5’ CGCTTGAGTCGGCAAAGAAAT 3’	5’ CTTCCCGTTGCTTGACGTTG 3’
Il-1β	5’ TGC CAC CTT TTG ACA GTG ATG 3’	5’ TGA TGT GCT GCT GCG AGA TT 3’
Trem2	5’ GACCTCTCCACCAGTTTCTCC 3’	5’ TACATGACACCCTCAAGGACTG 3’
Gfap	5’ CCAAACTGGCTGATGTCTACC 3’	5’ GCTTCATGTGCCTCCTGTCTA 3’
ApoE	5’ CTTCTGGGATTACCTGCGCT 3’	5’ GTCCTCCATCAGTACCGTTCAG 3’
Ctsd	5' GCC TCC GGT CTT TGA CAA CTT 3'	5' CAC CAA GCA TTA GTT CTC CTC C 3'

Table 2 - Details of the human primers used for Real-Time qPCR.

Gene	Forward Primer	Reverse Primer
RPL19	5' GGGCATAGGTAAGCGGAAGG 3'	3'TCAGGTACAGGCTGTGATACA 3'
MTOR	5' TCGCTGAAGTCACACAGACC 3'	5'CTTTGGCATATGCTCGGCAC 3'
PRKAA1	5' GGGTGAAGATCGGCCACTAC 3'	5' CCTACCACATCAAGGCTCCG 3'
ULK1	5' CACCCACCCAGTTCCAAACA 3'	5' AACTTGAGGAGATGGCGTGT 3'
BECN1	5' AACCAGATGCGTTATGCCCA 3'	5' TCCATTCCACGGGAACACTG 3'
PIK3C3	5' GCTGTCCTGGAAGACCCAAT 3'	5' TTCTCACTGGCAAGGCCAAA 3'
LC3B	5' AGAAGGCGCTTACAGCTCAA 3'	5' AGATTGGTGTGGAGACGCTG 3'
WIPI2	5' CTTGGACTCTGCCTCTCACG 3'	5' TGTAGGCAAGTCTCGTTGGG 3'
P62	5' TGAAACACGGACACTTCGG 3'	5' TCAGGAAATTCACACTCGGATC 3'

1.2. Antibodies

Table 3 – Details of the primary antibodies used in Western Blot analysis.

Primary antibody	Host	Commercial source	Reference	Dilution
Anti-NPC1	Rabbit	Novus Bio	NB400-148	1:1000
Anti-CYP46A1	Mouse	Santa Cruz Biotech	sc-136148	1:500
Anti-LC3A/LC3B	Rabbit	Thermo Fisher Scientific Inc.	PA1-16931	1:2000
Anti-P62	Mouse	Abcam	ab56416	1:2000
Anti-β-actin	Mouse	Sigma-Aldrich, Inc.	A5541	1:20000
Anti-p-P70S6K	Rabbit	R&D Systems	AF8965	1:1000
Anti-P70S6K	Rabbit	R&D Systems	AF8962	1:1000

Table 4 - Details of the secondary antibodies used for Western Blot analysis.

Secondary antibody	Host	Commercial source	Reference	Dilution
Anti-rabbit horseradish peroxidase	Goat	Bio-Rad	1706515	1:5000
Anti-mouse horseradish peroxidase	Goat	Bio-Rad	1721011	1:5000

Table 5 - Details of the primary antibodies used for immunohistochemistry.

Primary antibody	Host	Commercial source	Reference	Dilution
anti-GFAP	Rabbit	MilliporeSigma	MAB360	1:500
anti-Iba-1	Rabbit	Wako Pure Chemicals	019-19741	1:100
anti-Calbindin	Mouse	MilliporeSigma	C9848	1:1500
anti-HA	Mouse	BioLegend	901513	1:1000

Table 6 - Details of the secondary antibodies used for immunohistochemistry.

Secondary antibody	Host	Commercial source	Reference	Dilution
Alexa Fluor™ 488 anti-mouse	Goat	ThermoFisher Scientific	A11001	1:200
Alexa Fluor™ 568 anti-rabbit	Goat	ThermoFisher Scientific	A11011	1:200
Alexa Fluor™ 488 anti-rabbit	Goat	ThermoFisher Scientific	A11008	1:200

Methods

1. NPC mouse model

1.1. Animals and treatment

All animal experiments were performed according to the 2010/63/EU Directive and National law (Decreto-Lei n.º 113/2013). Animal facilities and the people involved in animal experiments are certified by the Portuguese regulatory entity, Direção Geral de Alimentação e Veterinária (DGAV). All the protocols executed were submitted to the Animal Welfare Committee (ORBEA) of IMM animal ethics committee and to DGAV. All animal experiments will be designed and conducted with commitment to the 3Rs.

The NPC mouse model used in this work was developed by Praggastis and colleagues and presents the knock-in of the $NPC1^{I1061T}$ mutation, the most prevalent human mutation which encodes a misfolded protein[67]. The $Npc1^{tm(I1061T)}$ mouse model faithfully recapitulates human NPC disease, with decreased motor coordination, brain lesions, particularly in the cerebellar area leading to Purkinje cell death, dendritic and axonal abnormalities, lipid storage, and premature death.

Homozygous mutants ($Npc1^{tm(I1061T)}$) and wild-type littermates ($Npc1^{+/+}$) were generated by crossing heterozygous mutant males and females, in-house. Mice were housed on a 12 h light-dark cycle with free access to a standard diet and water *ad libitum*, under standardized conditions. Both male and female mice were used as experimental animals.

After being anesthetized by isoflurane inhalation, a group of wild-type mice ($Npc1^{+/+}$) received a retro-orbital injection with a dose of $5x10^{11}$ vg (viral genomes) of adeno-associated viral (AAV) vector AAVPHPeB.HA.GFP (WT-GFP), while $Npc1^{tm(I1061T)}$ mice received either the same dose of AAVPHPeB.HA.GFP (NPC-GFP) or AAVPHPeB.HA.CYP (NPC-CYP). Mice were injected at 5 weeks of age and their weight was tracked daily, in order to evaluate their growth. They were weighed weekly from 5 weeks of age, and throughout the duration of the experience.

Mice were euthanized at week 12 and the blood and brain were quickly collected. To minimize the number of animals used, one brain hemisphere was immediately fixed in 4% paraformaldehyde solution (PFA), and then further impregnated in gelatin and frozen to be

processed for histology. The other hemisphere was dissected for the isolation of specific brain regions and the tissues were immediately frozen at -80 °C, for future protein, RNA, and DNA isolation. Additionally, the liver was weighed and collected, and other tissues, such as the heart, lung, and intestine were also isolated and stored at -80 ºC, for further processing.

1.2. Tissue sample preparation

In order to obtain homogeneous samples of each mouse's brain tissue, frozen tissues isolated from the cortex and cerebellum were ground in liquid nitrogen with a mortar and pestle. The collected ground tissues were separated and stored at -80 ºC until used for DNA, RNA, or protein isolation.

2. Cell culture

2.1. HeLa cells and primary human fibroblasts

The NPC cellular models used in this work were the NPC1-Knock Out (NPC1-KO) HeLa cells and fibroblast cells from NPC human patients carrying the I1061T mutation.

The NPC1-KO cell line was a kind gift from Dr. Wim Annaert[152]. It was generated through the knock-out of the NPC1 protein in HeLa cells using CRISPR/Cas9 genome editing. NPC-KO and WT HeLa cell lines were maintained in high glucose Dulbecco's Modified Eagle Medium (DMEM; Sigma-Aldrich, Inc., MO, USA), at 37 °C in humidified 5% CO_2. The media was supplemented with 10% heat-inactivated fetal bovine serum, 2 mM L-glutamine, 100 units/mL penicillin, and 100 µg/mL streptomycin (Gibco®, Thermo Fisher Scientific Inc., Bedford, USA).

Primary human fibroblast cultures from skin biopsies with clinical and/or morphological diagnosis of Niemann-Pick type C disease, NPC1 (I1061T), as well as wild-type (WT) controls were kindly provided by Doctor Lúcia Lacerda from the National Health Institute Dr. Ricardo Jorge Centro de Genética Médica Dr. Jacinto de Magalhães, Portugal. The fibroblasts were cultured in low glucose (1 mg glucose/L) DMEM supplemented with 10% heat-inactivated fetal bovine serum (FBS), 2 mM L-glutamine, 250 µg/ml fungizone, 10 mg/ml kanamycin, and 100 units/mL penicillin and 100 µg/mL streptomycin (Gibco®, Life Technologies), and maintained at 37 °C in humidified 5% CO_2.

2.2. Cell transduction

Adenovirus encoding GFP (adGFP) or FLAG-tagged CYP46A1 (adCYP) were generated by using the pAdTrack/pAdEasy system and quantified. Both HeLa cells and human fibroblasts were transduced overnight with adenovirus at a titer of 3.75 x 10^7 green fluorescent units (gfu) per ml of media.

WT and NPC1-KO HeLa cells were grown in T75 culture flasks, trypsinized, centrifuged at 500 *g* for 5 min, and plated at a density of 250 000 cells/mL for RNA extraction, or 175 000 cells/mL for total protein extraction. Cultured cells were transduced with either adGFP or adCYP, and after 24 h the media was changed. Cells were maintained for another 24 or 48 h, depending on the endpoint analysis.

Primary human fibroblasts were also transduced with either adGFP or adCYP, for 96 h.

3. RNA isolation and reverse transcription

RNA was isolated from the cerebellum and cortex tissue of each mouse, as well as from HeLa cells transduced with adGFP or adCYP, using TRIzol reagent[153]. For that, either the cultured cells or mice tissue were resuspended and dissociated in 1 mL of TRIzol Reagent (Thermo Fisher Scientific Inc.), with posterior lysate collection and incubation at room temperature for 5 min. Afterward, 200 µL chloroform was added, and the samples were agitated vigorously for 15 sec, incubated for 2-3 min at room temperature, and centrifuged at 12.000 *g* for 15 min at 4 °C.

Centrifugation leads to phase separation, as an aqueous phase (top layer containing the RNA), an interphase, corresponding to precipitated DNA, and an organic phase (bottom layer) are formed. The aqueous phase was recovered, and 500 µL of isopropanol were added, followed by incubation for 10 min at room temperature and centrifugation at 12.000 *g* for 10 min at 4 °C. The resulting pellet was washed with 70% ethanol in diethylpyrocarbonate (DEPC)-treated water and allowed to air-dry. The RNA was resuspended in molecular biology grade water and incubated in a water bath at 55 °C for 10 minutes. RNA quantification was performed in the Nanodrop spectrophotometer (Thermo Fisher Scientific Inc.). The samples were stored at -80 °C until further use.

Before proceeding to cDNA synthesis, the RNA of each tissue or cellular sample was treated with DNAse I Recombinant enzyme (Roche Diagnostics GmbH, Mannheim, Germany). For

that, 1 µg of RNA was first diluted with molecular biology grade water to a final volume of 8 µL, with posterior addition of 1 µL of incubation buffer 10X, and of 0.1 U/µL DNAse I and water until a final volume of 10 µL. The samples were then heated at 37 °C for 30 min, followed by 10 min at 75 °C, in a VWR Thermal Cycler (VWR International LLC, USA). To synthesize the cDNA, 5 ng/µL of random hexamer mix (NZYTech, Lda., Lumiar, Portugal) and 0.5 mM dNTPs NZYMix (NZYTech, Lda.) were added to 5 µL of the DNAse-treated samples. After a 5 min incubation at 65 °C, 100 U of NZY Tech Reverse Transcriptase enzyme (NZYTech), diluted in reaction buffer 1X, and 2 µL of reaction buffer 10X were added to the mix, in order to reach a final volume of 20 µL. The samples were then incubated at 25 °C for 10 min, followed by 50 min at 50 °C, and 5 min at 85 °C. Until further use, the cDNA samples were stored at -20 °C.

4. Real-Time Quantitative Polymerase Chain Reaction (RT-qPCR)

For detection and quantification of mRNA expression levels in mouse cerebellum and cortex, as well as in the adGFP and adCYP-transduced HeLa cells**,** RT-qPCR was run in 384-well optical reaction plates containing a final volume of 5 µl per well, corresponding to 2 µL of cDNA diluted in Mili-Q water and 3 µL of target gene master mix, being each sample run in duplicate for each assayed gene. The reaction components, 1X SensiFAST™ SYBR® Hi-ROX Kit (Meridian Bioscience Inc., Cincinnati, Ohio, EUA) and 300 nM of specific primers (STAB Vida, Caparica, Portugal) for mice samples (Table 1) and for HeLa cells (Table 2), were prepared for each target gene, pre-mixed, and pipetted into the reaction plate.

The RT-qPCR was performed in a QuantStudio 7 Flex Real-Time PCR System (Thermo Fisher Scientific Inc.), being used a cycling program comprised of three stages: an initial denaturation at 95 °C for 2 min, the amplification stage of 40 cycles of 95 °C for 5 sec and 60 °C for 30 sec for annealing and extension, followed by a melting curve analysis. The mRNA levels of the genes of interest in the cerebellum and cortex samples of mice were normalized to the housekeeping genes, *Rpl19* and *Rpl29*, and for the HeLa cells were normalized to the *RPL19* levels. Reference genes were selected using the NormFinder tool[154]. The normalized levels are presented as fold change from controls using the $^{\Delta\Delta}$Ct method.

5. Preparation of total protein extracts

For total protein extraction either the frozen dissociated animal tissue or the transduced HeLa cells and fibroblasts, were homogenized in lysis buffer (50 mM Tris-HCl (pH 7.5), 180 mM NaCl, 1 mM EDTA, and 1% Triton), supplemented with 1 mM dithiothreitol (DTT), 1 mM sodium orthovanadate, 10 mM sodium fluoride and protease inhibitors cocktail (Roche, Switzerland). Lysates were incubated on ice for 30 min. After sonicating for 4 times, 4 sec each cycle, samples were centrifuged at 13,000 *g* for 15 min, at 4 °C, and the supernatants were collected and stored at -80 °C.

Quantification of total protein levels was performed by the Bradford method, using Bio-Rad Protein Assay Reagent (Bio-Rad Laboratories, Hercules, CA, USA), according to the manufacturer's protocol.

6. Western Blotting and immunodetection

The levels of the proteins of interest were determined by Western blot analysis. Protein samples isolated from HeLa cells and human fibroblasts were denatured for 5 min at 95 °C using a mixture of 1:1 (v/v) sample/ 2X SDS buffer (0.25 mM Tris-HCL (pH 6.8), 4% SDS, 40% glycerol, 0.2% bromophenol blue, 1% 2β-mercaptoethanol). The denatured proteins were then separated on a 12.5% or 10% sodium dodecyl sulfate-polyacrylamide gel electrophoresis (SDS-PAGE).

The gel was then electrotransferred to an activated polyvinylidene difluoride (PVDF) membrane (Immobilon®-P, MilliporeSigma, Burlington, Massachusetts, USA). The membranes were then stained with amido black 1X (Sigma-Aldrich, Inc.) and air dried at room temperature. After re-hydration with ethanol, the membranes were then incubated with the specific primary antibodies described in Table 3 and, posteriorly, with the correspondent secondary antibodies, described in Table 4.

The membranes were processed for protein detection using WesternBright™ ECL (Advansta Corporation, Menlo Park, CA, USA) Western blotting detection reagent or SuperSignal™ West Femto Maximum Sensitivity Substrate (Thermo Fisher Scientific Inc.) in a ChemiDoc™ MP imaging system (Bio-Rad Laboratories). The relative intensities of protein bands were analyzed

using the Image Lab Software Version (Bio-Rad Laboratories). β-actin was used as the loading control.

7. Total cholesterol assay

The Amplex® Red Cholesterol Assay Kit (Sigma-Aldrich), was used to evaluate the levels of both free cholesterol and cholesteryl esters in mice cerebellum and cortex protein extracts. The cholesteryl esters are hydrolyzed by cholesterol esterase into cholesterol, which is then oxidized by cholesterol oxidase to yield H_2O_2. In the presence of horseradish peroxidase (HRP), 10-acetyl-3,7-dihydroxyphenoxazine (Amplex® Red reagent) reacts with H_2O_2 producing a highly fluorescent resorufin.

The assay was performed according to the manufacturer's instructions. A 20 mM stock solution of Amplex® Red was first prepared by dissolving Amplex® Red reagent in dimethyl sulfoxide (DMSO). Then, 200 U/ml HRP, 200 U/ml cholesterol oxidase, and 200 U/ml cholesterol esterase stock solutions were prepared by dissolving the respective lyophilized powders in the necessary amount of 1X reaction buffer prepared from the 5X reaction buffer stock solution supplied by the kit.

The total protein extracts prepared from cerebellum and cortex mouse samples, as described in section 5, were diluted 1:50 in 1X reaction buffer. A volume of 50 µl of each sample was then placed into a 96-well microplate for fluorescence-based assays in duplicates. Next, a cholesterol calibration curve and a negative control without cholesterol were prepared and applied in the same 96-well microplate. Since Amplex® Red is unstable in the presence of dithiothreitol (DTT), the DTT-containing lysis buffer used in section 5 was also used in the calibration curve.

The reaction was initiated through the addition of 50 µL of the reaction mixture containing 300 µM of Amplex® Red reagent, as well as 2 U/mL HRP, 2 U/mL cholesterol oxidase, and 0.2 U/ml cholesterol esterase in 1X reaction buffer. This resulted in a final concentration of 150 µM Amplex® Red reagent in the reaction mix and a final reaction volume of 100 µl per well.

After an incubation of 30 min at 37 °C, the fluorescence was measured in the Varioskan LUX Multimode Microplate Reader (Thermo Fisher Scientific Inc.) with excitation at 560 nm and emission detection at 585 nm. The background was corrected by subtracting the negative

control and normalization of the results was obtained through protein quantification using Bradford reagent, as described in section 5.

8. Histological processing

The brain hemisphere reserved for immunohistochemistry was immediately fixed in PFA 4% for 24 to 48 h. Afterward, the hemispheres were sequentially transferred to a 15% and 30% saccharose solution for 24 h each. The tissue was then embedded in gelatin and frozen at -80 °C. Brains were processed in 12 µm thick sagittal slices using the cryostat. Brain embedding and processing was performed by the Comparative Pathology Unit at Instituto de Medicina Molecular João Lobo Antunes (iMM).

8.1. Immunohistochemistry and filipin staining

To assess microglia and astrocytes activation, Anti-ionized calcium-Binding Adapter Molecule 1 (Iba-1) and GFAP immunohistochemistry were performed, respectively, in parasagittal cerebellum slices of each mouse. Mice cerebellum sections were also immunostained for Calbindin and the HA-Tag, in order to allow visualization of the Purkinje cells and the ectopically expressed CYP46A1, respectively. For all antibodies, the same procedure was followed.

Briefly, slices were air-dried for 1 h and rehydrated in PBS for 10 min, before incubation with blocking solution (goat serum 5% and Triton X-100 0.2% in PBS) for 1 h, in a humid chamber protected from light and at room temperature. After blocking, the slices were then probed with either the anti-Iba-1, -GFAP, -Calbindin, or -HA-Tag primary antibody diluted as described in Table 5 in blocking solution, overnight, in a humid chamber at 4 °C, and protected from light. Unbound primary antibodies were washed with PBS 3 times and the slices were incubated for 1 h at room temperature with the respective secondary antibodies, diluted in blocking solution, as described in Table 6, and DAPI (1:2000; Biotium), for nuclear staining, for 1 h in a humid chamber protected from light and at room temperature. After being washed with PBS 3 times, the slices were then mounted.

Fluorescence visualization was performed in an AxioScope.A1 microscope (Zeiss, Germany) with an AxioCam HRm camera (Zeiss). Morphological analysis and fluorescence

quantification were performed using NIH ImageJ 1.46r software. To further assess astrocytic morphological features, the fluorescence of the slices stained for GFAP was also visualized in a Leica TCS SP8 Confocal Microscope (Leica Microsystems, Germany) and the Leica Application Suite X software (Leica Microsystems).

For unesterified cholesterol staining, mice brain slices were dyed with filipin III (F4767, Sigma-Aldrich). Briefly, the slices were air-dried and rehydrated in PBS, and, posteriorly, 0.05 mg/mL filipin III was added for 2 h in a humid chamber protected from light and at room temperature. The slices were then washed in PBS 3 times and mounted.
Fluorescence visualization was performed in an AxioScope.A1 microscope with an AxioCam HRm camera. Blinded analysis of the filipin score of the cortex region of the stained sections was carried out by two independent reviewers, as the sections were previously independently coded by a third party. A scale of 0-6 was used to evaluate filipin staining intensity as an indicator of relative cholesterol storage, being 0 corresponding to no accumulation, and 6 corresponding to extensive storage. After scoring, the third-party code was broken and the results of all sections were averaged for each mice group (WT-GFP, NPC-GFP, and NPC-CYP).

8.2. Purkinje cell count

For the Purkinje cell visualization and count, the 12 μm thick sagittal mice cerebellum slices were stained with Cresyl Violet. Briefly, the sections were air-dried and stained with filtered Cresyl Violet (Sigma-Aldrich) at 60 °C, for 3 min. Subsequently, the sections were differentiated in 96% ethanol with acetic acid for 1 min and then dehydrated in a series of ethanol consisting of 96% ethanol and then 100% ethanol, for 1 min in each solution. The sections were then clarified in xylene for 1 min. Finally, sections were mounted using Entellan mounting medium (Merck, Rahway, New Jersey, U.S.) and then air-dried.

The number of Purkinje cells in each cerebellar lobule (I-X) of the Cresyl Violet-stained sections was manually counted under a 40X objective. The length of the Purkinje cell layers was manually traced and measured using ImageJ software analysis (National Institutes of Health). The results are presented as the number of Purkinje cells/mm, reflecting the number of cells per length of cell layer for each cerebellar lobe.

9. Statistical analysis

GraphPad Prism 9 was used to perform statistical analysis. The Shapiro-Wilk test was performed to test if the data fit a normal distribution. One-way ANOVA, followed by Tukey's multiple comparisons test was used when data fit a normal distribution. When data failed to pass the normality test, the Kruskal-Wallis test was performed, followed by Dunn's multiple comparisons test.

Part III - Results

1. CYP46A1 ectopic expression in Npc1$^{tm(I1061T)}$ mice

Previous *in vitro* studies from our group have suggested that CYP46A1 ectopic expression in NPC cellular models leads to a remarkable amelioration of the pathological phenotype of intracellular cholesterol accumulation (Moutinho et al., unpublished results). In order to determine whether *in vivo* CYP46A1 ectopic expression was able to improve disease phenotype, CYP46A1 expression was increased in the Npc1$^{tm(I1061T)}$ mice model through AAV gene-mediated therapy. A group of Npc1$^{tm(I1061T)}$ mice was administered with a dose of 5x10^{11} vg (viral genomes) of AAVPHPeB.HA.CYP vector (NPC-CYP), or the same dose of AAVPHPeB.HA.GFP vector (NPC-GFP). In parallel, a group of wild-type mice (Npc1$^{+/+}$) received the AAVPHPeB.HA.GFP (WT-GFP) vector, in the same dose, as a control.

The efficiency of AAV delivery to the cerebellum of the WT-GFP and NPC-GFP mice was confirmed through visualization, in parasagittal brain sections, of GFP expression in the Purkinje cells of the cerebellum (Figure 5).

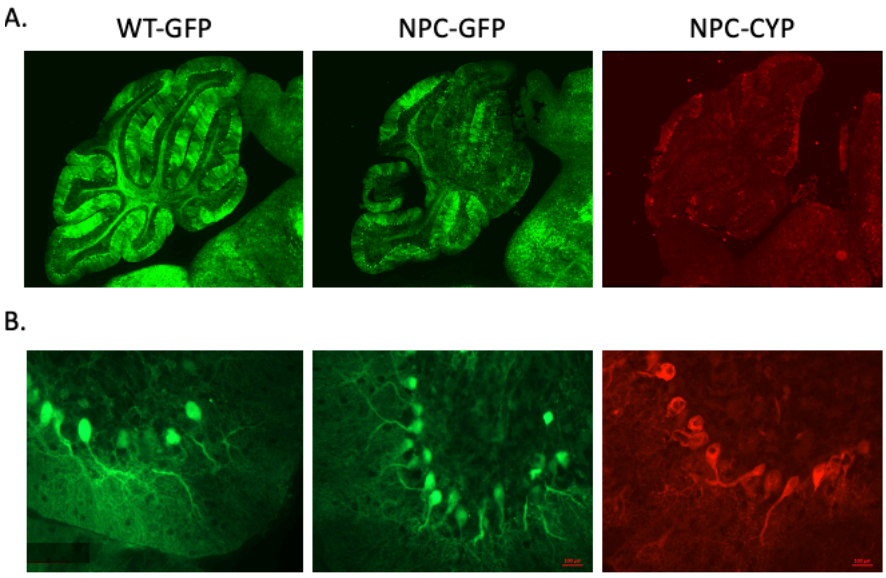

Figure 5 - Correct delivery of AAV encoding for GFP and CYP46A1 in mouse cerebellum. Wild-type mice received a retro-orbital injection with a dose of 5x10^{11} vg (viral genomes) of AAVPHPeB.HA.GFP (WT-GFP) vector, while Npc1$^{tm(I1061T)}$ mice received the same dose of AAVPHPeB.HA.GFP (NPC-GFP) or AAVPHPeB.HA.CYP46A1 (NPC-CYP). Mice were injected at day 35 and sacrificed at 12 weeks of age. AVV-mediated GFP expression in WT-GFP and NPC-GFP mouse cerebellum, and AAV-mediated HA-tag expression in NPC-CYP mouse brain (Panel A). Microphotographs of more detailed Purkinje cells of cerebellar lobule X of each mouse, expressing GFP (WT-GFP and NPC-GFP) or HA-tag (NPC-CYP) (40x) (Panel B).

The correct delivery of CYP46A1 to the brain in NPC-CYP mice was confirmed by fluorescence visualization of the HA-tag.

Weight loss is one of the hallmarks of the NPC disease and has already been described for this animal model[67]. Therefore, we tracked mice's weight weekly from the AAV injection onwards. As expected, a lower weight gain was observed in NPC females from week 10 and at 12 weeks, for males, compared to the WT animals (Figure 6). However, from week 10 onward, the body weight gain in NPC-CYP female mice followed a tendency to stabilize, and at week 12, the percentage of body weight gain of NPC-CYP female mice was significantly higher (approximately 15%), compared to NPC-GFP female mice. This difference was, however, not observed in males.

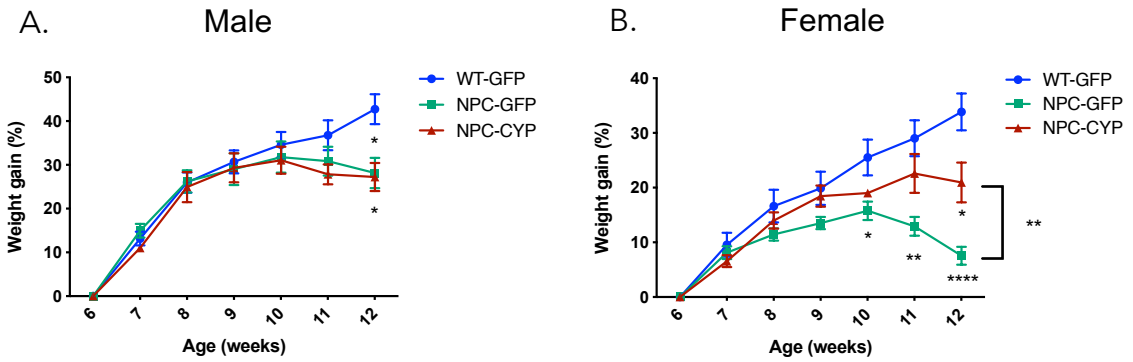

Figure 6 - Effect of CYP46A1 expression in mouse body weight gain over time. Wild-type mice received a retro-orbital injection with a dose of $5x10^{11}$ vg (viral genomes) of AAVPHPeB.HA.GFP (WT-GFP) vector, while $Npc1^{tm(I1061T)}$ mice received the same dose of AAVPHPeB.HA.GFP (NPC-GFP) or AAVPHPeB.HA.CYP46A1 (NPC-CYP). Mice were injected at day 35 and their weight was tracked weekly until 12 weeks of age. Data is presented in percentage of weight gain in relation to the weight presented by each animal at 6 weeks: male (A) and female mice (B). Statistical analysis was performed by ANOVA one-way tests followed by Tukey's multiple comparisons test (*p<0.05, **p<0.01, ****p<0.0001).

In NPC disease, besides the neurological features, liver-associated pathologies are also present in patients[155]. Therefore, the effect of CYP46A1 ectopic expression on two liver-injury-related parameters, namely the liver-to-body weight ratio and levels of alanine aminotransferase (ALT) was evaluated in mice serum (Figure 7).

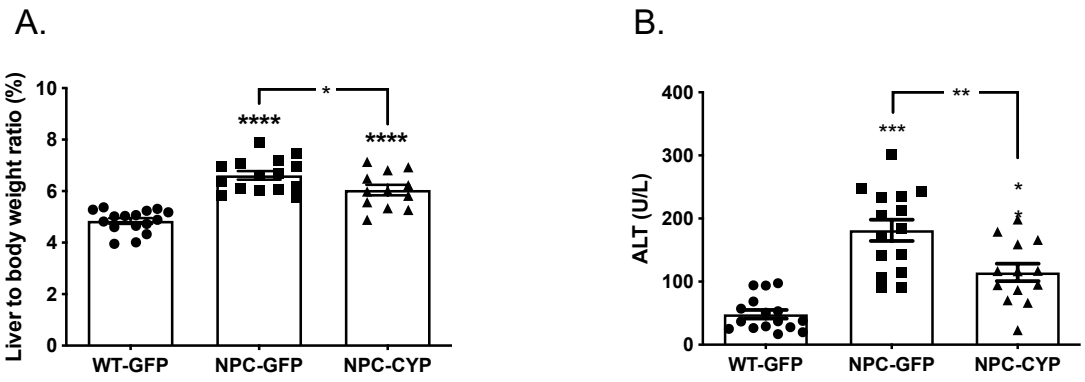

Figure 7 - Effect of CYP46A1 expression in liver-injury-related parameters. Liver-to-body weight ratio (shown in percentage) (A), and the levels of alanine aminotransferase (ALT) in the serum (U/L), were quantified in wild-type mice injected with $5x10^{11}$ vg (viral genomes) AAV-GFP (WT-GFP) vector, and of $Npc1^{tm(I1061T)}$ mice that received the same dose of AAV-GFP (NPC-GFP) or AAV-CYP (NPC-CYP). Mice were injected at day 35 and euthanized at 12 weeks of age. Data represents mean values ± SEM and statistical analysis was performed by one-way ANOVA followed by Tukey post-hoc test or by Kruskal-Wallis followed by Dunn's post-hoc test (*p<0.05, **p<0.01, ***p<0.001, ****p<0.0001).

A significant increase of 1.4- fold in the liver-to-body weight was observed in NPC-GFP mice, compared to WT-GFP. The hepatomegaly observed was partially corrected by CYP46A1, as the levels of liver-to-body weight were significantly reduced by 10% in NPC-CYP mice, compared to NPC-GFP. In agreement, we observed an increase in serum ALT levels of approximately 3.8, that was also reverted by CYP46A1 expression, since we observed a significant decrease of approximately 35% in the levels of this biomarker of liver dysfunction. Overall, these results suggest that CYP46A1 expression has a positive impact on general health indicators of NPC animals.

2. Effect of CYP46A1 ectopic expression on brain cholesterol homeostasis impairment in NPC disease

Due to the importance of CYP46A1 in brain cholesterol homeostasis, we further evaluated the impact of CYP46A1 expression on brain cholesterol levels. We started by quantifying total cholesterol levels in mice cerebellum and cortex samples using the Amplex® Red Reagent (Figure 8). No significant differences in total cholesterol levels were observed between the different experimental groups, in the two brain regions.

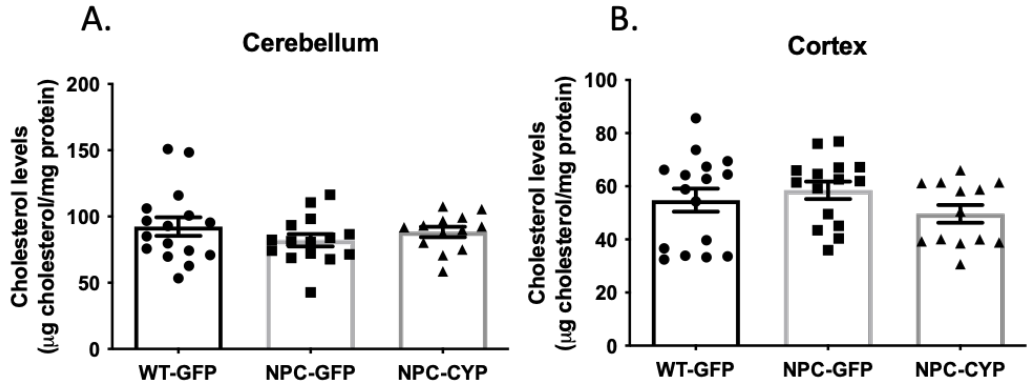

Figure 8 - Effect of CYP46A1 expression on cholesterol accumulation in the cerebellum and cortex of NPC mice. Total cholesterol levels in the cerebellum (A) and cortex (B) of wild-type mice injected with $5x10^{11}$ vg (viral genomes) AAV-GFP (WT-GFP) vector, and of $Npc1^{tm(I1061T)}$ mice that received the same dose of AAV-GFP (NPC-GFP) or AAV-CYP (NPC-CYP). Mice were injected at day 35 and euthanized at 12 weeks of age. Data represents mean values±SEM and is presented in micrograms of cholesterol per milligrams of protein (µg/mg).

Despite the fact that no differences were observed in the overall brain cholesterol content, the NPC disease is characterized by an intracellular accumulation of cholesterol, and consequently by significant changes in cholesterol homeostasis, therefore, we evaluated the transcriptional profile of genes involved in cholesterol metabolism. Total mRNA was isolated from the cerebellum and cortex of WT-GFP, NPC-GFP, and NPC-CYP mice, and the transcript levels of genes responsible for cholesterol synthesis and uptake, transport, and esterification were quantified by RT-qPCR (Figure 9). For the characterization of the effect of CYP46A1 increased expression on cholesterol synthesis, the transcript levels of Hmgcr and Hmgcs1 genes were quantified, as *Hmgcr* catalyzes mevalonate synthesis, the rate-limiting step in the cholesterol synthesis pathway, and *Hmgcs1* catalyzes the conversion of Acetyl-CoA into HMG-CoA, the necessary substrate[156]. A significant decrease in the mRNA levels of both genes was observed in NPC-GFP mice cerebellum (Figure 9A and B) and cortex samples (Figure 9G and H), compared to WT-GFP littermates (0.9- and 0.7-fold in the cerebellum, respectively, and 0.8-fold for both genes in the cortex). Both in the cerebellum and cortex, CYP46A1 ectopic expression was able to restore the expression levels of Hmgcr and Hmgcs1 to values similar to those found in WT-GFP mice, which corresponded to an increase of approximately 1.2 and 1.6-fold in the cerebellum, respectively, and 1.3- and 1.7-fold in the cortex, compared to NPC-GFP mice.

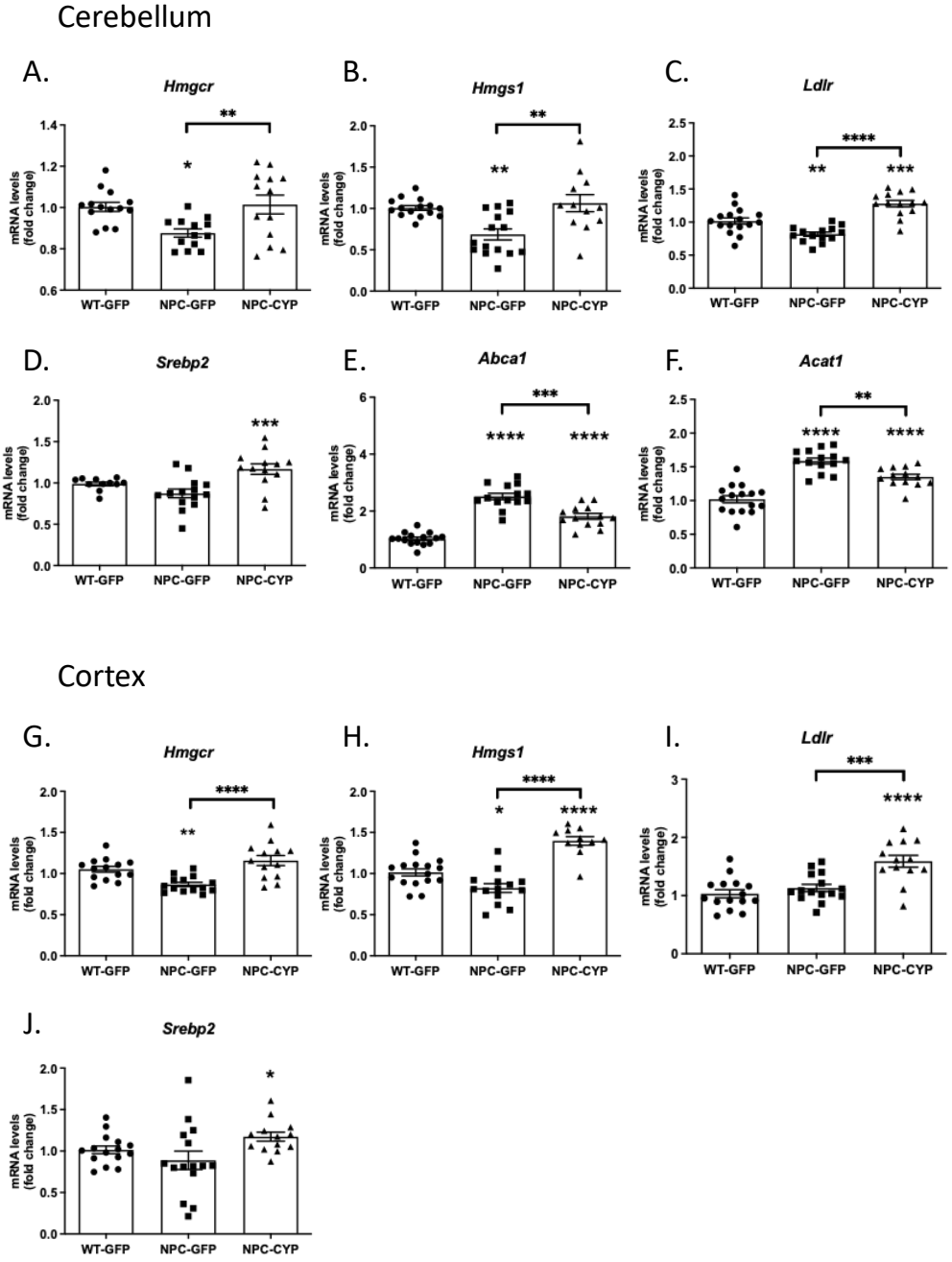

Figure 9 - CYP46A1 expression corrects cholesterol homeostasis in NPC. Wild-type mice received a retro-orbital injection with a dose of $5x10^{11}$ vg (viral genomes) of AAVPHPeB.HA.GFP (WT-GFP) vector, while $Npc1^{tm(I1061T)}$ mice received the same dose of AAVPHPeB.HA.GFP (NPC-GFP) or AAVPHPeB.HA.CYP46A1 (NPC-CYP). Mice were injected at day 35 and sacrificed at 12 weeks of age. mRNA was extracted from cerebellum and cortex samples and mRNA levels of genes involved in cholesterol synthesis, transport, or metabolism were measured by RT-qPCR. mRNA levels of Hydroxymethylglutaryl-CoA reductase (Hmgcr) (A), Hydroxymethylglutaryl-CoA synthase (Hmgs1) (B), Low-Density Lipoprotein Receptor (Ldlr) (C), *Sterol regulatory element-binding protein 2* (Srebp2) (D), ATP Binding Cassette Subfamily A Member 1 (Abca1) (E), and Acetyl-CoA acetyltransferase (Acat1) (F) were calculated for the cerebellum samples, and Hmgcr (G), Hmgs1 (H), Ldlr (I), and Srebp2 (J) for the cortex samples as well. Values were normalized to *Rpl19* and *Rpl29* as reference genes and plotted as a fold change over the average mRNA levels detected in WT-GFP mice samples. Data represents mean values ±SEM (*p<0.05, **p<0.01, ***p<0.001, ****p<0.0001).

Additionally, the mRNA levels of Ldlr, an important player in cholesterol uptake, were significantly decreased in the cerebellum samples of NPC-GFP mice, compared to WT-GFP (0.8-fold) (Figure 9C), although a similar significant decrease was not observed in the cortex (Figure 9I). Interestingly, once again CYP46A1 ectopic expression could repair the decrease in Ldlr mRNA levels, as in the cerebellum it increased Ldlr transcript levels 1.3-fold relative to WT-GFP animals. Similarly, in the cortex, we could observe a significant increase of about 1.5-fold in NPC-CYP when compared with WT-GFP.

SREBP2 is the key transcription factor that regulates the expression of the majority of genes involved in cholesterol synthesis and uptake[29], including HMGCR, HMGCS, and LDLR. Despite the changes induced by the NPC phenotype in the mRNA levels of those genes, both in the cerebellum and cortex, no changes were observed for the Srebp2 transcript levels (Figure 9D and J). This result is not surprising, taking into account that the activation of this transcription factor is a complex regulatory program that requires processing and nuclear translocation of an inactive precursor that is synthesized in the ER[29]. However, in NPC-CYP animals a significant 1.3-fold increase in Srebp2 mRNA levels was detected in the cerebellum and cortex (Figure 9D and J). This increase occurs concomitantly with the increase in the Ldlr mRNA levels, previously described. Altogether, these results demonstrate that CYP46A1 is, at least, partially restoring SREBP2-mediated gene regulation in the brain of NPC animals, suggesting an improvement in the ER function as the cholesterol sensor of the cell.

Another mediator of cholesterol homeostasis is the membrane cholesterol transporter ABCA1 which represents an important pathway for excess cellular cholesterol efflux. In the brain, ABCA1 is particularly abundant in Purkinje cells[156]. Our results show a significant increase in *Abca1* mRNA levels in NPC-GFP mice, in comparison to WT-GFP littermates (2.5-fold) (Figure 9E). Again, CYP46A1 ectopic expression partially reverted this increase, leading to a decrease of approximately 28% in NPC-CYP mice.

Transcript levels of Acat1 were also assessed in the cerebellum, as this enzyme is responsible for the esterification of cholesterol for storage. NPC animals have a significant 1.6-fold increase in Acat1 mRNA levels, relative to WT-GFP, while CYP46A1 expression reverted this effect, leading to a 15% downregulation in Acat1 mRNA levels (Figure 9F).

Our transcriptomic analysis confirmed an extensive dysregulation of cholesterol metabolism-related gene expression in this NPC animal model, that is characterized by a significant decrease

in cholesterol synthesis and uptake, and an increase in cholesterol efflux and esterification. Importantly, CYP46A1 ectopic expression was able to revert all those changes, confirming the *in vivo* beneficial effect.

Having concluded that CYP46A1 ectopic expression is able to correct the mRNA levels of genes involved in cholesterol homeostasis, we assessed whether CYP46A1 was also able to revert the pathological accumulation of cholesterol in LE/L compartments. For that, parasagittal brain sections of WT-GFP, NPC-GFP, and NPC-CYP mice were stained with filipin III, which labels unesterified cholesterol (Figure 10).

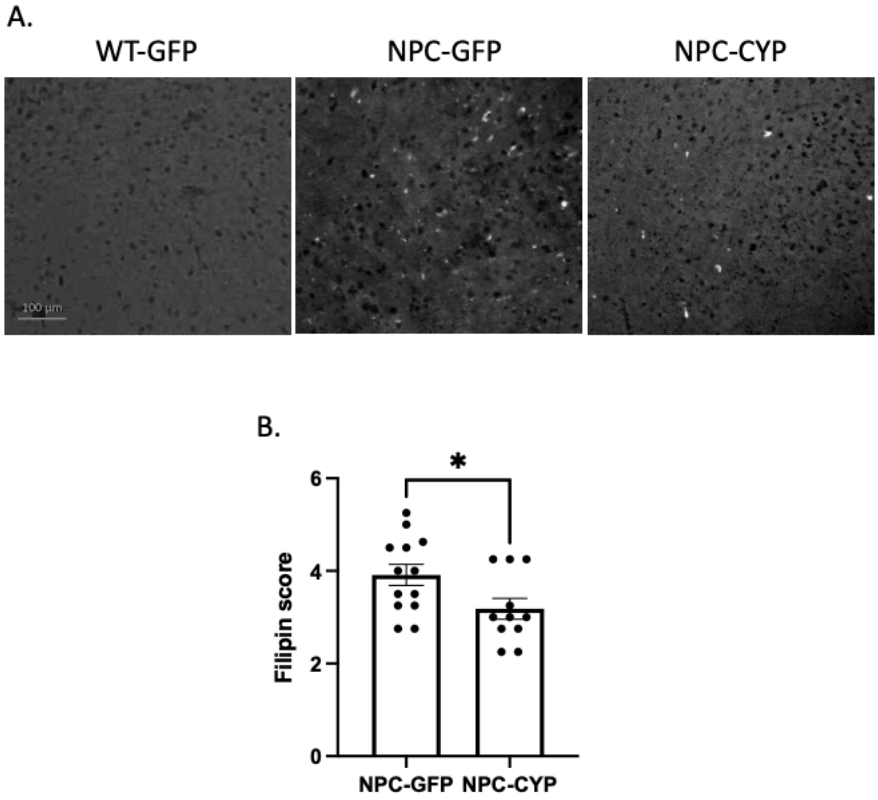

Figure 10 - CYP46A1 ectopic expression corrects cholesterol accumulation in the late endosomes/lysosomes (LE/L). Wild-type mice received a retro-orbital injection with a dose of $5x10^{11}$ vg (viral genomes) of AAVPHPeB.HA.GFP (WT-GFP) vector, while $Npc1^{tm(I1061T)}$ mice received the same dose of AAVPHPeB.HA.GFP (NPC-GFP) or AAVPHPeB.HA.CYP46A1 (NPC-CYP). Mice were injected at day 35 and sacrificed at 12 weeks of age. Unesterified cholesterol in the cortex region of mice brain slices was assessed via filipin III labeling. Cortex slices were analyzed in a blinded fashion on a scale of 0 – 6, being 0 corresponding to no accumulation, registered in WT mice sections, and 6 corresponding to extensive storage. Images representative of the mean score of WT-GFP, NPC-GFP, and NPC-CYP mice (0, 4, and 3, respectively) are shown in panel A (10x). Data are presented in image B as mean values ± SEM, Mann-Whitney test was performed (*$p<0.05$).

Blinded analysis of the filipin accumulation in the cortex region was carried out using a scale of 0-6 to evaluate filipin staining intensity as an indicator of relative cholesterol storage, in which 0 corresponds to no accumulation, and 6 corresponds to extensive storage. After scoring, the results of all sections were averaged for each mice group (WT-GFP, NPC-GFP, and NPC-CYP). A representative image is presented in Figure 10A. As expected, WT-GFP mice did not display any cholesterol accumulation (Figure 10A), while NPC-GFP mice showed an aggravated and localized cholesterol accumulation, which translated to a higher filipin III score. Importantly, NPC-CYP mice exhibited a significant decrease in filipin III staining score when compared to NPC-GFP mice. This decrease in filipin-positive cells, of approximately 19%, reflects a correcting effect by CYP46A1 ectopic expression of cholesterol accumulation that occurs in NPC1 LE/L compartments (Figure 10B).

3. Effect of CYP46A1 ectopic expression on neuroinflammatory hallmarks of NPC disease

Neuroinflammation is one of the hallmarks of NPC disease, being the cerebellum one of the most affected regions, as evidenced by microglia activation, which has been suggested to be an important contributor to neurodegeneration in NPC1[157]. Therefore, the effect of CYP46A1 ectopic expression on the mRNA levels of classic markers of pro- and anti-inflammatory DAM microglia phenotype was assessed in NPC mice cerebellum (Figure 11).

Microglia activation was first confirmed in NPC mice cerebellum by the significant increase of 14.3- and 3.7-fold, observed in the mRNA levels of markers of microgliosis, such as Cd68 (Figure 11A) and Itgax (Figure 11B), when compared to the WT littermates[79]. Interestingly, this increase was significantly reverted by CYP46A1 ectopic expression, leading to a decrease of approximately 27% in the mRNA levels of those markers. This result suggests that CYP46A1 may have a positive impact in the neuroinflammatory phenotype of NPC disease.

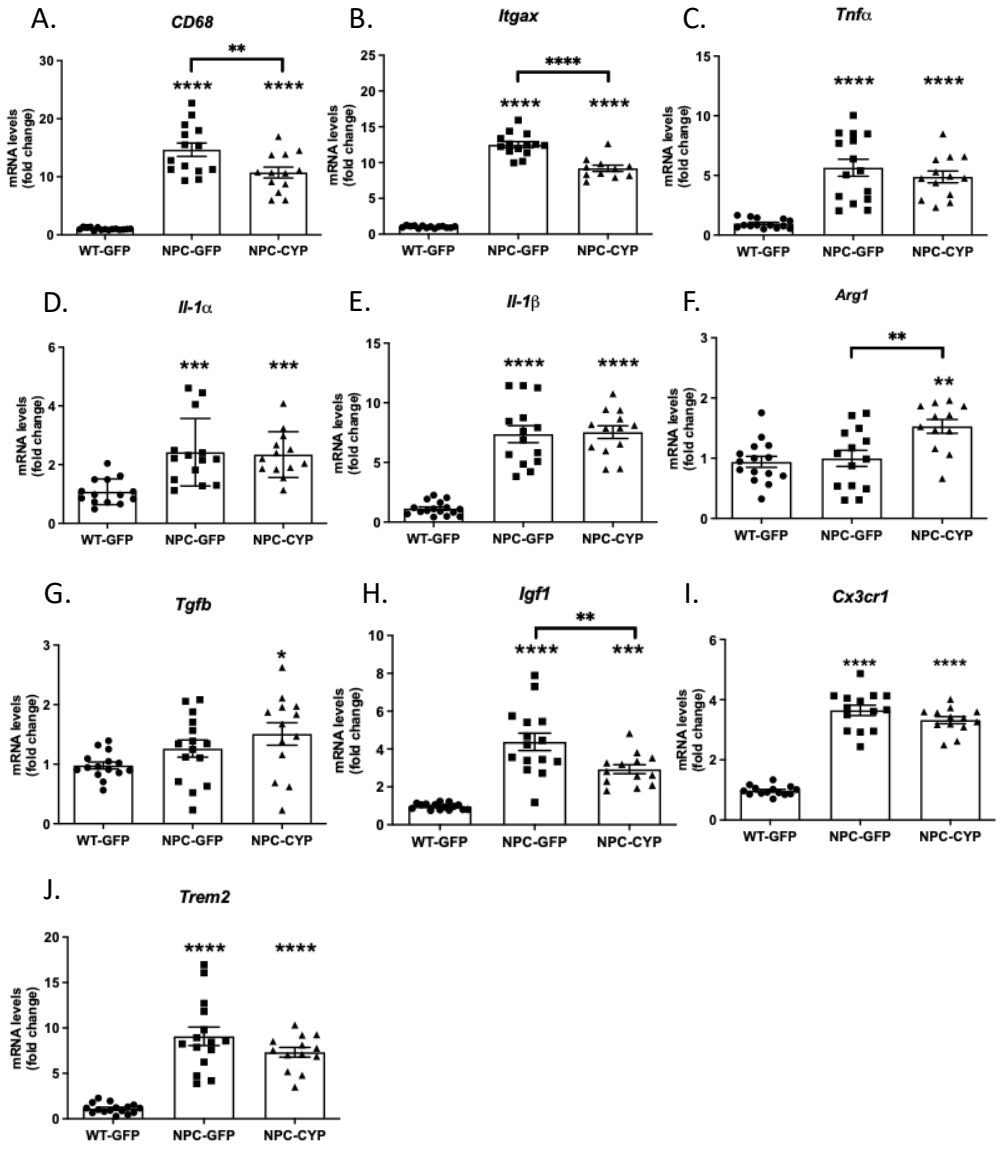

Figure 11 - Effect of CYP46A1 ectopic expression in the microglia profile of NPC mice. Wild-type mice received a retro-orbital injection with a dose of $5x10^{11}$ vg (viral genomes) of AAVPHPeB.HA.GFP (WT-GFP) vector, while $Npc1^{tm(I1061T)}$ mice received the same dose of AAVPHPeB.HA.GFP (NPC-GFP) or AAVPHPeB.HA.CYP46A1 (NPC-CYP). Mice were injected at day 35 and sacrificed at 12 weeks of age. mRNA was extracted from the cerebellum samples and transcript levels were measured by RT-qPCR using *Rpl19* and *Rpl29* as reference genes. mRNA levels of Cluster of Differentiation 68 (CD68) (A), Integrin Subunit Alpha X (Itgax) (B), Tumor necrosis factor α (Tnfα) (C), Interleukin (IL)-1α (Il-1α) (D), Il-1β (E), Arginase 1 (Arg1) (F), Transforming growth factor β (Tgfβ) (G), Insulin-like growth factor-1 (Igf1) (H), C-X_3-C Motif Chemokine Receptor 1 (Cx_3cr1) (I), and Triggering receptor expressed on myeloid cells 2 (Trem2) (J) were calculated and plotted as a fold change over the average mRNA levels detected in WT-GFP mice samples and represented as mean values ±SEM (*p<0.05, **p<0.01, ***p<0.001, ****p<0.0001).

This cerebellar microglial activation in NPC mice was accompanied by an increase in the mRNA levels of the pro-inflammatory cytokines Tnfα, Il-1α, and Il-1β , detected in NPC-GFP mice, when compared to WT-GFP, however, no changes were observed in NPC-CYP mice,

indicating that the mRNA levels of the genes were not affected by CYP46A1 ectopic expression (Figure 11C, D and E, respectively). Interestingly, significant differences in the levels of Il-1β were observed between NPC-GFP male and female mice, since female NPC-GFP mice presented significantly higher transcript levels (1.4-fold) when compared to male NPC-GFP mice (Figure 12).

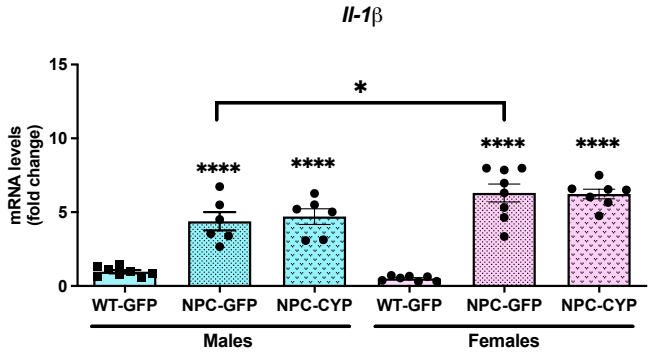

Figure 12 - Sex-specific differences in cytokine expression levels in NPC mice. Wild-type mice received a retro-orbital injection with a dose of $5x10^{11}$ vg (viral genomes) of AAVPHPeB.HA.GFP (WT-GFP) vector, while $Npc1^{tm(I1061T)}$ mice received the same dose of AAVPHPeB.HA.GFP (NPC-GFP) or AAVPHPeB.HA.CYP46A1 (NPC-CYP). Mice were injected at day 35 and sacrificed at 12 weeks of age. mRNA was extracted from the cerebellum samples and transcript levels were measured by RT-qPCR using *Rpl19* and *Rpl29* as reference genes. mRNA levels of Il-1β were calculated and plotted for male and female mice as a fold change over the average mRNA levels detected in the correspondent WT-GFP mice samples and represented as mean values ±SEM (*p<0.05, ****p<0.0001).

Regarding microglia markers that typically indicate an anti-inflammatory response, the transcript levels of Arg1, Tgfβ and Igf1 were also quantified. ARG1 is a marker of anti-inflammatory microglia activation profile that is usually associated with tissue repair and phagocytosis[158]. Interestingly, although Arg1 transcript levels observed in NPC-GFP mice were similar to those found in WT-GFP, CYP46A1 ectopic expression led to a significant increase of 1.5-fold in NPC-CYP mice, compared to NPC-GFP (Figure 11F). Similarly, the mRNA levels of Tgfβ, a cytokine also produced when the microglia activation profile is anti-inflammatory, and involved in healing[158], did not register differences from WT-GFP to NPC mice (Figure 11G). However, as for Arg1 levels, a significant increase of 1.5-fold was observed in NPC-CYP mice Tgfβ levels, compared to WT-GFP, suggesting a tendency for CYP46A1 to promote the levels of this anti-inflammatory cytokine. Regarding Igf1,, which has been described as a neuroprotective factor involved in the neuroinflammatory response to brain injury[159], there is an up-regulation of the transcript levels in NPC-GFP mice of about 4.5-fold,

which was corrected by CYP46A1 expression, leading to a 33% decrease compared to NPC-GFP mice (Figure 11H).

CX_3CR1, the receptor of the CX3CL1 chemokine that acts as a regulator of microglia activation in response to brain injury or inflammation, may promote the activation of microglia and stimulate the release of inflammatory factors in pathologic frames[160]. Indeed, in NPC-GFP mice, a significant increase in Cx_3cr1 levels was registered (3.7-fold) compared to WT-GFP, which remained unaltered in the case of CYP46A1 ectopic expression (Figure 11I).

Additionally, the transcript levels of Trem2 were also determined, due to its function as a regulator of microglia activation in response to brain injury or inflammation, promoting activation and stimulating the release of inflammatory factors in pathologic frames, along with having also been described to be associated with microglial phagocytosis as well as regulation of cholesterol metabolism in microglia[60]. The levels registered a significant increase (8-fold) in NPC-GFP mice, compared to WT-GFP, and no alterations were observed after CYP46A1 expression (Figure 11J). There are still inconsistencies regarding whether this DAM protein signaling functions in a pro-inflammatory (damaging) or anti-inflammatory (reparative) manner, however, it has recently been described that the transition between activation stages of DAM is dependent on TREM2 signaling, highlighting its role in the modulation of microglia function[161].

Overall, CYP46A1 ectopic expression corrects the increase in mRNA levels of some pro-inflammatory biomarkers in NPC mice, such as Cd68 and Itgax, while it does not affect the expression of pro-inflammatory cytokines such as Tnfα, Il-1α, and Il-1β. Interestingly, CYP46A1 expression significantly up-regulates the expression levels of Arg1 and Tgfβ. Altogether, our results suggest that, concomitant with the correction of cholesterol homeostasis, CYP46A1 may lead to a decrease in neuroinflammation.

Subsequently to the analysis of the mRNA levels of microglia activation markers, which suggests CYP46A1 ectopic expression is promoting alterations in the microglia profile in NPC mice, microglia activation was further analyzed in specific regions of the mice's cerebellum, based on Iba-1 immunostaining. Previous results from our group suggested Iba-1 protein levels are differently modulated in male and female mice cerebellum, as a significant increase was only registered in NPC-GFP male mice, compared to the corresponding control (WT-GFP), which was reverted by CYP46A1 (Brito, 2020). For that reason, Iba-1 immunostaining images

are presented in separate panels for male and female mice for each cerebellar region, namely the deep nuclei, and the inner granular and molecular layers of the IV-V cerebellar lobules, with the subsequent quantification (Figures 13, 14, and 15).

As previously observed by Western-blot analysis, an increase in the fluorescence levels of the Iba-1 microglial marker was confirmed in NPC-GFP male mice, compared to WT-GFP, in the deep cerebellar nuclei (Figure 13B), and in the inner granular and molecular layers of lobules IV-V (Figures 14B and 15B, respectively).

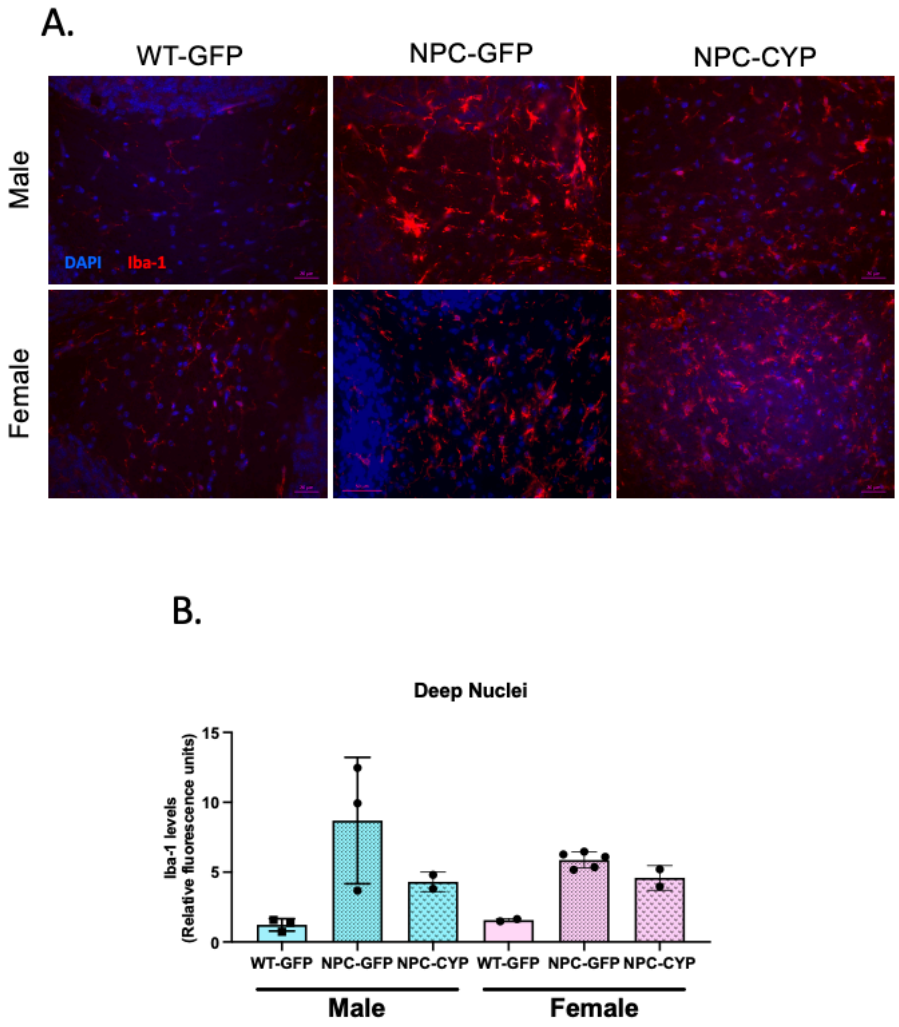

Figure 13 - Effect of CYP46A1 in the expression levels of the microglial activation marker Iba-1 in the deep cerebellar nuclei of NPC mice. Wild-type mice received a retro-orbital injection with a dose of $5x10^{11}$ vg (viral genomes) of AAVPHPeB.HA.GFP (WT-GFP) vector, while $Npc1^{tm(I1061T)}$ mice received the same dose of AAVPHPeB.HA.GFP (NPC-GFP) or AAVPHPeB.HA.CYP46A1 (NPC-CYP). Mice were injected at day 35 and sacrificed at 12 weeks of age. Parasagittal brain sections from these animals were immunostained with anti-Iba-1 antibody (red) and nuclei were stained with DAPI (blue). Fluorescent microscopy photographs of the deep cerebellar nuclei region (A) were taken and Iba-1 levels were quantified

with Image J (B). Data represents mean values ± SEM and is expressed as relative fluorescence units (scale bar: 20 µm). ANOVA one-way tests were performed followed by Tukey's multiple comparisons test.

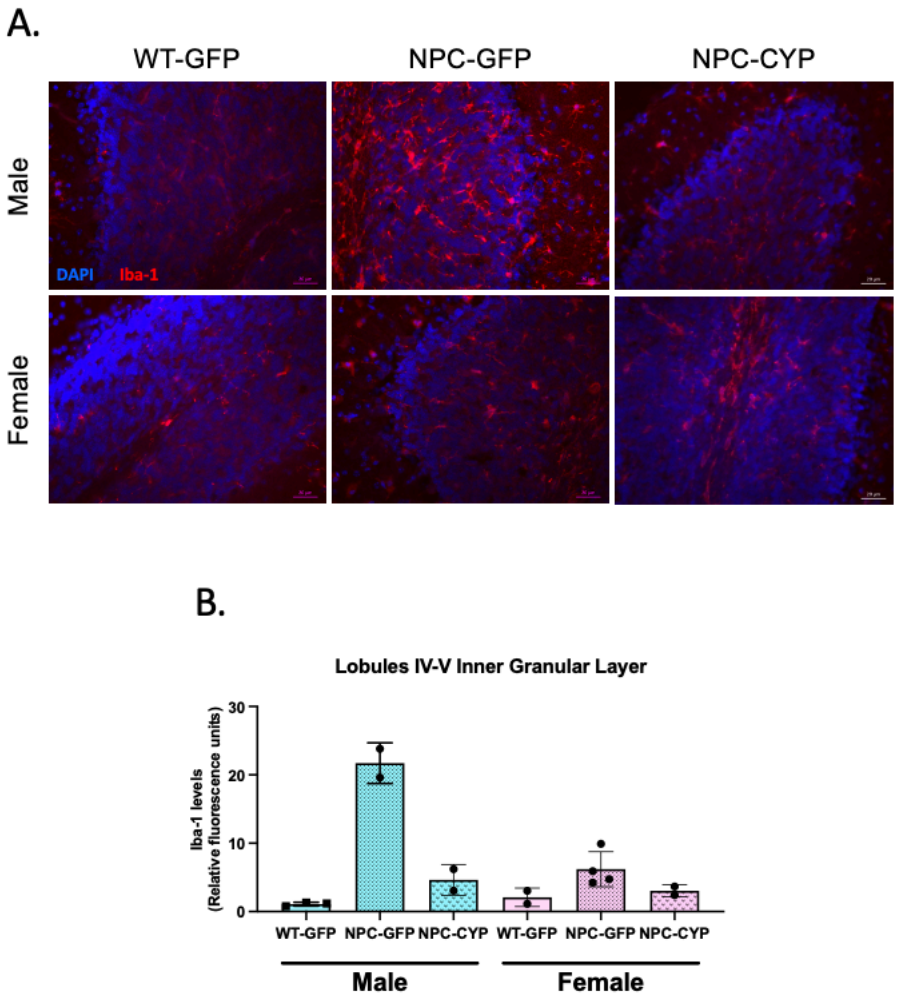

Figure 14 - Effect of CYP46A1 in the expression levels of the microglial activation marker Iba-1 in the inner granular layer of the cerebellar cortex. Wild-type mice received a retro-orbital injection with a dose of $5x10^{11}$ vg (viral genomes) of AAVPHPeB.HA.GFP (WT-GFP) vector, while $Npc1^{tm(I1061T)}$ mice received the same dose of AAVPHPeB.HA.GFP (NPC-GFP) or AAVPHPeB.HA.CYP46A1 (NPC-CYP). Mice were injected at day 35 and sacrificed at 12 weeks of age. Parasagittal brain sections from these animals were immunostained with anti-Iba-1 antibody (red) and nuclei were stained with DAPI (blue). Microphotographs of the inner granular layer of the cerebellar lobules IV-V were taken (A), and Iba-1 levels were quantified with Image J (B). Data represents mean values ± SEM and is expressed as relative fluorescence units (scale bar: 20 µm). ANOVA one-way tests were performed followed by Tukey's multiple comparisons test.

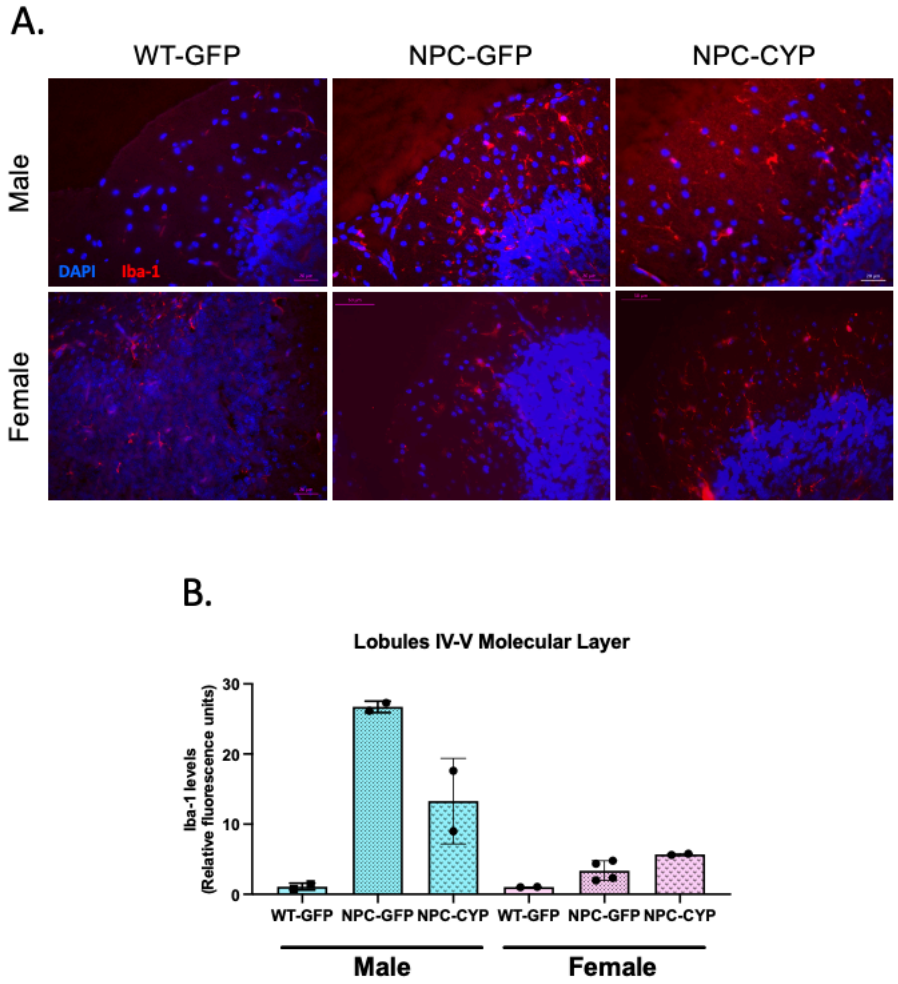

Figure 15 - Effect of CYP46A1 in the expression levels of the microglial activation marker Iba-1 in the molecular layer of the cerebellar cortex. Wild-type mice received a retro-orbital injection with a dose of $5x10^{11}$ vg (viral genomes) of AAVPHPeB.HA.GFP (WT-GFP) vector, while $Npc1^{tm(I1061T)}$ mice received the same dose of AAVPHPeB.HA.GFP (NPC-GFP) or AAVPHPeB.HA.CYP46A1 (NPC-CYP). Mice were injected at day 35 and sacrificed at 12 weeks of age. Parasagittal brain sections from these animals were immunostained with anti-Iba-1 antibody (red) and nuclei were stained with DAPI (blue). Microphotographs of the molecular layer of the cerebellar lobules IV-V were taken (A), and Iba-1 levels were quantified with Image J (B). Data represents mean values ± SEM and is expressed as relative fluorescence units (scale bar: 20 μm). ANOVA one-way tests were performed followed by Tukey's multiple comparisons test.

This increase was also observed in the cerebellar deep nuclei of female NPC mice, although not as evident in the cerebellar lobules' layers, similar to the previous protein level quantification. A tendency was observed for CYP46A1 ectopic expression to correct the increase in Iba-1 positive cells in all the analyzed cerebellar regions with the exception of the molecular layer of lobules IV-V of female mice (Figure 15B).

Neuroinflammation associated with astrogliosis is also present in NPC[79]. Astrogliosis-related gene expression was assessed in NPC mice by RT-qPCR and the transcript levels of Gfap and ApoE, were quantified in mice brain tissue (Figure 16A, B, and C). The cerebellum mRNA levels of Gfap and ApoE, as well as the cortex mRNA levels of ApoE, were significantly increased in NPC-GFP mice, compared to WT-GFP (11.3- and 3.2-fold increase in the cerebellum, respectively, and 1.4-fold for the ApoE levels in the cortex), confirming the expected glial activation. In the cerebellum, CYP46A1 was not able to revert this increase while in the cortex the ApoE mRNA levels were restored to control levels, in NPC-CYP mice. In line with what we observed for Gfap mRNA levels, previous results from our lab showed an increase in GFAP protein levels in NPC mice cerebellum (Brito, 2020).

Consistent with the increase in inflammatory gene mRNA levels in the cerebellum samples, increased astrocytic activation was observed in the NPC mice parasagittal cerebellum sections stained for GFAP. The cerebellum regions observed by confocal microscopy, namely the deep nuclei and inner granular layer (Figure 16D and E, respectively), registered a demarked increase in GFAP labeling in NPC-GFP mice, compared to WT-GFP, reflecting the expected astrocytic reactive changes in NPC mice. No evident differences were observed between NPC-GFP and NPC-CYP mice, suggesting that CYP46A1 ectopic expression does not recover the astrogliosis present in the cerebellum of NPC animals.

Bergmann glia (BG) fibers localized in the molecular layer of the cerebellum were also visualized by GFAP fluorescent labeling (Figure 16F). Mutation of the NPC1 protein has been suggested to alter the normal pattern of BG differentiation, and defects in the BG morphogenesis have previously been described in the $Npc1^{nmf164}$ mice model, which displayed BG with radial shafts that were enlarged and of irregular caliber, compared to WT littermates[161]. Indeed, we also observed this altered morphology when comparing NPC to WT mice, with enlarged radial fibers in NPC mice. As a correct development of BG is crucial for cerebellar function, including synaptic activity[162], it was assessed whether CYP46A1 expression would revert the pathologic alterations. However, no differences were observed comparing NPC-GFP and NPC-CYP mice.

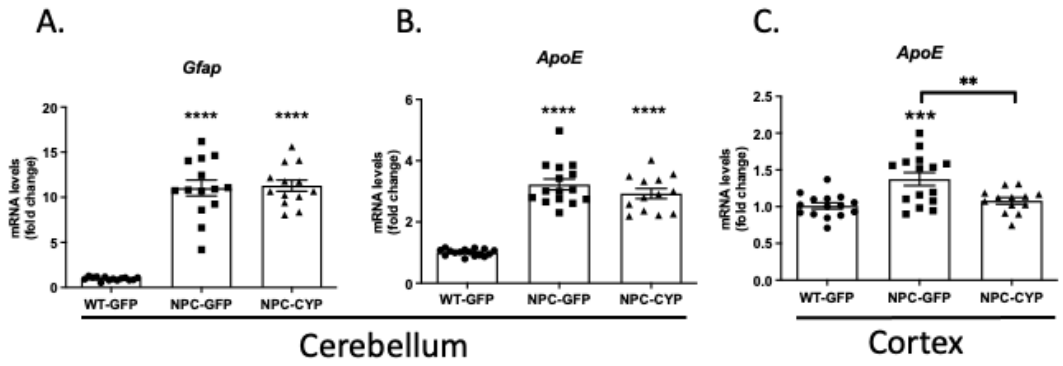
A.
Gfap
mRNA levels (fold change)
20
15
10
5
0
****
****
WT-GFP
NPC-GFP
NPC-CYP
B.
ApoE
mRNA levels (fold change)
6
4
2
0
****
****
WT-GFP
NPC-GFP
NPC-CYP
Cerebellum
C.
ApoE
mRNA levels (fold change)
2.5
2.0
1.5
1.0
0.5
0.0
**
***
WT-GFP
NPC-GFP
NPC-CYP
Cortex

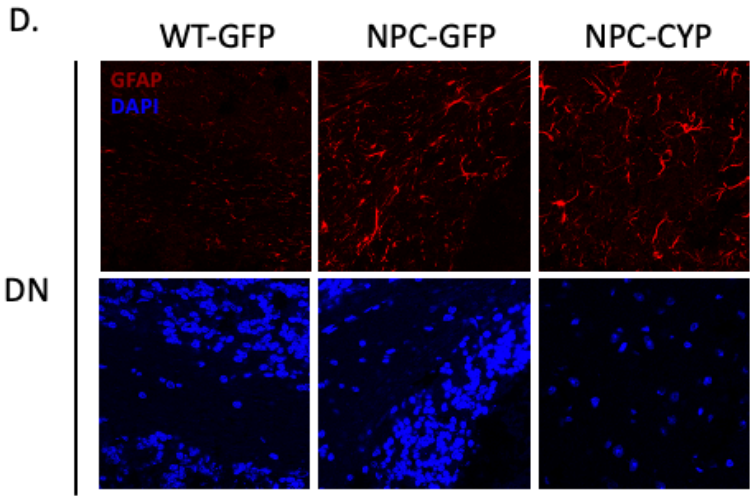
D.
WT-GFP
NPC-GFP
NPC-CYP
GFAP
DAPI
DN

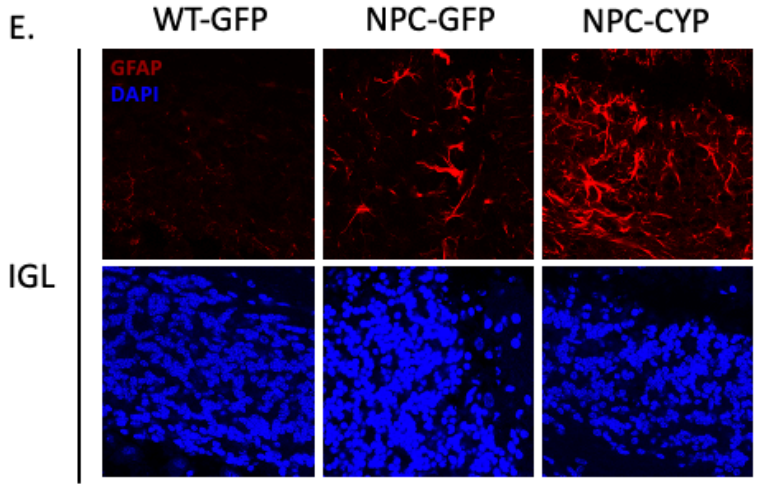
E.
WT-GFP
NPC-GFP
NPC-CYP
GFAP
DAPI
IGL

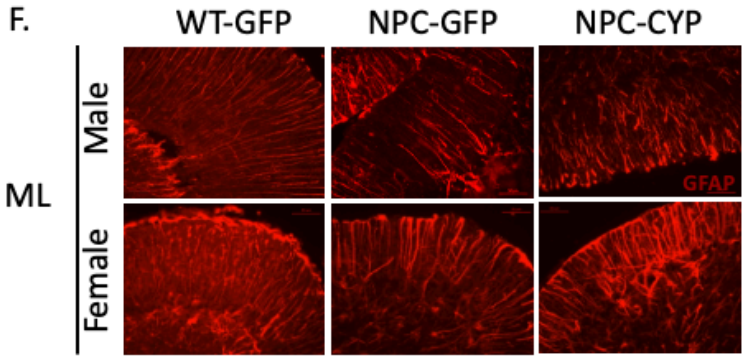
F.
WT-GFP
NPC-GFP
NPC-CYP
ML
Male
Female
GFAP

Figure 16 - CYP46A1 ectopic expression in NPC mice cerebellum does not affect astrogliosis. Wild-type mice received a retro-orbital injection with a dose of $5x10^{11}$ vg (viral genomes) of AAVPHPeB.HA.GFP (WT-GFP) vector, while $Npc1^{tm(I1061T)}$ mice received the same dose of AAVPHPeB.HA.GFP (NPC-GFP) or AAVPHPeB.HA.CYP46A1 (NPC-CYP). Mice were injected at day 35 and sacrificed at 12 weeks of age. mRNA was extracted from the cerebellum and cortex samples and transcript levels were measured by RT-qPCR using *Rpl19* and *Rpl29* as reference genes. mRNA levels in the cerebellum of Gfap (A), and ApoE (B), as well as of ApoE in the cortex samples (C), were calculated and plotted as a fold change over the average mRNA levels detected in WT-GFP mice samples and represented as mean values ±SEM (*p<0.05, **p<0.01, ***p<0.001, ****p<0.0001). Parasagittal brain sections were immunostained with anti-GFAP antibody (red), and nuclei of the deep nuclei and inner granular layer were stained with DAPI (blue). Representative confocal microscopy photographs of astrocyte morphology/activation in the deep nuclei (D) and inner granular layer of lobules IV-V (E) and representative fluorescent microscopy photographs of Bergmann glia fibers in the molecular layer of lobules IV-V (F).

4. Effect of CYP46A1 ectopic expression on neuronal cell death in NPC disease

Cerebellar ataxia, as a result of the severe loss of Purkinje neurons, is a cardinal symptom of NPC disease. The previously described beneficial effects of CYP46A1 expression in restoring brain cholesterol homeostasis and reducing neuroinflammation in NPC animals led us to evaluate if CYP46A1 would display a correcting effect on Purkinje cell density. For the visualization of the Purkinje cells, mice parasagittal cerebellum sections were stained with Cresyl Violet, and the number of Purkinje cells per mm of cell layer length, of each cerebellar lobule was counted for the WT-GFP, NPC-GFP, and NPC-CYP mice (Figure 17A and B). As expected, neuronal loss was evident in NPC mice, with a significant decrease in Purkinje cell density in NPC-GFP mice compared to WT-GFP littermates. This decrease was more striking in the anterior zone, which comprises the cerebellar lobules I-V, compared to the central zone, which includes the lobules IX-X. These region-specific differences result from the progressive neurodegenerative process where Purkinje cell loss starts from the anterior zone to the posterior zone[163]. Even though still noticeable, neuronal loss was least apparent in the lobules IX-X, where Purkinje cells are still mostly preserved in the later stages of the disease. Comparing the Purkinje cell density between NPC-GFP and NPC-CYP mice, surprisingly, there were no striking differences, indicating that CYP46A1 ectopic expression did not reverse the Purkinje cell degeneration process.

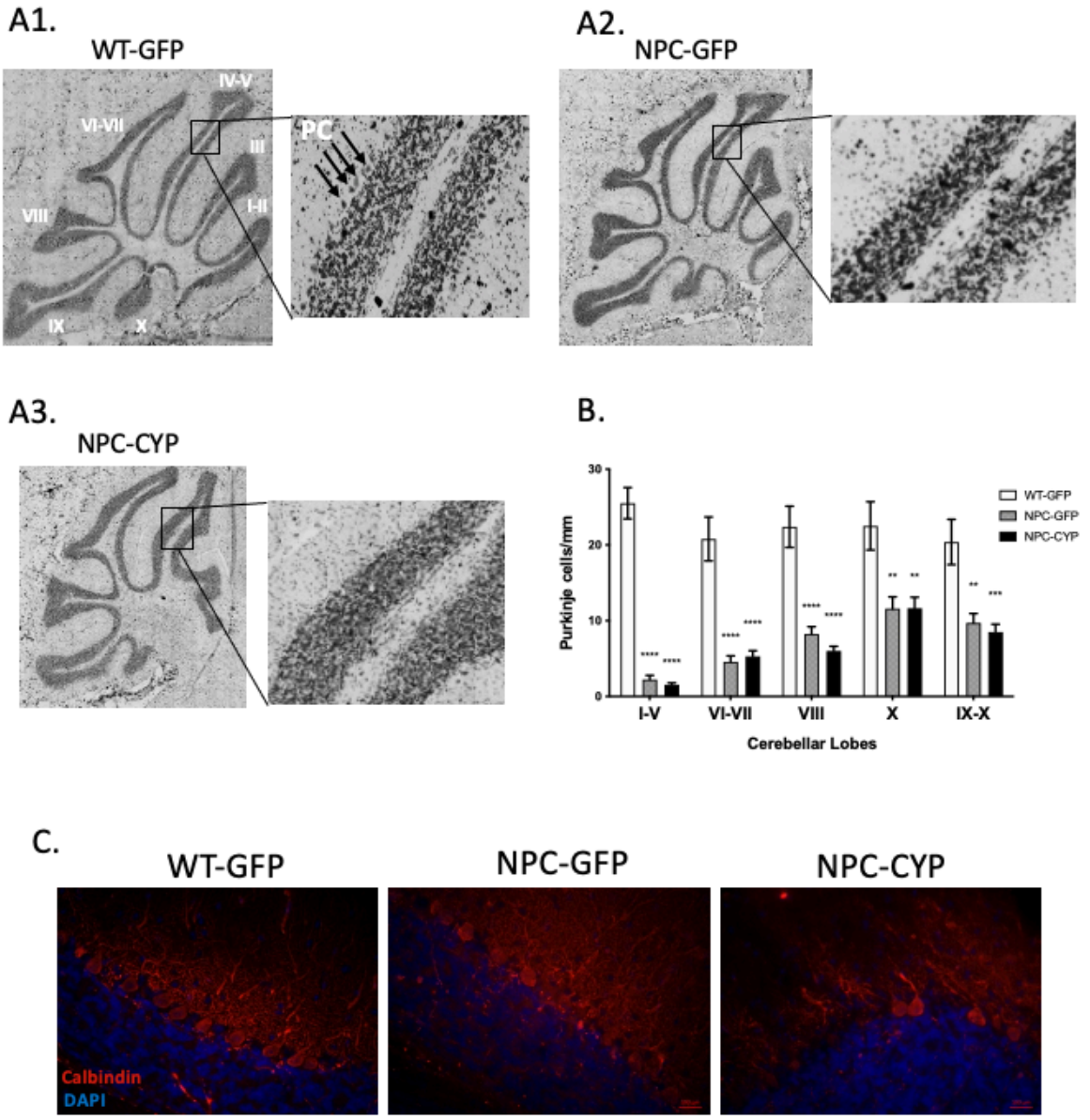

Figure 17 - Effect of CYP46A1 ectopic expression on cerebellar/Purkinje cell neuropathology. Wild-type mice received a retro-orbital injection with a dose of $5x10^{11}$ vg (viral genomes) of AAVPHPeB.HA.GFP (WT-GFP) vector, while $Npc1^{tm(I1061T)}$ mice received the same dose of AAVPHPeB.HA.GFP (NPC-GFP) or AAVPHPeB.HA.CYP46A1 (NPC-CYP). Mice were injected at day 35 and sacrificed at 12 weeks of age. Parasagittal brain sections from these animals were subjected to Cresyl Violet staining, allowing the visualization of Purkinje cells in the cerebellum. WT-GFP (A1), NPC-GFP (A2), and NPC-CYP (A3) Purkinje cells (PC) were counted, and the length of the Purkinje cells layers was measured in each cerebellar lobe, allowing the determination of the Purkinje cell density (B). Data are presented as mean values ± SEM. ANOVA one-way tests were performed followed by Tukey's multiple comparisons test (*p<0.05, **p<0.01, ***p<0.001 and ****p<0.0001 vs WT-GFP). For further confirmation of Purkinje cell loss, parasagittal brain sections from these animals were also subjected to calbindin and DAPI staining, as calbindin allows the visualization of Purkinje cells. Similar regions of the lobules IV-V of the calbindin-stained cerebellum of WT-GFP, NPC-GFP, and NPC-CYP mice are represented (Panel C).

In order to further confirm Purkinje cell loss, mice parasagittal cerebellum sections were processed for immunofluorescent staining for calbindin, a protein belonging to the large superfamily of cytoplasmic calcium-binding proteins, that is expressed in the brain and particularly concentrated in the Purkinje cells[164] (Figure 17C). The stained sections revealed a similar loss in Purkinje cell number, reflecting a demarked degeneration between NPC-GFP mice and WT-GFP littermates, which is not corrected by CYP46A1 ectopic expression.

5. Effect of CYP46A1 ectopic expression on autophagic flux dysfunction in NPC disease

NPC disease is also featured by autophagic flux impairment, which has been suggested, in previous studies from our group, to be partially corrected in NPC mice by CYP46A1 ectopic expression, as a decrease in LC3II/I levels was observed in the cortex of NPC-CYP when compared to WT-GFP mice (Brito, 2020).

As defects in lysosomal function are associated with autophagy impairment in NPC, we first determined if the mRNA levels of the lysosomal enzyme Cathepsin D were affected in NPC mice cerebellum (Figure 18).

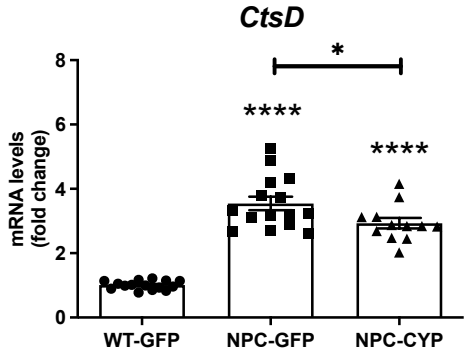

Figure 18 - CYP46A1 ectopic expression partially corrects the mRNA levels of Cathepsin D (CtsD) in NPC mice cerebellum. Wild-type mice received a retro-orbital injection with a dose of $5x10^{11}$ vg (viral genomes) of AAVPHPeB.HA.GFP (WT-GFP) vector, while $Npc1^{tm(I1061T)}$ mice received the same dose of AAVPHPeB.HA.GFP (NPC-GFP) or AAVPHPeB.HA.CYP46A1 (NPC-CYP). Mice were injected at day 35 and sacrificed at 12 weeks of age. mRNA was extracted from cerebellum samples and transcript levels were measured by RT-qPCR using *Rpl19* and *Rpl29* as reference genes. mRNA levels of cathepsin D were calculated and values were plotted as a fold change over the average mRNA levels detected in WT-GFP mice samples and represented as mean values ±SEM (*p<0.05 and ****p<0.0001).

Indeed, a significant increase was observed in NPC-GFP animals compared to WT-GFP mice, while CYP46A1 ectopic expression was able to partially rescue this lysosomal deregulation, leading to a decrease of 17% in the Cathepsin D transcript levels in NPC-CYP mice. These results further confirm a beneficial effect of CYP46A1 expression in restoring lysosomal/autophagic activity *in vivo*.

In order to better understand the role of CYP46A1 in correcting the autophagic flux in NPC disease, we analyzed markers of autophagy activation in cellular models of NPC disease, by analyzing LC3II/I levels and p62 protein levels, p70S6K phosphorylation, and mRNA levels of mTOR pathway and autophagy core markers. We started by analyzing if CYP46A1 ectopic expression could correct the accumulation of lipidated LC3 levels characteristic of the impairment in autophagic flux observed in the NPC disease. For that, we transduced fibroblasts from NPC human patients carrying the I1601T mutation with adenovirus coding for CYP46A1 (adCYP) or a control virus (adGFP) (Figure 19). As expected, we observed a 2-fold increase in LC3II/I ratio in NPC fibroblasts, compared to WT. Once more, CYP46A1 expression led to a correcting effect in the accumulation of LC3-II-containing vesicles comparable to WT fibroblasts.

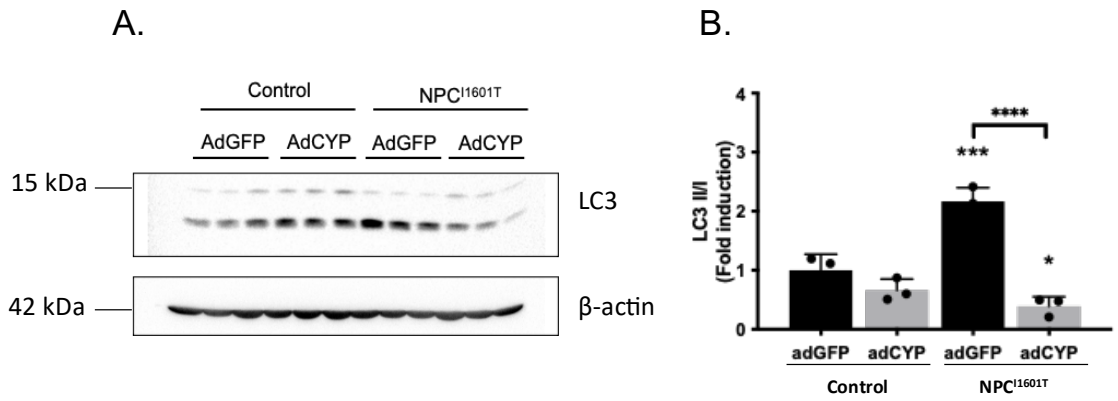

Figure 19 - Effect of CYP46A1 expression on LC3II/I ratio in fibroblasts from NPC patients carrying the I1061T mutation. CYP46A1 expression was increased in WT and NPC fibroblast cells by administration of CYP46A1 adenovirus (adCYP). For control, other WT and NPC fibroblast cells were also administered GFP adenovirus (adGFP). Total extracts were prepared and analyzed by Western Blot. The immunoblots shown are representative of the results obtained in three different experiments (A). Protein levels were calculated and plotted for WT and NPC fibroblast cells (B) (*p<0.05, ***p<0.001, and ****p<0.0001).

To further dissect the mechanisms by which CYP46A1 is promoting the restoration of the endo-lysosomal and autophagic flux in NPC, we used a human cellular model, the NPC1-KO HeLa

cells. We started by confirming the previously reported effect of CYP46A1 in correcting LC3II/I levels. For that, NPC1-KO HeLa cells were transduced with CYP46A1-encoding adenovirus or control virus, for 48 and 72 h (NPC1-KO adGFP/adCYP), and, in parallel, WT HeLa cells were transduced with adGFP control vector (WT adGFP). The protein levels of LC3II/I, p62 levels, and phospho-p70S6K/p70S6K were evaluated by Western-blot analysis, to assess the autophagic flux status (Figure 20).

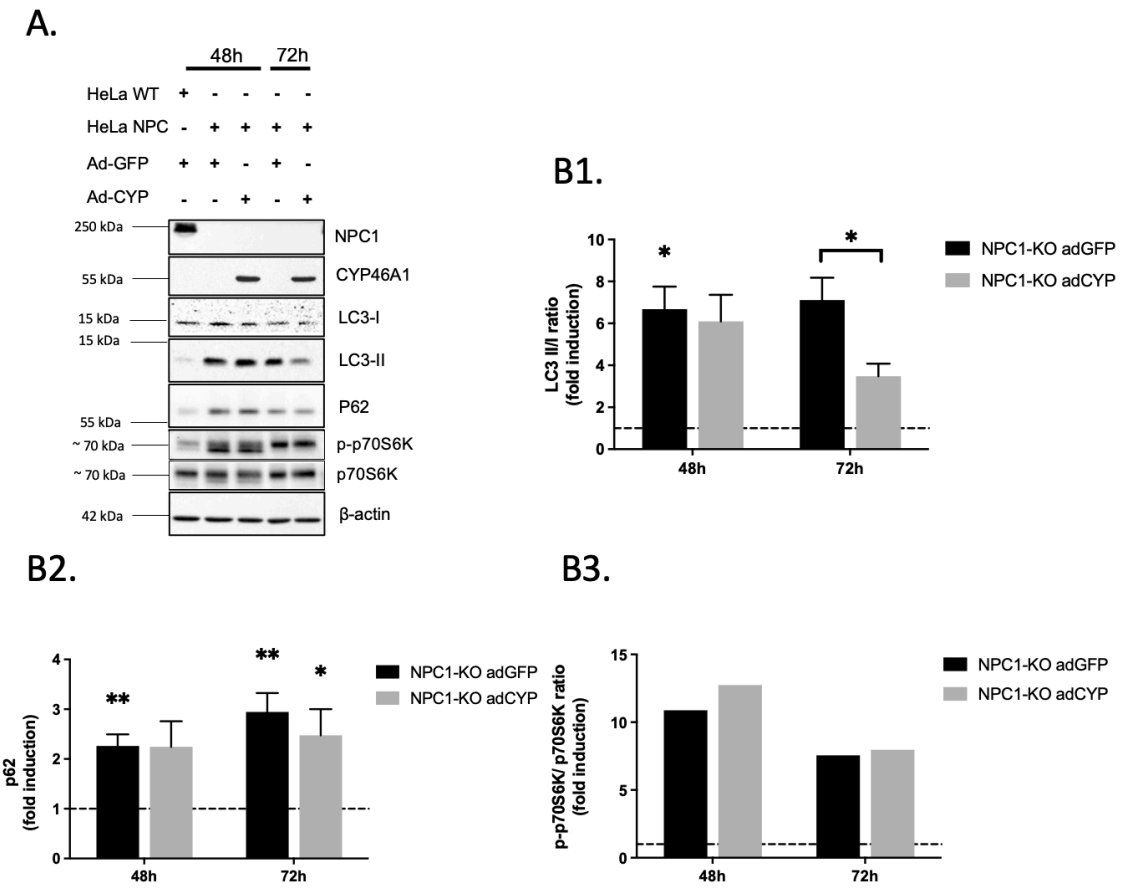

Figure 20 - Effect of CYP46A1 ectopic expression on autophagy markers in NPC1-KO HeLa cells. CYP46A1 expression was increased in WT and NPC1-KO HeLa cells by transduction with CYP46A1 adenovirus (adCYP). To be used as control, WT and NPC1-KO HeLa cells were transduced with GFP-encoding adenovirus (adGFP). Total extracts were prepared from treatment time points 48 and 72 h and analyzed by Western Blot. The immunoblots shown are representative of the results obtained in 2 to 4 independent experiments (A). Levels of LC3II/I, p62, and phospho-p70S6K/p70S6K (p-p70S6K/p70S6K) were calculated and plotted (B1, B2, and B3 respectively) (*p<0.05, **p<0.01).

As expected, LC3II/I levels were significantly increased in NPC1-KO adGFP cells compared to WT adGFP, at both time points, 48 and 72 h (6.7- and 5.7-fold, respectively). However, at 72 h of treatment, CYP46A1 expression led to a significant decrease of LC3II/I ratio in NPC1-KO cells, compared to NPC1-KO adGFP (0.6-fold), confirming the previous results obtained

in other models of the disease. Similar to the LC3II/I ratio, the protein levels of p62, another widely used autophagy marker, were also significantly increased in NPC1-KO adGFP cells compared to WT adGFP, at both time points (2.3-fold at 48h, and 3-fold at 72h). However, p62 protein levels remained elevated in NPC1-KO adCYP cells, suggesting that the autophagy flux block is not being fully reverted by CYP46A1, particularly the degradation of p62 in the autolysosomal vesicles. Additionally, mTOR complex 1 (mTORC1) hyperactivation has been described in NPC models[165]. Since this complex is a major modulator of autophagy inhibition we evaluated if CYP46A1 could positively impact the normalization of mTORC1 activity. The phosphorylation status of the mTOR downstream target p70S6K was used to assess mTOR activation. The results presented in Figure B3 are from two independent experiments with high variability. Nevertheless, an increased phosphorylation status of p70S6K was registered in NPC1-KO adGFP cells, compared to WT adGFP. However, no differences were observed after CYP46A1 expression, suggesting that, despite the improvement in the autophagic flux, CYP46A1 is not able to revert the endogenous signal responsible for the activation of this specific pathway. However, more experiments must be done to confirm this result.

To gain a deeper insight into the effect of CYP46A1 in the autophagy status of NPC1-KO HeLa cells we analyzed the transcript levels of genes involved in the mTOR pathway and of diverse markers of autophagy activation by RT-qPCR (Figure 21). The mRNA levels of MTOR, the key component of the autophagy inhibitor mTORC1 complex, and ULK1, which plays a key role in autophagy initiation, are downregulated in NPC1-KO adGFP, compared to the control, CYP46A1 expression did not affect ULK1 expression levels. In parallel, the transcript levels of PRKAA1 (AMPK), a negative regulator of the mTORC1 complex, were also assessed, although no significant differences were observed.

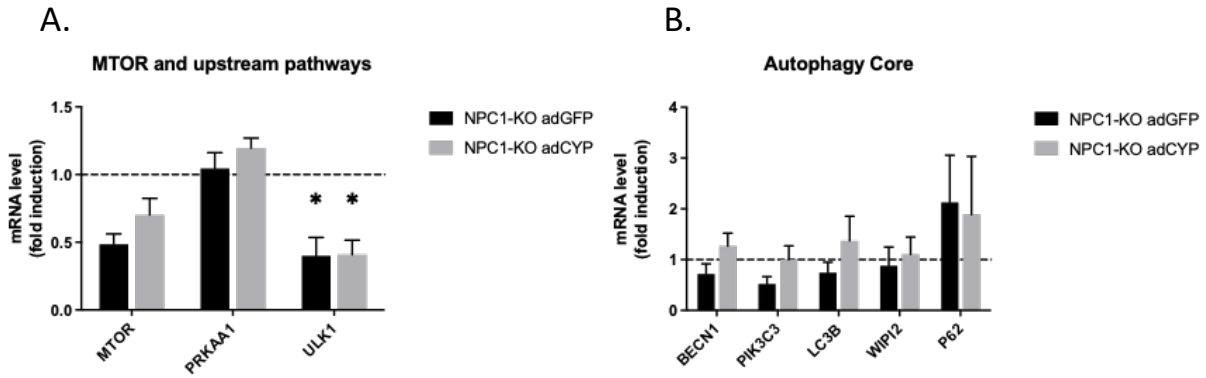

Figure 21 - Effect of CYP46A1 ectopic expression on the mRNA levels of markers of mTOR pathway and of autophagy core genes in NPC1-KO HeLa cells. WT and NPC1-KO HeLa cells were transduced with an adenoviral vector encoding CYP46A1 (adCYP) or with a control vector (adGFP). mRNA was extracted and levels of genes involved in mTOR and upstream pathways (A) and in autophagy (B) were measured by RT-qPCR. mRNA levels of Mammalian Target of Rapamycin (MTOR), Protein Kinase AMP-Activated Catalytic Subunit Alpha 1 (prkaa1), Unc-51 Like Autophagy Activating Kinase 1 (ULK1), Beclin 1 (BECN1), Phosphatidylinositol 3-Kinase Catalytic Subunit Type 3 (PIK3C3), Microtubule-Associated Protein 1 Light Chain 3b (LC3B), WD Repeat Domain, Phosphoinositide Interacting 2 (WIPI2), and of Sequestosome 1 (P62) were quantified. Values were normalized to *RPL19* as a reference gene and plotted as a fold change over the average mRNA levels detected in WT-GFP samples. Data represent mean values ±SEM of 4 to 6 independent experiments (*$p<0.05$ vs. WT-GFP).

Overall, the transcript levels of several autophagy markers analyzed, namely, BECN1, PIK3C3, LC3B, and WIPI2 showed a tendency for a decrease in NPC1-KO adGFP compared to WT adGFP (Figure 21B), while CYP46A1 ectopic expression seems to increase the expression levels of these genes, to values similar to those found in WT cells. Additionally, in agreement with what was observed at the protein levels, the increased mRNA levels of P62 registered in NPC-KO adGFP cells were not significantly affected by CYP46A1 ectopic expression. Although these preliminary results require further confirmation, the autophagy-related transcriptome analysis points to a global downregulation of autophagy markers and players, that seems to be partially corrected by CYP46A1, further elucidating the molecular mechanisms by which this neuronal-specific cytochrome P450 is promoting the autophagic flux in NPC cells.

Part IV - Discussion and future perspectives

The NPC disease originates from mutation of the NPC1 protein, which is responsible for the egress and recycling of lipoprotein-derived cholesterol from LE/L towards the ER or plasma membrane[66]. The accumulation of unesterified cholesterol in LE/L and deregulation of cholesterol homeostasis are the main hallmarks of this progressive and fatal neurodegenerative and lysosomal storage disorder[166].

Considering the role of CYP46A1, the neuron-specific enzyme that catalyzes the major brain cholesterol removal pathway, we hypothesized that increasing the expression of CYP46A1 would be beneficial in NPC. Indeed, previous studies from our group demonstrated that ectopic expression of CYP46A1 in fibroblasts of NPC patients carrying the I1061T mutation led to a remarkable amelioration of the cholesterol accumulation in LE/L and, overall, of the pathological phenotype (Moutinho et al., unpublished results).

To understand if CYP46A1 could improve the pathological NPC phenotype *in vivo*, the $NPC1^{tm(I1061T)}$ mouse model was used. This model has the knock-in of the $NPC1^{I1061T}$ mutation, the most prevalent in human NPC patients, which encodes a misfolded protein that has reduced half-life, as it is targeted for ER-associated degradation[167]. Therefore, the pathologic features faithfully recapitulate those in human NPC disease, including the characteristic decreased motor coordination, brain lesions, particularly in the cerebellar area leading to Purkinje cell death, dendritic and axonal abnormalities, lipid storage, and premature death.

In this *in vivo* model, CYP46A1 ectopic expression ameliorated liver-injury-related parameters, namely liver-to-body weight, and serum levels of alanine aminotransferase, by significantly reversing the pathological increase observed in NPC mice. Body weight loss is a hallmark of NPC disease and CYP46A1 was able to partially prevent the decrease in body weight gain of NPC female mice. This effect was, however, not observed in males. In fact, upon handling, the male mice appeared to display an aggravated disease phenotype, which could be due to variability in disease symptomatology[67].

Total cholesterol levels were also determined in NPC mice's cerebellum and cortex, where no differences were observed between the experimental groups. In fact, although NPC is characterized by cholesterol accumulation, it is also featured by severe progressive neurodegeneration, which results in demyelination and loss of the associated cholesterol, which

blocks out the unesterified cholesterol accumulation. This way, previous reports have detected a decrease in cholesterol levels in specific areas, such as the midbrain, brainstem, and spinal cord, where demyelination is most prominent[168-170]. However, as different regions of the CNS display variable amounts of white matter, demyelination does not affect the cerebellum and cortex regions at such an impactful rate, which explains why these regions did not register the described decrease in cholesterol levels. This way, and despite the absence of an effect regarding CYP46A1 ectopic expression in NPC mice, the characteristic intracellular unesterified cholesterol accumulation was confirmed in the Npc1$^{tm(I1061T)}$ mice model, due to an increase in filipin staining of mice parasagittal brain sections consistent to what was previously described in this model[171]. Strikingly, the significant decrease in filipin labeling registered in NPC-CYP mice, compared to NPC-GFP, suggested that CYP46A1 ectopic expression promotes a redistribution of the accumulated cholesterol within the cells, in agreement with our *in vitro* data.

Furthermore, the gene expression analysis that we performed suggested that the cerebellar and cortex cells appear to be adapting to this cholesterol mobilization. The dysregulated cholesterol homeostasis observed in the NPC phenotype was consistent with what had been previously described by our group (Brito, 2020) and was characterized by a significant decrease in cholesterol synthesis (*Hmgr* and *Hmgs1*) and uptake (*Ldlr*), along with increased cholesterol efflux (*Abca1*) and esterification (*Acat1*). This deregulation was significantly recovered by CYP46A1 ectopic expression, as it was able to restore to levels similar to those registered in WT-GFP, confirming an *in vivo* beneficial effect. This effect is most likely due to the cholesterol redistribution, and consequent decrease of LE/L cholesterol loading promoted by CYP46A1 expression, leading SREBP2, a key transcription factor that regulates cholesterol synthesis and uptake, to sense a decrease in accumulated cholesterol, therefore initiating a process towards cholesterol synthesis. This is also suggested by CYP46A1 ectopic expression being able to revert the decreasing tendency of Srebp2 transcript levels registered in NPC-GFP mice, a tendency that could be translated into an indication of increased cholesterol availability at the ER, as the levels in NPC-CYP mice even overcame those registered in WT-GFP[172]. It would be interesting to evaluate the nuclear localization of SREBP2 in the brain of NPC-GFP and NPC-CYP mice.

Overall, the results suggest that CYP46A1 normalizes cholesterol homeostasis in the brain and is promoting the egress of cholesterol from the LE/L compartments by an alternative pathway,

that is either independent of the NPC1 protein or that works in parallel to the NPC1-mediated route. In the future, understanding the mediators of this effect would be of interest, as cholesterol metabolism dysregulation is featured in a variety of pathologic conditions, for which new targets could therefore be described. Alternatives to be studied in the future may include CYP46A1 promoting an ABCA1-mediated efflux of endolysosomal cholesterol, as overexpression of this transporter in NPC-deficient fibroblasts has been shown to reduce the accumulation of cholesterol[173,174], or promoting a vesicle-mediated transport pathway such as [^{3}H]cholesterol efflux via HDL re-secretion, which is independent of the disturbed cholesterol uptake pathway via the LDLR[175]. Also, although NPC1 constitutes the major pathway, it has been shown to be dispensable for the RIDα/ORP1L-dependent egress route of LDL-cholesterol to an ER pool of cholesterol that is accessible to ACAT1 for esterification and storage in lipid droplets[176]. In fact, RIDα has previously been reported to be able to rescue the cholesterol storage in NPC fibroblasts by increasing lipid droplets' formation via a mechanism that depends on ORP1L[176,177]. As preliminary results have suggested CYP46A1 increases lipid droplets in the NPC mice liver, this option would be interesting to be further addressed, although this effect has not yet been assessed in the brain tissue.

The fact that cholesterol homeostasis regulators are responding and adapting to the corrections being promoted by CYP46A1 further indicates that the enzyme is leading to a recovery of cholesterol deregulation. Therefore, the effect of CYP46A1 ectopic expression was further assessed regarding other pathologic aspects characteristic of the NPC disease that are aggravated by cholesterol accumulation, namely lysosomal dysfunction. As cholesterol accumulation mainly occurs at the lumen and limiting membrane of LE/L, it results in enlarged lysosomes that present defects at a morphological, trafficking, and functional level[165]. Lysosomal dysfunction was confirmed by elevated mRNA levels of Cathepsin D in the cerebellum of NPC mice. Indeed, higher levels and increased activity of Cathepsin D have previously been identified in the Npc1$^{-/-}$ mice model[131]. This dysregulation was partially reverted in NPC-CYP mice, suggesting CYP46A1 ectopic expression could ameliorate this outcome.

Another consequence of cholesterol accumulation within the LE/L in NPC is the hyperactivation and recruitment of mTORC1 at the lysosomal surface[165]. The mTORC1 activation requires a cholesterol-regulated motif, contained in the lysosomal transmembrane protein SLC38A9, and occurs due to stimulation by accumulated cholesterol of the protein

complex also involved in amino acid-dependent mTORC1 activation, composed of GTPases, their membrane anchor Ragulator, and the lysosomal amino acid permease SLC38A9[165, 178-181]. In a non-pathologic frame, the NPC1 protein not only regulates cholesterol export from lysosomes, decreasing, therefore, the trigger for mTORC1 activation, but also binds to SLC38A9, further inhibiting the complex's signaling[165,178]. Upon phosphorylation by the PI3K/AKT signal transduction pathway, the activated mTORC1 promotes the phosphorylation of p70S6K, among other downstream targets[182]. The phosphorylation status of p70S6K is, therefore, a widely used marker of mTOR activity and was analyzed in the used NPC cellular model containing the knock-out of NPC1 protein (NPC1-KO HeLa cells)[183]. Indeed, the described mTORC1 hyperactive state was corroborated by the immunoblotting results, where increased phosphorylation of the p70S6K protein in NPC1-KO ad-GFP HeLa cells, compared to WT ad-GFP HeLa cells, was detected.

Preliminary studies from our group had previously assessed whether CYP46A1 increased expression would be able to correct this autophagy flux impairment in NPC. For that, the levels of LC3II/I ratio were measured by immunoblotting in the cortex of AAV-CYP and -GFP-treated NPC1$^{tm(I1061T)}$ mice. As preliminary results from our group showed that the increase of LC3II/I levels in NPC-GFP mice was partially corrected by CYP46A1 ectopic expression, we further investigated the correcting role of CYP46A1 by resorting to other NPC models, namely human NPC1^{I1061T} fibroblasts and NPC1-KO HeLa cells. The human NPC1^{I1061T} patients' fibroblast cells were first used to show the effect of CYP46A1 ectopic expression on lysosomal cholesterol accumulation. A similar response was obtained in both models regarding LC3II/I levels, as there was a significant increase observed in NPC fibroblast and NPC1-KO HeLa cells treated with ad-GFP, which was consistent with previous reports, that also described an increase in LC3II levels in NPC models[136,184,185]. Even though the mechanism through which alterations in cholesterol homeostasis in lipid-storage disorders might perturb autophagy has still to be completely understood, the increase in LC3II/I levels in the NPC models has previously been described to be due to an impairment in autophagosome maturation, as they fail to fuse with late endosomes, compromising amphisome formation, as previously mentioned[136].

Autophagy dysfunction was also corroborated upon quantification of the transcript levels of autophagy core genes BECN1, PIK3C3, LC3B, and WIPI2 in NPC mice cerebellum. These genes were downregulated in NPC mice and the results also pointed to CYP46A1 ectopic expression being able to revert this global decrease. Although these corrections of autophagy

at the transcriptional level promoted by CYP46A1 were not significant, the block in autophagosome maturation (and further degradation) present in NPC1-KO HeLa cells was significantly corrected by CYP46A1, as a robust decrease was registered in LC3II/I ratio in NPC1-KO ad-CYP cells. As the autophagic cargo clearance is being restored in the ad-CYP-transduced NPC1 mutant cells, and CYP46A1 is promoting the re-establishment of the autophagic flux, these alterations are eventually sensed by the cell's autophagy controlling mechanisms, which might be leading to signaling for the autophagy core genes transcript levels to be increased. Interestingly, SREBP2 has been shown to directly activate autophagy genes during cell sterol depletion, conditions known to induce both autophagy and nuclear SREBP2 levels. Additionally, SREBP2 knockdown during nutrient depletion decreased autophagosome formation and lipid droplet association of the autophagosome targeting protein LC3[186]. Since we observe an increase in SREBP2 transcript levels, it would be interesting to see if the CYP46A1 effect is dependent on the restoration of cholesterol homeostasis and SREBP2 activation. In order to further understand how CYP46A1 is promoting the re-establishment of the autophagy flux, we have initiated experiments to evaluate the colocalization of LC3- and Rab7-positive vesicles in NPC1-KO ad-GFP/ad-CYP HeLa cells, in order to assess if CYP46A1 is promoting amphisome formation, which we intend on proceeding to develop in the future.

Consistent with previous studies[136,184,185], the autophagy block late in the pathway observed in the NPC1-KO HeLa cells was also associated with an accumulation of autophagy substrate p62, which targets specific cargo for autophagic clearance, promoting its engulfment into the forming autophagosomes[187,188]. Although CYP46A1 promoted autophagosome degradation - as verified by a decrease in LC3II/I ratio, the accumulation of p62 protein was not affected by CYP46A1. This, along with Cathepsin D mRNA levels in NPC-CYP mice not being entirely reverted to values similar to WT-GFP, suggests that the lysosomal proteolytic capacity may not be fully recovered by CYP46A1. Previous studies by Davis et al. have disclosed how NPC-affected lysosomes display profound proteolytic impairment, likely due to a depletion of several hydrolases that could originate either from their transcriptional inhibition or defective trafficking[165]. An increased propensity for membrane damage has also been shown for NPC-affected lysosomes, which could further promote a decrease in hydrolases, due to consequent leakage[165,189]. Although the factors that promote this membrane damage are still to be determined, possible causes include either accumulation of cholesterol, forming discontinuities and leading to alterations in the limiting membrane fluidity, or accumulation of undigested cargo within the lumen, that can pierce through the membrane. Either the extensive hydrolase

depletion or leakage may be explanatory as to why the lysosomal function is only partially restored by CYP46A1. Therefore, further studies designed to quantify resident lysosomal hydrolases in the cellular models used in this work, NPC1-KO Hela cells, or human patient fibroblast cells would be of interest. Quantification of important markers including Cathepsin Z protease, the acid lipase (LIPA), or other enzymes involved in the degradation of glycans and glycosphingolipids, such as galactosylceramidase (GALC) and N-acetyl-alpha-glucosaminidase (NAGLU), which have all been suggested by previous studies to be decreased in $Npc1^{-/-}$ mice, would further elucidate CYP46A1 effect[165].

Microgliosis is the first evidence of neuroinflammation in NPC, and previous studies have suggested that targeting this hallmark decreases the rate of neuronal loss, slowing disease progression and therefore increasing the longevity of NPC mice[68]. The microglia activation profile of $Npc1^{-/-}$ mice has been previously described through single-cell transcriptome analysis, consisting of deregulation of pro- and anti-inflammatory markers, which was in accordance with our transcriptomics' results[60]. The NPC-associated microglia profile was characterized by the upregulation of pro-inflammatory markers *Cd68* and *Itgax* - indicators of the NPC microglia's reactive amoeboid state, as well as of pro-inflammatory cytokines *Tnfα*, *Il-1α*, and *Il-1β*. Interestingly, sex-specific differences were observed in the transcript levels of Il-1β, which have never been described in this animal model or in NPC patients, and, therefore, identifying the factors that contribute to this effect may lead to the development of novel therapeutic strategies to treat NPC disease. Regarding microglia markers that typically indicate an anti-inflammatory response, Arg1 and Tgfβ transcript levels were not altered in the NPC phenotype, while Igf1 levels were significantly increased. Levels of the modulator of microglia function Trem2 also registered a significant increase in NPC mice. Only the increase in Cx_3cr1 transcript levels was not in conformity with what has previously been described, which could be explained due to our analysis being directed to cerebellum tissue, while the mentioned description was based on single-cell analysis. Also, the use of different animal models may underlie some of the observed differences.

CYP46A1 ectopic expression recovered the dysregulation of some pro-inflammatory biomarkers in NPC mice, as Cd68 and Itgax levels were corrected, while the levels of pro-inflammatory cytokines Tnfα, Il-1α, and Il-1β were not affected. CYP46A1 expression also promotes markers of anti-inflammatory microglia profile, by significantly up-regulating the levels of Arg1 and Tgfβ. Overall, these results suggest CYP46A1 to be leading to a decrease in

neuroinflammation, by promoting the correction of the deregulated levels of some microglia pro-inflammatory markers while promoting anti-inflammatory markers, correlated to a more neuroprotective and healing activation profile. Subsequent to transcriptomic studies of NPC microglia still being limitedly available, future studies regarding a deeper characterization in NPC would be of interest. Also, exploring the effect of CYP46A1 expression on a wider variety of microglial activation markers and modulators, namely the anti-inflammatory IL-10, which affects the microglia activation profile, would be elucidative[190].

This overall correcting effect of CYP46A1 towards microglial activation was further confirmed by a tendency to decrease the dysregulated Iba-1 levels observed in NPC mice. As observed in previous results (Brito, 2020), there is an increase in Iba-1 protein levels in the NPC mice cerebellum, which is mostly present in male mice. Although in male mice the effect was more demarked, a tendency for CYP46A1 to revert Iba-1 increased levels was also observed in female mice, except in the molecular layer. Due to the variability in the microglial activation marker levels, it would be interesting to further assess the NPC microglia morphology in future studies. Also, as recent studies have reported microglial phagocytic capacity to be altered in NPC, with increased uptake being observed[66], a possible therapeutic potential for modulation of microglial activation has been suggested and should be further analyzed.

As the neurodegenerative cascade initiated by microglia activation in NPC leads to astrocytosis, the effect of CYP46A1 was assessed on this neuroinflammatory hallmark as well. A significant increase in Gfap and ApoE transcript levels was detected, as previously registered in this animal model[67], which was further confirmed by GFAP immunostaining in mice brain sections. However, our preliminary results suggest that the increased cerebellar astrocytic activation was not recovered by CYP46A1.

Although crucial pathological features of the disease including cholesterol homeostasis, lysosomal and autophagy dysfunction, as well as microglia activation, were improved in response to CYP46A1 ectopic expression, no ameliorations were observed regarding the NPC-characteristic Purkinje cell death in mice cerebellum. Unesterified cholesterol accumulation has frequently been indicated as the main cause of neuronal cell death and most developed drug screenings have been directed to LE/L cholesterol storage and modulation of cholesterol regulation. That includes HDAC inhibitors, which have been reported to reduce the cholesterol accumulation in fibroblasts derived from NPC patients and are extensively indicated as viable therapeutics for NPC. However, the fact that restoring cholesterol homeostasis is not sufficient

to entirely revert the disease phenotype has already been previously suggested, as, besides cholesterol, the NPC-affected LE/L of most cell types also accumulate other lipids, namely glycosphingolipids, which have been shown to be centrally involved in the neuropathogenesis of the disorder. In fact, the only approved drug for NPC is miglustat, which efficiently crosses the BBB and inhibits the glycosphingolipids' synthesis pathway by blocking the key enzyme glucosylceramide synthase, leading to delayed onset of neurological dysfunction and reduced neuronal cell death in human patients and other NPC models[192]. This suggests a more in-depth analysis of the accumulated lipids and the mechanisms leading to Purkinje cell death in NPC should be addressed.

Overall, the results presented in this work demonstrate that CYP46A1-mediated correction of cholesterol homeostasis in NPC mice is not sufficient to prevent neuronal cell death. Nevertheless, CYP46A1 was able to revert several pathological aspects of this disease, namely cholesterol metabolism normalization, autophagic flux regularization, and decreased neuroinflammation, which are also present in several other neurodegenerative disorders, and may represent a valid therapeutic approach to be used concomitantly with other drugs and in different disease contexts.

References

1. Russell, D. W., Halford, R. W., Ramirez, D. M. O., Shah, R. & Kotti, T. Cholesterol 24-hydroxylase: An enzyme of cholesterol turnover in the brain. *Annu. Rev. Biochem.* **78**, 1017–1040 (2009).

2. Mahley, R. W. & Rall, S. C. Apolipoprotein E: Far more than a lipid transport protein. *Annu. Rev. Genomics Hum. Genet.* **1**, 507–537 (2000).

3. Posse de Chaves, E. I., Rusinol, A. E., Vance, D. E., Campenot, R. B. & Vance, J. E. Role of lipoproteins in the delivery of lipids to axons during axonal regeneration. *J. Biol. Chem.* **272**, 30766–30773 (1997).

4. Mauch, D. H. *et al.* CNS Synaptogenesis Promoted by Glia-Derived Cholesterol. *Science.* **294**, 1354–1357 (2001).

5. Xu, G. *et al.* Relationship between abnormal cholesterol synthesis and retarded learning in rats. *Metabolism.* **47**, 878–882 (1998).

6. A, L. *et al.* Cholesterol reduction impairs exocytosis of synaptic vesicles. *J Cell Sci* **123**, 595–605 (2010).

7. Liu, Q. *et al.* Amyloid precursor protein regulates brain apolipoprotein E and cholesterol metabolism through lipoprotein receptor LRP1. *Neuron* **56**, 66–78 (2007).

8. Zhang, J. & Liu, Q. Cholesterol metabolism and homeostasis in the brain. *Protein Cell* **6**, 254–264 (2015).

9. Davison, A. N. *Brain sterol metabolism*. *Advances in lipid research* **3**, 171–196 (1965).

10. Cuzner, M. L., Davison, A. N. & Gregson, N. A. Turnover of brain mitochondrial membrane lipids. *Biochem. J.* **101**, 618–626 (1966).

11. Ohyama, Y. *et al.* Studies on the transcriptional regulation of cholesterol 24-hydroxylase (CYP46A1): Marked insensitivity toward different regulatory axes. *J. Biol. Chem.* **281**, 3810–3820 (2006).

12. Wustner, D., Mondal, M., Tabas, I. & Maxfield, F. R. Direct observation of rapid internalization and intracellular transport of sterol by macrophage foam cells. *Traffic* **6**, 396–412 (2005).

13. Dietschy, J. M. & Turley, S. D. Cholesterol metabolism in the baboon. *Curr. Opin. Lipidol.* **12**, 105–112 (2001).

14. Dietschy, J. M. & Turley, S. D. Cholesterol metabolism in the central nervous system during early development and in the mature animal. *J. Lipid Res.* 1375–1397 (2004).

15. Björkhem, I., Lütjohann, D., Breuer, O., Sakinis, A. & Wennmalm, Å. Importance of a Novel Oxidative Mechanism for Elimination of Brain Cholesterol. *J. Biol. Chem.* **272**, 30178–30184 (1997).

16. Xie, C., Lund, E. G., Turley, S. D., Russell, D. W. & Dietschy, J. M. Quantitation of two pathways for cholesterol excretion from the brain in normal mice and mice with neurodegeneration. *J. Lipid Res.* **44**, 1780–1789 (2003).

17. Shafaati, M., O'Driscoll, R., Björkhem, I. & Meaney, S. Transcriptional regulation of Cholesterol 24-hydroxylase by histone deacetylase inhibitors. *Biochem. Biophys. Res. Commun.* **378**, 689–694 (2009).

18. Meaney, S., Bodin, K., Diczfalusy, U. & Björkhem, I. On the rate of translocation in vitro and kinetics in vivo of the major oxysterols in human circulation: Critical importance of the position of the oxygen function. *J. Lipid Res.* **43**, 2130–2135 (2002).

19. Li-Hawkins, J., Lund, E. G., Bronson, A. D. & Russell, D. W. Expression cloning of an oxysterol 7α-hydroxylase selective for 24- hydroxycholesterol. *J. Biol. Chem.* **275**, 16543–16549 (2000).

20. Lütjohann, D. *et al.* Cholesterol homeostasis in human brain: Evidence for an age-dependent flux of 24S-hydroxycholesterol from the brain into the circulation. *Proc. Natl. Acad. Sci. U. S. A.* **93**, 9799–9804 (1996).

21. Pitas, R. E., Boyles, J. K., Lee, S. H., Foss, D. & Mahley, R. W. Astrocytes synthesize apolipoprotein E and metabolize apolipoprotein E-containing lipoproteins. *Biochim. Biophys. Acta (BBA)/Lipids Lipid Metab.* **917**, 148–161 (1987).

22. Kim, W., Weickert, C. & Garner, B. Role of ATP-binding cassette transporters in brain lipid transport and neurological disease. *J Neurochem* **104**, 1145–1166 (2008).

23. Wellington, C. *et al.* ABCA1 mRNA and protein distribution patterns predict multiple different roles and levels of regulation. *Lab Invest* **82**, 273–283 (2002).

24. Koldamova, R. *et al.* 22R-hydroxycholesterol and 9-cis-retinoic acid induce ATP-binding cassette transporter A1 expression and cholesterol efflux in brain cells and decrease amyloid beta secretion. *J Biol Chem* **278**, 13244–13256 (2003).

25. Roheim, P., Carey, M., Forte, T. & Vega, G. Apolipoproteins in human cerebrospinal fluid. *Proc Natl Acad Sci USA* **76**, 646–649 (1979).

26. Minagawa, H. *et al.* Mechanism underlying apolipoprotein E (ApoE) isoform-dependent lipid efflux from neural cells in culture. *J Neurosci Res* **87**, 2498–2508 (2009).

27. Lahiri, D. Apolipoprotein-E as a target for developing new therapeutics for Alzheimer's disease based on studies from protein, RNA, and regulatory region of the gene. *Mol Neurosci* **23**, 225–233 (2004).

28. Ko, M., Zou, K. & Minagawa, H. Cholesterol-mediated neurite outgrowth is differently regulated between cortical and hippocampal neurons. *J Biol Chem* **52**, 42759–42765 (2005).

29. Brown, M. & Goldstein, J. A proteolytic pathway that controls the cholesterol content of membranes, cells, and blood. *Proc Natl Acad Sci* **96**, 11041–11048 (1999).

30. Lund, E. G., Guileyardo, J. M. & Russell, D. W. cDNA cloning of cholesterol 24-hydroxylase,

a mediator of cholesterol homeostasis in the brain. *Proc. Natl. Acad. Sci. U. S. A.* **96**, 7238–7243 (1999).

31. Lütjohann, D. *et al.* Cholesterol dynamics in the foetal and neonatal brain as reflected by circulatory levels of 24S-hydroxycholesterol. *Acta Paediatr. Int. J. Paediatr.* **90**, 652–657 (2001).

32. Mast, N. *et al.* Broad Substrate Specificity of Human Cytochrome P450 46A1 Which Initiates Cholesterol Degradation in the Brain. *Biochemistry* **42**, 14284–14292 (2003).

33. Bodin, K. *et al.* Metabolism of 4β-hydroxycholesterol in humans. *J. Biol. Chem.* **277**, 31534–31540 (2002).

34. Mast, N., Charvet, C., Pikuleva, I. A. & Stout, C. D. Structural basis of drug binding to CYP46A1, an enzyme that controls cholesterol turnover in the brain. *J. Biol. Chem.* **285**, 31783–31795 (2010).

35. Mellon, S. H. & Griffin, L. D. Neurosteroids: biochemistry and clinical significance. *TRENDS Endocrinol. Metab.* **13**, 35–43 (2002).

36. Abildayeva, K. *et al.* 24(S)-hydroxycholesterol participates in a liver X receptor-controlled pathway in astrocytes that regulates apolipoprotein E-mediated cholesterol efflux. *J Biol Chem* **281**, 12799–12808 (2006).

37. Koldamova, R. & Lefterov, I. Role of LXR and ABCA1 in the pathogenesis of Alzheimer's disease - implications for a new therapeutic approach. *Curr Alzheimer Res* **4**, 171–178 (2007).

38. Lund, E. G. *et al.* Knockout of the cholesterol 24-hydroxylase gene in mice reveals a brain-specific mechanism of cholesterol turnover. *J. Biol. Chem.* **278**, 22980–22988 (2003).

39. Janowski, B. A., Willy, P. J., Devi, T. R., Falck, J. R. & Mangelsdorf, D. J. An oxysterol signalling pathway mediated by the nuclear receptor LXRα. *Nature* **383**, 728–731 (1996).

40. Lehmann, J. M. *et al.* Activation of the nuclear receptor LXR by oxysterols defines a new hormone response pathway. *J. Biol. Chem.* **272**, 3137–3140 (1997).

41. Forman, B. M., Ruan, B., Chen, J., Schroepfer, G. J. & Evans, R. M. The orphan nuclear receptor LXRa is positively and negatively regulated by distinct products of mevalonate metabolism. *Proc. Natl. Acad. Sci. U. S. A.* **94**, 10588–10593 (1997).

42. Milagre, I. *et al.* Transcriptional regulation of the human CYP46A1 brain-specific expression by Sp transcription factors. *J. Neurochem.* **106**, 835–849 (2008).

43. Wang, L. *et al.* Liver X receptors in the central nervous system: From lipid homeostasis to neuronal degeneration. *Proc. Natl. Acad. Sci. U. S. A.* **99**, 13878–13883 (2002).

44. Shafaati, M. *et al.* Enhanced production of 24S-hydroxycholesterol is not sufficient to drive liver X receptor target genes in vivo. *J. Intern. Med.* **270**, 377–387 (2011).

45. Kotti, T. J., Ramirez, D. M. O., Pfeiffer, B. E., Huber, K. M. & Russell, D. W. Brain cholesterol

turnover required for geranylgeraniol production and learning in mice. *Proc. Natl. Acad. Sci. U. S. A.* **103**, 3869–3874 (2006).

46. Kotti, T., Head, D. D., McKenna, C. E. & Russell, D. W. Biphasic requirement for geranylgeraniol in hippocampal long-term potentiation. *Proc. Natl. Acad. Sci. U. S. A.* **105**, 11394–11399 (2008).

47. Moutinho, M. *et al.* Cholesterol 24S-Hydroxylase Overexpression Inhibits the Liver X Receptor (LXR) Pathway by Activating Small Guanosine Triphosphate-Binding Proteins (sGTPases) in Neuronal Cells. *Mol. Neurobiol.* **51**, 1489–1503 (2015).

48. Moutinho, M. *et al.* Neuronal cholesterol metabolism increases dendritic outgrowth and synaptic markers via a concerted action of GGTase-I and Trk. *Sci. Rep.* **6**, 1–18 (2016).

49. Maioli, S. *et al.* Is It Possible to Improve Memory Function by Upregulation of the Cholesterol 24S-Hydroxylase (CYP46A1) in the Brain? *PLoS One* **8**, 2–9 (2013).

50. Fu, B. Y. *et al.* Cholesterol 24-hydroxylase (CYP46A1) polymorphisms are associated with faster cognitive deterioration in Chinese older persons: A two-year follow up study. *Int. J. Geriatr. Psychiatry* **24**, 921–926 (2009).

51. Nunes, M. J. *et al.* Sp proteins play a critical role in histone deacetylase inhibitor-mediated derepression of CYP46A1 gene transcription. *J. Neurochem.* **113**, 418–431 (2010).

52. Meng, J. *et al.* The anti-tumor histone deacetylase inhibitor SAHA and the natural flavonoid curcumin exhibit synergistic neuroprotection against amyloid-beta toxicity. *PLoS One* **9**, 1–11 (2014).

53. Ryu, H. *et al.* Sp1 and Sp3 are oxidative stress-inducible, antideath transcription factors in cortical neurons. *J. Neurosci.* **23**, 3597–3606 (2003).

54. Dynan, W. S. & Tjian, R. The promoter-specific transcription factor Sp1 binds to upstream sequences in the SV40 early promoter. *Cell* **35**, 79–87 (1983).

55. Mast, N. *et al.* Crystal structures of substrate-bound and substrate-free cytochrome P450 46A1, the principal cholesterol hydroxylase in the brain. *Proc. Natl. Acad. Sci. U. S. A.* **105**, 9546–9551 (2008).

56. Shafaati, M. *et al.* The antifungal drug voriconazole is an effi cient inhibitor of brain cholesterol 24s-hydroxylase in vitro and in vivo. *J. Lipid Res.* **51**, 318–323 (2010).

57. Mast, N. *et al.* In silico and intuitive predictions of CYP46A1 inhibition by marketed drugs with subsequent enzyme crystallization in complex with fluvoxamine. *Mol. Pharmacol.* **82**, 824–834 (2012).

58. Mast, N. *et al.* Pharmacologic stimulation of Cytochrome P450 46A1 and Cerebral Cholesterol Turnover in Mice. *J. Biol. Chem.* **289**, 3529–3538 (2014).

59. Carstea, E. D. *et al.* Niemann-Pick C1 Disease Gene: Homology to Mediators of Cholesterol Homeostasis. *Science.* **277**, 228–231 (1997).

60. Cougnoux, A. *et al.* Single cell transcriptome analysis of Niemann–Pick disease, type C1 cerebella. *Int. J. Mol. Sci.* **21**, 1–23 (2020).

61. Patterson, M. C., Vecchio, D., Prady, H., Abel, L. & Wraith, J. E. Miglustat for treatment of Niemann-Pick C disease: a randomised controlled study. *Lancet Neurol.* **6**, 765–772 (2007).

62. Pineda, M. *et al.* Miglustat in patients with Niemann-Pick disease Type C (NP-C): A multicenter observational retrospective cohort study. *Mol. Genet. Metab.* **98**, 243–249 (2009).

63. Farmer, C. A. *et al.* Long-term neuropsychological outcomes from an open-label phase 1/2a trial of 2-hydoxypropyl-β-cyclodextrins (VTS-270) in Niemann-Pick Disease, Type C1. *CNS Drugs* **33**, 677–683 (2019).

64. Vanier, M. T. Niemann-Pick disease type C. *Orphanet J. Rare Dis.* 1–16 (2010).

65. Davies, J. P. & Ioannou, Y. A. Topological analysis of Niemann-Pick C1 protein reveals that the membrane orientation of the putative sterol-sensing domain is identical to those of 3-hydroxy-3-methylglutaryl-CoA reductase and sterol regulatory element binding protein cleavage-activating. *J. Biol. Chem.* **275**, 24367–24374 (2000).

66. Colombo, A. *et al.* Loss of NPC1 enhances phagocytic uptake and impairs lipid trafficking in microglia. *Nat. Commun.* **12**, 1–20 (2021).

67. Praggastis, M. *et al.* A murine Niemann-Pick C1 I1061T knock-In model recapitulates the pathological features of the most prevalent human disease allele. *J. Neurosci.* **35**, 8091–8106 (2015).

68. Cougnoux, A. *et al.* Microglia activation in Niemann-Pick disease, type C1 is amendable to therapeutic intervention. *Hum. Mol. Genet.* **27**, 2076–2089 (2018).

69. Cougnoux, A. *et al.* Necroptosis inhibition as a therapy for Niemann-Pick disease, type C1: Inhibition of RIP kinases and combination therapy with 2-hydroxypropyl-β-cyclodextrin. *Mol. Genet. Metab.* **125**, 345–350 (2018).

70. Kavetsky, L. *et al.* Increased interactions and engulfment of dendrites by microglia precede Purkinje cell degeneration in a mouse model of Niemann Pick Type-C. *Sci. Rep.* **9**, 1–15 (2019).

71. Lloyd-Evans, E. *et al.* Niemann-Pick disease type C1 is a sphingosine storage disease that causes deregulation of lysosomal calcium. *Nat. Med.* **14**, 1247–1255 (2008).

72. Yu, W. *et al.* Altered cholesterol metabolism in Niemann-Pick type C1 mouse brains affects mitochondrial function. *J. Biol. Chem.* **280**, 11731–11739 (2005).

73. Loftus, S. K. *et al.* Rescue of neurodegeneration in Niemann-Pick C mice by a prion-promoter-driven Npc1 cDNA transgene. *Hum. Mol. Genet.* **11**, 3107–3114 (2002).

74. Prasad, A., Fischer, W. A., Maue, R. A. & Henderson, L. P. Regional and developmental expression of the Npc1 mRNA in the mouse brain. *J. Neurochem.* **75**, 1250–1257 (2000).

75. Ong, W. Y. *et al.* Neurodegeneration in Niemann-Pick type C disease mice. *Exp. Brain Res.* **141**,

218–231 (2001).

76. Suzuki, H., Sakiyama, T., Harada, N., Abe, M. & Tadokoro, M. Pathologic changes of glial cells in murine model of Niemann-Pick disease type C: Immunohistochemical, lectin-histochemical and ultrastructural observations. *Pediatr. Int.* **45**, 1–4 (2003).

77. Graeber, M. B., Li, W. & Rodriguez, M. L. Role of microglia in CNS inflammation. *FEBS Lett.* **585**, 3798–3805 (2011).

78. Veerhuis, R., Nielsen, H. M. & Tenner, A. J. Complement in the brain. *Mol. Immunol.* **48**, 1592–1603 (2011).

79. Cologna, S. M. *et al.* Human and Mouse Neuroinflammation Markers in Niemann-Pick Disease, Type C1. *J Inherit Metab Dis.* **37**, 1–18 (2015).

80. Baudry, M., Yao, Y., Simmons, D., Liu, J. & Bi, X. Postnatal development of inflammation in a murine model of Niemann-Pick type C disease: Immunohistochemical observations of microglia and astroglia. *Exp. Neurol.* **184**, 887–903 (2003).

81. Reemst, K., Noctor, S. C., Lucassen, P. J. & Hol, E. M. The indispensable roles of microglia and astrocytes during brain development. *Front. Hum. Neurosci.* **10**, 1–28 (2016).

82. Butovsky, O. & Weiner, H. L. Microglial signatures and their role in health and disease. *Nat. Rev. Neurosci.* **19**, 622–635 (2018).

83. Bachiller, S. *et al.* Microglia in neurological diseases: A road map to brain-disease dependent-inflammatory response. *Front. Cell. Neurosci.* **12**, 1–17 (2018).

84. Martinez, F. O. & Gordon, S. The M1 and M2 paradigm of macrophage activation: Time for reassessment. *F1000Prime Rep.* **6**, 1–13 (2014).

85. Holtman, I. R. *et al.* Induction of a common microglia gene expression signature by aging and neurodegenerative conditions: a co-expression meta-analysis. *Acta Neuropathol. Commun.* **3**, 31 (2015).

86. Keren-Shaul, H. *et al.* A Unique Microglia Type Associated with Restricting Development of Alzheimer's Disease. *Cell* **169**, 1276-1290.e17 (2017).

87. Loftus, S. K. *et al.* Murine model of Niemann-Pick C disease: mutation in a cholesterol homeostasis gene. *Science.* **277**, 232–235 (1997).

88. Ransohoff, R. M. & Brown, M. A. Innate immunity in the central nervous system. *J. Clin. Invest.* **122**, 1164–1171 (2012).

89. Mott, R. T. *et al.* Neuronal expression of CD22: novel mechanism for inhibiting microglial proinflammatory cytokine production. *Glia* **46**, 369–379 (2004).

90. German, D. C. *et al.* Neurodegeneration in the Niemann-Pick C mouse: Glial involvement. *Neuroscience* **109**, 437–450 (2002).

91. Suzuki, M. *et al.* Endosomal accumulation of Toll-like receptor 4 causes constitutive secretion

of cytokines and activation of signal transducers and activators of transcription in Niemann-Pick disease type C (NPC) fibroblasts: A potential basis for glial cell activation in the NPC brain. *J. Neurosci.* **27**, 1879–1891 (2007).

92. Tanaka, J., Nakamura, H. & Miyawaki, S. Cerebellar involvement in murine sphingomyelinosis: A new model of Niemann-Pick Disease. *J. Neuropathol. Exp. Neurol.* **47**, 291–300 (1998).

93. Patel, S. C. *et al.* Localization of Niemann-Pick C1 protein in astrocytes: Implications for neuronal degeneration in Niemann-Pick type C disease. *Proc. Natl. Acad. Sci. U. S. A.* **96**, 1657–1662 (1999).

94. Vance, J. E. Dysregulation of cholesterol balance in the brain: Contribution to neurodegenerative diseases. *DMM Dis. Model. Mech.* **5**, 746–755 (2012).

95. FW, P. Outsourcing in the brain: do neurons depend on cholesterol delivery by astrocytes? *Bioessays* **25**, 72–78 (2003).

96. Zhang, M. *et al.* Astrocyte-only Npc1 reduces neuronal cholesterol and triples life span of Npc1-/- mice. *J. Neurosci. Res.* **86**, 2848–2856 (2008).

97. Patel, S. C. *et al.* Astrocytes synthesize and secrete the lipophilic ligand carrier apolipoprotein D. *Neuroreport* **6**, 653–657 (1995).

98. Kimelberg, H. K., Goderie, S. K., Higman, S., Pang, S. & Waniewski, R. A. Swelling-induced release of glutamate, aspartate and taurine from astrocyte cultures. *J. Neurosci* **10**, 1583–1591 (1990).

99. Wu, Y.-P., Kubota, A. & Suzuki, K. Neuronal death and reactive glial changes in the brain of the Niemann-Pick disease type C mouse. *Neurosci. Abstr.* **25**, 1118 (1999).

100. Reggiori, F. & Klionsky, D. J. Autophagosomes: Biogenesis from scratch? *Curr. Opin. Cell Biol.* **17**, 415–422 (2005).

101. Mizushima, N. Autophagy: Process and function. *Genes Dev.* **21**, 2861–2873 (2007).

102. Beth Levine & Guido Kroemer. Autophagy in the Pathogenesis of Disease. *Cell.* **132**, 27–42 (2008).

103. Biswas, D. *et al.* ATP-induced autophagy is associated with rapid killing of intracellular mycobacteria within human monocytes/macrophages. *BMC Immunol.* **9**, (2008).

104. Mizushima, N. & Levine, B. Autophagy in mammalian development and differentiation. *Nat Cell Biol.* **12**, 823–830 (2010).

105. Kaushik, S. & Cuervo, A. M. *The coming of age of chaperone-mediated autophagy*. *Nat Rev Mol Cell Biol.* **19**, 365–381 (2019).

106. Klionsky, D. J. The molecular machinery of autophagy: Unanswered questions. *J. Cell Sci.* **118**, 7–18 (2005).

107. Finkbeiner, S. The autophagy lysosomal pathway and neurodegeneration. *Cold Spring Harb.*

Perspect. Biol. **12**, 1–19 (2020).

108. Klionsky, T. S. and D. J. Autophagy in Health and Disease: A Double-Edged Sword Takahiro. *Bone* **23**, 1–7 (2008).

109. Gutierrez, M. G. *et al.* Autophagy is a defense mechanism inhibiting BCG and Mycobacterium tuberculosis survival in infected macrophages. *Cell* **119**, 753–766 (2004).

110. Lum, J. J. *et al.* Growth factor regulation of autophagy and cell survival in the absence of apoptosis. *Cell* **120**, 237–248 (2005).

111. Takenouchi, T., Fujita, M., Sugama, S., Kitani, H. & Hashimoto, M. The role of the P2X7 receptor signaling pathway for the release of autolysosomes in microglial cells. *Autophagy* **5**, 723–724 (2009).

112. Ao, X., Zou, L. & Wu, Y. Regulation of autophagy by the Rab GTPase network. *Cell Death Differ.* **21**, 348–358 (2014).

113. Perera, R. M. & Zoncu, R. The Lysosome as a Regulatory Hub. *Annu. Rev. Cell Dev. Biol.* **32**, 223–253 (2016).

114. Jiang, P. & Mizushima, N. LC3- and p62-based biochemical methods for the analysis of autophagy progression in mammalian cells. *Methods* **75**, 13–18 (2015).

115. Kabeya, Y. *et al.* LC3, a mammalian homolog of yeast Apg8p, is localized in autophagosome membranes after processing ((2000). *EMBO J.* **19**, 5720–5728 (2000).

116. Kabeya, Y. *et al.* LC3, GABARAP and GATE16 localize to autophagosomal membrane depending on form-II formation. *J. Cell Sci.* **117**, 2805–2812 (2004).

117. Tanida, I., Minematsu-Ikeguchi, N., Ueno, T. & Kominami, E. Lysosomal turnover, but not a cellular level, of endogenous LC3 is a marker for autophagy. *Autophagy* **1**, 84–91 (2005).

118. Tanida, I., Ueno, T. & Kominami, E. LC3 conjugation system in mammalian autophagy. *Int. J. Biochem. Cell Biol.* **36**, 2503–2518 (2004).

119. Tanida, I., Tanida-Miyake, E., Ueno, T. & Kominami, E. The human homolog of Saccharomyces cerevisiae Apg7p is a protein-activating enzyme for multiple substrates including human Apg12p, GATE-16, GABARAP, and MAP-LC3. *J. Biol. Chem.* **276**, 1701–1706 (2001).

120. Tanida, I., Tanida-Miyake, E., Komatsu, M., Ueno, T. & Kominami, E. Human Apg3p/Aut1p homologue is an authentic E2 enzyme for multiple substrates, GATE-16, GABARAP, and MAP-LC3, and facilitates the conjugation of hApg12p to hApg5p. *J. Biol. Chem.* **277**, 13739–13744 (2002).

121. Mizushima, N., Ohsumi, Y. & Yoshimori, T. Autophagosome formation in mammalian cells. *Cell Struct. Funct.* **27**, 421–429 (2002).

122. Kuma, A. *et al.* The role of autophagy during the early neonatal starvation period. *Nature* **432**, 1032–1036 (2004).

123. Komatsu, M. *et al.* Impairment of starvation-induced and constitutive autophagy in Atg7-deficient mice. *J. Cell Biol.* **169**, 425–434 (2005).

124. Hara, T. *et al.* Suppression of basal autophagy in neural cells causes neurodegenerative disease in mice. *Nature* **441**, 885–889 (2006).

125. Ravikumar, B., Duden, R. & Rubinsztein, D. C. Aggregate-prone proteins with polyglutamine and polyalanine expansions are degraded by autophagy. *Hum. Mol. Genet.* **11**, 1107–1117 (2002).

126. Iwata, A. *et al.* Increased susceptibility of cytoplasmic over nuclear polyglutamine aggregates to autophagic degradation. *Proc. Natl. Acad. Sci. U. S. A.* **102**, 13135–13140 (2005).

127. Fortun, J., Dunn, W. A., Joy, S., Li, J. & Notterpek, L. Emerging Role for Autophagy in the Removal of Aggresomes in Schwann Cells. *J. Neurosci.* **23**, 10672–10680 (2003).

128. Ravikumar, B. *et al.* Inhibition of mTOR induces autophagy and reduces toxicity of polyglutamine expansions in fly and mouse models of Huntington disease. *Nat. Genet.* **36**, 585–595 (2004).

129. Komatsu, M. *et al.* Loss of autophagy in the central nervous system causes neurodegeneration in mice. *Nature* **441**, 880–884 (2006).

130. Singh, R. *et al.* Autophagy regulates lipid metabolism. *Nature* **458**, 1131–1135 (2009).

131. Liao, G. *et al.* Cholesterol accumulation is associated with lysosomal dysfunction and autophagic stress in Npc1-/- mouse brain. *Am. J. Pathol.* **171**, 962–975 (2007).

132. Man, S. M. & Kanneganti, T. D. Regulation of lysosomal dynamics and autophagy by CTSB/cathepsin B. *Autophagy* **12**, 2504–2505 (2016).

133. Qiao, L. *et al.* Lysosomal enzyme cathepsin D protects against alpha-synuclein aggregation and toxicity. *Mol. Brain* **1**, 17 (2008).

134. Ko, D. C. *et al.* Cell-autonomous death of cerebellar purkinje neurons with autophagy in niemann-pick type C disease. *PLoS Genet.* **1**, 0081–0095 (2005).

135. Pacheco, C. D., Kunkel, R. & Lieberman, A. P. Autophagy in Niemann-Pick C disease is dependent upon Beclin-1 and responsive to lipid trafficking defects. *Hum. Mol. Genet.* **16**, 1495–1503 (2007).

136. Sarkar, S. *et al.* Impaired autophagy in the lipid storage disorder Niemann–Pick type C1 disease. *Cell Rep.* **12**, 1302–1315 (2013).

137. Ishibashi, S., Yamazaki, T. & Okamoto, K. Association of autophagy with cholesterol-accumulated compartments in Niemann-Pick disease type C cells. *J Clin Neurosci.* **16**, 954–9 (2009).

138. Paulina Ordonez, M. *et al.* Disruption and therapeutic rescue of autophagy in a human neuronal model of Niemann pick type C1. *Hum. Mol. Genet.* **21**, 2651–2662 (2012).

139. Roney, J. C. *et al.* Lipid-mediated motor-adaptor sequestration impairs axonal lysosome delivery leading to autophagic stress and dystrophy in Niemann-Pick type C. *Dev Cell.* **56**, 1452–1468 (2021).

140. Walkley, S. U. Cellular pathology of lysosomal storage disorders. *Brain Pathol.* **8**, 175–193 (1998).

141. Walkley, S. U., Sikora, J., Micsenyi, M., Davidson, C. & Dobrenis, K. Lysosomal Compromise and Brain Dysfunction: Examining the Role of Neuroaxonal Dystrophy. *Biochem Soc Trans.* **38**, 1436–1441 (2010).

142. Bonifacino, J. S. & Neefjes, J. Moving and Positioning the Endolysosomal System. *Curr Opin Cell Biol.* **47**, 1–8 (2017).

143. Farías, G. G., Guardia, C. M., De Pace, R., Britt, D. J. & Bonifacino, J. S. BORC/kinesin-1 ensemble drives polarized transport of lysosomes into the axon. *Proc. Natl. Acad. Sci. U. S. A.* **114**, E2955–E2964 (2017).

144. Petrov, A. M. *et al.* CYP46A1 Activation by Efavirenz Leads to Behavioral Improvement without Significant Changes in Amyloid Plaque Load in the Brain of 5XFAD Mice. *Neurotherapeutics* **16**, 710–724 (2019).

145. Hudry, E. *et al.* Adeno-associated virus gene therapy with cholesterol 24-hydroxylase reduces the amyloid pathology before or after the onset of amyloid plaques in mouse models of alzheimer's disease. *Mol. Ther.* **18**, 44–53 (2010).

146. Boussicault, L. *et al.* CYP46A1, the rate-limiting enzyme for cholesterol degradation, is neuroprotective in Huntington's disease. *Brain* **139**, 953–970 (2016).

147. Kacher, R. *et al.* CYP46A1 gene therapy deciphers the role of brain cholesterol metabolism in Huntington's disease. *Brain* **142**, 2432–2450 (2019).

148. Vanier, M. T. Complex lipid trafficking in Niemann-Pick disease type C. *J. Inherit. Metab. Dis.* **38**, 187–199 (2015).

149. Reddy, J. V, Ganley, I. G. & Pfeffer, S. R. Clues to neuro-degeneration in Niemann-Pick type C disease from global gene expression profiling. *PLoS One* **20;1**, e19 (2006).

150. Mitroi, D. N. *et al.* NPC 1 enables cholesterol mobilization during long-term potentiation that can be restored in Niemann–Pick disease type C by CYP 46A1 activation. *EMBO Rep.* **20**, 1–18 (2019).

151. Pikuleva, I. Targeting cytochrome P450 46A1 and brain cholesterol 24-hydroxylation to treat neurodegenerative diseases. *Explor. Neuroprotective Ther.* **1**, 159–172 (2021).

152. Tharkeshwar, A. K. *et al.* A novel approach to analyze lysosomal dysfunctions through subcellular proteomics and lipidomics: The case of NPC1 deficiency. *Sci. Rep*. **7**, 1–20 (2017).

153. Simões, A. E. S. *et al*. Efficient recovery of proteins from multiple source samples after trizol® or trizol®LS RNA extraction and long-term storage. *BMC Genomics* **14**, (2013).

154. Andersen, C. L., Jensen, J. L. & Ørntoft, T. F. Normalization of real-time quantitative reverse transcription-PCR data: a model-based variance estimation approach to identify genes suited for normalization, applied to bladder and colon cancer data sets. *Cancer Res.* **64**, 5245–50 (2004).

155. Erickson, R. P., Bhattacharyya, A., Hunter, R. J., Heidenreich, R. A. & Cherrington, N. J. Liver disease with altered bile acid transport in Niemann-Pick C mice on a high-fat, 1% cholesterol diet. *Am. J. Physiol. - Gastrointest. Liver Physiol.* **289**, 300–307 (2005).

156. Hirsch-Reinshagen, V. *et al*. Deficiency of ABCA1 impairs apolipoprotein E metabolism in brain. J. Biol. Chem. **279**, 41197–41207 (2004).

157. Langmade, S. J. *et al*. Pregnane X receptor (PXR) activation: A mechanism for neuroprotection in a mouse model of Niemann-Pick C disease. *Proc. Natl. Acad. Sci. U. S. A*. **103**, 13807–13812 (2006).

158. Subramaniam, S. R. & Federoff, H. J. Targeting microglial activation states as a Therapeutic Avenue in Parkinson's disease. Front. Aging Neurosci. **9**, 1–18 (2017).

159. Labandeira-Garcia, J. L., Costa-Besada, M. A., Labandeira, C. M., Villar-Cheda, B. & Rodríguez-Perez, A. I. Insulin-like growth factor-1 and neuroinflammation. *Front. Aging Neurosci.* **9**, 1–9 (2017).

160. Pawelec, P., Ziemka-nalecz, M., Sypecka, J. & Zalewska, T. The Impact of the CX3CL1/CX3CR1 Axis in Neurological Disorders. Cells **9**, 2277 (2020).

161. Caporali, P. et al. Developmental delay in motor skill acquisition in niemann-pick C1 mice reveals abnormal cerebellar morphogenesis. *Acta Neuropathol. Commun.* **4**, 1–18 (2016).

162. Buffo, A. & Rossi, F. Origin, lineage and function of cerebellar glia. Prog Neurobiol **109**, 42–63 (2013).

163. Higashi, Y., Murayama, S., Pentchev, P. & Suzuki, K. Cerebellar degeneration in the Niemann-Pick type C mouse. *Acta Neuropathol*. **85**, 175–184 (1993).

164. Laure-Kamionowska, M. & Málińska, D. Calbindin positive Purkinje cells in the pathology of human cerebellum occurring at the time of its development. *Folia Neuropathol.* **47**, 300–305 (2009).

165. Davis, O. B. *et al*. NPC1-mTORC1 Signaling Couples Cholesterol Sensing to Organelle Homeostasis and Is a Targetable Pathway in Niemann-Pick Type C. *Dev. Cell* **56**, 260-276.e7 (2021).

166. Trilck, M. *et al*. Niemann-Pick type C1 patient-specific induced pluripotent stem cells display disease specific hallmarks. *Orphanet J. Rare Dis.* **8**, 1–12 (2013).

167. Gelsthorpe, M. E. *et al.* Niemann-Pick type C1 I1061T mutant encodes a functional protein that is selected for endoplasmic reticulum-associated degradation due to protein misfolding. *J. Biol. Chem.* **283**, 8229–8236 (2008).

168. Li, H. *et al*. Molecular, anatomical, and biochemical events associated with neurodegeneration

in mice with Niemann-Pick type C disease. *J. Neuropathol. Exp. Neurol.* **64**, 323–333 (2005).

169. Santiago-Mujica, E. *et al*. Hepatic and neuronal phenotype of NPC1−/− mice. *Heliyon* **5**, e01293 (2019).

170. Xie, C., Turley, S., Pentchev, P. & Dietschy, J. Cholesterol balance and metabolism in mice with loss of function of Niemann-Pick C protein. *Am. J. Physiol*. **276**, e336-44 (1999).

171. Davidson, J. *et al*. 2-Hydroxypropyl-β-cyclodextrin is the active component in a triple combination formulation for treatment of Niemann-Pick C1 disease. *Biochim. Biophys. Acta - Mol. Cell Biol. Lipids* **1864**, 1545–1561 (2019).

172. Brown, M. S. & Goldstein, J. L. The SREBP pathway: Regulation of cholesterol metabolism by proteolysis of a membrane-bound transcription factor. *Cell* **89**, 331–340 (1997).

173. Lu, A. Endolysosomal cholesterol export: More than just NPC1. *BioEssays* **44**, 1–12 (2022).

174. Boadu, E., Nelson, R. C. & Francis, G. A. ABCA1-dependent mobilization of lysosomal cholesterol requires functional Niemann-Pick C2 but not Niemann-Pick C1 protein. *Biochim. Biophys. Acta - Mol. Cell Biol. Lipids* **1821**, 396–404 (2012).

175. Pagler, T. A., Neuhofer, A., Laggner, H., Strobl, W. & Stangl, H. Cholesterol efflux via HDL resecretion occurs when cholesterol transport out of the lysosome is impaired. *J. Lipid Res.* **48**, 2141–2150 (2007).

176. Cianciola, N. L., Greene, D. J., Morton, R. E. & Carlin, C. R. Adenovirus RIDα uncovers a novel pathway requiring ORP1L for lipid droplet formation independent of NPC1. *Mol. Biol. Cell* **24**, 3209–3225 (2013).

177. Cianciola, N. L. & Carlin, C. R. Adenovirus RID-α activates an autonomous cholesterol regulatory mechanism that rescues defects linked to Niemann-Pick disease type C. *J. Cell Biol*. **187**, 537–552 (2009).

178. Castellano, B. M. *et al*. Lysosomal cholesterol activates mTORC1 via an SLC38A9-Niemann-Pick C1 signaling complex. *Science* **355**, 1306–1311 (2017).

179. Sancak, Y. *et al*. Ragulator-Rag complex targets mTORC1 to the lysosomal surface and is necessary for its activation by amino acids. *Cell* **141**, 290–303 (2010).

180. Wang, S. *et al*. The amino acid transporter SLC38A9 is a key component of a lysosomal membrane complex that signals arginine sufficiency to mTORC1. *Science* **347**, 188–194 (2015).

181. Wyant, G. A. *et al*. mTORC1 activator SLC38A9 is required to efflux essential amino acids from lysosomes and use protein as a nutrient. *Cell* **171**, 642–654 (2017).

182. Leal, P. *et al.* AKT/mTOR substrate p70S6k is frequently phosphorylated in gallbladder cancer tissue and cell lines. *Onco. Targets. Ther.* **6**, 1373–1384 (2013).

183. Hartmann, B. P70S6 kinase phosphorylation for pharmacodynamic monitoring. *Clin. Chim. Acta* **413**, 1387–1390 (2012).

184. Ilnytska, O. *et al*. Enrichment of NPC1-deficient cells with the lipid LBPA stimulates autophagy, improves lysosomal function, and reduces cholesterol storage. *J. Biol. Chem*. **297**, 100813 (2021).

185. Elrick, M. J., Yu, T., Chung, C. & Lieberman, A. P. Impaired proteolysis underlies autophagic dysfunction in Niemann-Pick type C disease. *Hum. Mol. Genet*. **21**, 4876–4887 (2012).

186. Seo, Y. K., Jeon, T., Chong, H. K., Beisinger, J. & Osborne, T. F. Genome-wide Localization of SREBP-2 in Hepatic Chromatin Predicts a Role in Autophagy. *Cell Metab.* **13**, 367–375 (2011).

187. Mizushima, N. & Yoshimori, T. How to interpret LC3 immunoblotting. *Autophagy* **3**, 542–545 (2007).

188. Liedtke, M., Völkner, C., Hermann, A. & Frech, M. J. Impact of Organelle Transport Deficits on Mitophagy and Autophagy in Niemann–Pick Disease Type C. *Cells* **11**, 1–24 (2022).

189. Grace Y., L. & David M., S. mTOR at the nexus of nutrition, growth, ageing and disease. *Nat. Rev. Mol. Cell Biol*. **21**, 183–203 (2020).

190. Laffer, B. et al. Loss of IL-10 Promotes Differentiation of Microglia to a M1 Phenotype. *Front. Cell. Neurosci*. **13**, 1–12 (2019).

191. Helquist, P., Maxfield, F. R., Wiech, N. L. & Wiest, O. Treatment of Niemann-Pick Type C Disease by Histone Deacetylase Inhibitors. *Neurotherapeutics* **10**, 688–697 (2013).

192. Zervas, M., Somers, K. L., Thrall, M. A. & Walkley, S. U. Critical role for glycosphingolipids in Niemann-Pick disease type C. *Curr. Biol*. **11**, 1283–1287 (2001).